Effect of Adenovirus-mediated Decorin Gene Therapy on Fibrotic Remodeling in Tissue-engineered Skin

by

Saahil Sanon

A thesis submitted in partial fulfillment of the requirements for the degree of

Master of Science

in

Experimental Surgery

Department of Surgery

University of Alberta

Abstract

Background:

Hypertrophic scar (HTS) is a fibroproliferative disorder of the skin that results in the development of painful, red, raised scar lesions. Transforming growth factor beta 1 (TGF-β1) has been implicated as a key driver of this disorder. Primarily, these effects include an increased deposition of collagen and matrix proteoglycans, as well as the suppressed expression of matrix-remodeling proteins like matrix metalloproteinase 1 (MMP-1). The proteoglycan decorin (DCN) has been shown to bind to and inactivate TGF-β1. Moreover, DCN plays a key role during collagen fibrillogenesis by regulating collagen fibril thickness and organization. Therefore, adenoviral (Ad5)-DCN gene therapy may have therapeutic effects for HTS.

Objectives:

This project used a co-cultured tissue-engineered *in vitro* model to explore anti-fibrotic matrix remodeling after treating HTS fibroblasts with Ad5-DCN for 18 hours. Anticipated results included increased DCN protein levels, reduced contraction, normalized orientation of the extracellular matrix, and elevated gene expression of MMP-1.

Methods:

Tissue-engineered skin was prepared by co-culturing fibroblasts and keratinocytes in collagen-glycosaminoglycan scaffolds for 17 days. Keratinocytes isolated from normal skin were used for all scaffolds while dermal fibroblasts were from one of four groups: 1) normal skin fibroblasts (n=12), 2) HTS fibroblasts (n=12), 3) HTS fibroblasts + Ad5-DCN (n=12), 4) HTS fibroblasts + Ad5-GFP (n=12). Contraction during culture was evaluated using digital analysis of matrix area. Histological sections were stained with picrosirius red and analyzed using fast

Fourier analysis to determine collagen organization. mRNA levels of TGF-β1, collagen 1 alpha 1 (COL1A1), MMP-1, and DCN were measured via RT-qPCR. Total collagen levels were evaluated using LC/MS for the amount of 4-hydroxyproline, while DCN protein was measured using ELISA and immunofluorescent staining. Repeated measures ANOVA with Holm-Bonferroni post-hoc analysis was used to assess significance, with $p<0.05$ being significant.

Results:

After day 17, tissue-engineered skin constructs created using Ad5-DCN-treated HTS fibroblasts were less contracted than those with untreated HTS fibroblasts. The Ad5-DCN-treated group showed elevations in both soluble and matrix-bound DCN protein levels, as well as increased mRNA expression of DCN. Normalized extracellular matrix remodeling was observed, as indicated by collagen orientation index and collagen bundle packing index values. This may be the result of elevated MMP-1, which was found to be increased 5-fold in mRNA expression by the Ad5-DCN-treated group as compared to the untreated HTS group. Additionally, COL1A1 mRNA and total collagen protein were both reduced in the Ad5-DCN group as compared to the HTS Fb group. No significant difference was found with respect to TGF-β1 mRNA expression between groups.

Conclusions:

Treatment of HTS fibroblasts with Ad5-DCN leads to improvement in contraction and matrix remodeling in a tissue-engineered *in vitro* model of the skin. Further *in vivo* study may lead to improved tissue-engineered skin for treatment of acute injuries or to assist in the reconstruction of HTS post-burn, possibly through systemic effects of by reducing scarring when used for skin resurfacing of local injuries.

Preface

The following thesis involves scientific experimentation on cells acquired from human patients. The research project involving the acquisition of human abdominoplasty tissue and site-matched hypertrophic/normal skin punch biopsies for *in vitro* experimentation, of which this thesis is a part, received ethics approval from the University of Alberta Research Ethics Board on 09/07/2015 and is entitled "Wound healing research" (protocol number Pro00023826). This thesis is also encompassed in the research project entitled "Development and characterization of dermal fibrosis following burn injury" (protocol number AUP00000344), which last received ethics approval from the University of Alberta Research Ethics Board on 11/26/2015.

Portions of Chapter 1 have been published as Sanon, S., Hart, D.A., Tredget, E.E., *Molecular and cellular biology of wound healing and skin regeneration*, in *Skin tissue engineering and regenerative medicine*, M.Z. Albanna, J.H. Holmes, Editors. 2016, Elsevier. p. 19-47. Saahil Sanon was responsible for the majority of the literature review and manuscript composition for this book chapter. Dr. David A. Hart was involved with the literature review and manuscript composition of sections regarding porcine hypertrophic scar models. His sections are not contained here, as they are outside the scope of this thesis. Dr. Edward E. Tredget was the supervisory author and was involved with concept formation of the manuscript.

Construction of the adenoviral vectors used for experimentation in Chapter 2 was carried out by Dr. Peter Kwan. The protocol used in the development of these viral vectors were included in this thesis for completeness. All other portions of Chapter 2 and the entirety of Chapter 3 are an original work by Saahil Sanon.

Acknowledgements

First of all, I would like to thank my supervisory committee, Dr. Edward Tredget, Dr. Jie Ding, and Dr. Adetola Adesida. The findings of this thesis would not have been possible without their expert guidance over the past two years. Moreover, the mentoring I have received from each of them has been integral in influencing me to pursue my future career path as a physician-scientist.

Next, I want to thank Dr. Thomas Churchill, Christina Smith, Lisa Brick, and Tracey Dean. Together, they have served as the backbone to my graduate education in the Department of Surgery, ensuring that I was well-adjusted to life in Edmonton and helping me to successfully navigate the administrative aspects of the university.

In addition, this thesis has only been achieved due to the support of the other members of my lab: Forest Zhu, Peter Kwan, Zengshuan Ma, Takashi Iwashina, Leah Campeau, and Jiajie Wu. They made my time in the lab quite enjoyable and were always willing to lend a helping hand or let me bounce new research ideas off of them.

I would also like to acknowledge the funding sources for this project, particularly the Firefighters' Burn Trust Fund and the Edmonton Civic Employees Fund. Scientific research, though amazingly beneficial, is also incredibly expensive to conduct. This work would not have been done without their support.

Finally, this section would not be complete without thanking my friends and family, particularly my parents, Ashish and Ritu Sanon, and my brother, Nikhil Sanon. This achievement would not have been possible without their continual encouragement and moral support.

Table of Contents

List of Tables

List of Figures

List of Abbreviations

α-SMA	Alpha-smooth muscle actin
Ad5-DCN	Adenoviral vector expressing recombinant decorin
Ad5-GFP	Adenoviral vector expressing enhanced green fluorescent protein
BSA	Bovine serum albumin
CAR	Coxsackievirus and adenovirus receptor
CBPI	Collagen bundle packing index
CEA	Cultured epithelial autograft
CGAG	Collagen-glycosaminoglycan
COI	Collagen orientation index
COL1A1	Collagen 1 alpha 1
CTGF	Connective tissue growth factor
DCN	Decorin
DHT	Dehydrothermal treatment
DMEM	Dulbecco's modified eagle's medium with l-glutamine
DMSO	Dimethyl sulfoxide
ECM	Extracellular matrix
EDC	1-ethyl-3-(3-dimethyl aminopropyl) carbodiimide hydrochloride

ELISA	Enzyme-linked immunosorbent assay
FBS	Fetal bovine serum
FGF	Fibroblast growth factor
GA	Gluteraldehyde
GAG	Glycosaminoglycan
GAPDH	Glyceraldehyde 3-phosphate dehydrogenase
GFP	Green fluorescent protein
HA	Hyaluronic acid
HEK	Human embryonic kidney
HKGS	Human keratinocyte growth supplement
HTS	Hypertrophic scar
HTS Fb	Hypertrophic scar fibroblasts
IFN	Interferon
IGF	Insulin-like growth factor
IL	Interleukin
KGF	Keratinocyte growth factor
LC/MS	Liquid chromatography/mass spectrometry
MCP	Monocyte chemotactic protein

MMP	Matrix metalloproteinase
MOI	Multiplicity of infection
MTT	3-(4,5-dimethylthiozol-2-yl)-2,5-diphenyl tetrazolium bromide
NS Fb	Normal skin fibroblasts
PBS	Phosphate-buffered saline
PCR	Polymerase chain reaction
PDGF	Platelet-derived growth factor
PFU	Plaque-forming unit
R-SMAD	Receptor-regulated SMAD
RT-qPCR	Reverse transcription quantitative polymerase chain reaction
SDF	Stromal-cell-derived factor
SEM	Scanning electron microscope/microscopy
SLRP	Small leucine-rich proteoglycan
TBSA	Total body surface area
TG	Transglutaminase
TGF	Transforming growth factor
TGFBR	Transforming growth factor-beta receptor
TIMP	Tissue inhibitor of metalloproteinase

TLR	Toll-like receptor
TNF	Tumor necrosis factor
VEGF	Vascular endothelial growth factor

Chapter 1 : Introduction

As the outer covering of the human body, skin is the body's largest organ system. It plays an integral role in protecting the body from its surrounding environment and maintains homeostasis using a variety of specialized cell types contained within its structure. Anatomically, human skin is composed of three distinct regions: epidermis, dermis and hypodermis. A disruption of this organization, whether through injury or disease, initiates a process of wound healing and regeneration to restore proper skin function. A multitude of cellular and molecular components are involved in ensuring this mechanism is properly carried out, abnormalities of which often lead to chronic wounding and/or fibroproliferative disorders of the skin. An understanding of both ideal and irregular wound healing provides additional insight into the underlying biology of the skin and can be used to guide the future development of therapeutics for skin disorders.

Basic Structure of the Skin

The epidermis forms the exterior portion of the skin and has a four-layered, stratified structure containing metabolically-active squamous cells in the inner layers and keratinized, dead cells in the outer layers [1]. Keratinocytes, the main cells that make up the epidermis, are differentiated from stem cells located in the stratum basale, the innermost epidermal layer. As the keratinocytes migrate upwards through the middle layers of the epidermis – the stratum spinosum and stratum granulosum– they undergo a programmed cell death process known as cornification [2]. The resulting highly-keratinized dead cells accumulate in the outermost layer of the epidermis, the stratum corneum, and are responsible for providing the skin's primary barrier against the environment. Tight junctions are also present in these upper epidermal layers and help to prevent the loss of water from the body [3]. In thicker skin located on the palms on

the hands and soles of the feet, a thin fifth layer called the stratum lucidum is located between the stratum granulosum and stratum corneum [4]. In addition to keratinocytes, the epidermis also contains melanocytes, Langerhans cells and Merkel cells. Melanocytes give the skin its pigmentation, thus protecting the body from solar radiation, Langerhans cells work with the immune system to prevent infection, and Merkel cells act as mechanoreceptors, giving the skin its touch sensation [5].

The dermis lies beneath the epidermis and provides the skin with mechanical support. Dermal strength results from its abundance of extracellular matrix (ECM), which is produced by fibroblasts, the primary cell type of the dermis. 70% of the dermal matrix consists of collagen fibers, with the rest consisting mostly of elastin fibers and proteoglycans [4]. Elastin fibers impart elasticity to the skin, while proteoglycans provide compressive strength and facilitate the movement of fluids, growth factors and cytokines. The dermis can be further sub-divided into two main layers: the papillary dermis and the reticular dermis **(Figure 1.1)**. The papillary dermis is located adjacent to the epidermis and contains upward projections called papillae which interdigitate with downward projections from the epidermis known as rete ridges [6]. The papillary dermis is mostly comprised of thin, loosely-connected type I and III collagen fibers arranged in a basket-weave orientation [4]. The deeper reticular dermis, on the other hand, is denser with ECM and more acellular than the papillary dermis. This layer mainly consists of thick bundles of type I collagen that are arranged more parallel to the epidermis [4]. Immune cells, like macrophages, lymphocytes, and mast cells, are also present in the dermis and monitor the skin for signs of disease [5]. Extensive blood and lymphatic vasculature is also found in the dermis, in addition to nervous tissue and sensory receptors, which are responsible for providing the epidermis and dermis with nourishment, immune protection, and sensation [5].

Binding the epidermis to the dermis is a thin structure called the basement membrane. In addition to stabilizing the dermo-epidermal interface against shear stresses, it acts as a gatekeeper to the movement of cells and bioactive molecules between the two layers and functions as a reservoir of growth factors and cytokines [3]. Structurally, the basement membrane is comprised of independent networks of laminin (the lamina lucida) and collagen IV (the lamina densa) [3]. These two layers are interspersed throughout with nidogen and perlecan molecules, as well as integrins [3, 4]. Collagen VII fibrils present in the lamina densa also help to anchor the basement membrane to the underlying collagen I and III fibers of the papillary dermis [4].

The third major layer of skin is the hypodermis, which is the skin's thickest region and is located directly below the dermis. This subcutaneous layer is primarily composed of fat cells, known as adipocytes, as well as blood vessels and nervous tissue [5]. The number of adipocytes in the hypodermis varies with location in the body and the general state of nutrition [6]. In addition to storing energy, adipocytes in the hypodermis form continuous lobules which amass into a fat pad, thus contributing to thermoregulation by providing insulation [5, 6].

Skin also contains additional appendages which further assist its regulatory function. Hairs are keratinized outgrowths from the skin produced by the hair follicle [5]. Hair follicles produce hair through a cyclical regeneration process, which is initiated and regulated by stem cells present in the hair follicle bulge [5]. Arrector pili muscles in the skin, when contracted, cause hairs to stand up straight and retain heat from the environment, thus assisting the body's thermoregulation process [6]. Sweat glands are coiled, tubular glands which span the entire thickness of the skin [6]. They contribute to thermoregulation by secreting a watery fluid on the surface of the skin, which cools the body upon evaporation. Sebaceous glands are connected with

the hair follicle and secrete an oily substance known as sebum, which is responsible for lubricating and maintaining the hair and epidermis [5, 6].

Normal Wound Healing Process

Upon injury to the skin, wound healing is immediately initiated in order to begin the process of repair and reinstate the skin's protective barrier. While in some organisms this mechanism regenerates an identical copy of the injured tissue, the wound healing process in adult humans most often leads to fibrosis and scar formation. This process involves a complex interplay of cells and bioactive molecules that can be grouped into four overlapping phases: hemostasis, inflammation, proliferation and remodeling [7] **(Figure 1.2)**.

Hemostasis, the initial phase of wound healing, takes place in the first few hours following an injury. Successful hemostasis will produce a fibrin clot to stop any bleeding and will initiate the subsequent inflammatory mechanism. Formation of the fibrin clot begins when von Willebrand factor binds to the exposed tissue, resulting in platelet aggregation and the formation of a platelet plug [8]. This plug, in addition to the clotting factors released from injured tissue, activates the various signaling pathways responsible for producing thrombin, which subsequently converts fibrinogen into a fibrin matrix [7, 8]. Platelets in the fibrin clot release chemotactic factors that are responsible for recruiting leukocytes to the injury site, thus beginning the inflammatory immune response [7].

Inflammation begins with the arrival of neutrophils into the wound site, which are present for about 2-5 days unless an infection occurs [7]. Neutrophils release chemical mediators like tumor necrosis factor (TNF)-α, interleukin (IL)-1β, and IL-6, in order to further amplify the immune response [7]. Monocytes are then recruited to the wound site after about three days,

where they differentiate into macrophages and engulf pathogens and cellular debris [7, 8]. Macrophages also secrete a variety of growth factors and cytokines, such as IL-1, platelet-derived growth factor (PDGF), transforming growth factor (TGF)-β1, TGF-α, fibroblast growth factor (FGF), insulin-like growth factor (IGF)-1, and vascular endothelial growth factor (VEGF), which indicate that these cells play a crucial role in transitioning from the inflammation to the proliferation phase [7, 8].

Proliferation is characterized by re-epithelialization, neovascularization and formation of granulation tissue. Re-epithelialization occurs within hours after injury and aims to cover the wound surface. Cells at the wound edge release cytokines and growth factors, such as epidermal growth factor, keratinocyte growth factor (KGF), and TGF-β1, in order to stimulate fibroblasts and keratinocytes to migrate into the wound bed from the wound periphery [5]. In addition, stem cells from the hair follicle bulge can differentiate into epidermal progenitor cells, further contributing to the restoration of epidermis, though the fact that they are eventually eliminated from the newly-formed tissue suggests that they only play a role in initiating the re-epithelialization process [9, 10]. Furthermore, hair follicles and other skin appendages are not usually regenerated after injury, suggesting that the restorative potential of these stem cells is muted by the lack of an appropriate niche [5]. Neovascularization, also known as angiogenesis, is critical to maintaining the newly-formed tissue by providing nutrition and gas exchange. VEGF, PDGF, basic FGF, and thrombin that are present at the site of injury bind to receptors on the endothelial cells of existing blood vessels and initiate sprout formation [7]. These vascular sprouts migrate towards the wound bed, with the help of matrix metalloproteinases (MMPs) secreted by vascular endothelial cells at the leading edge as well as the urokinase-type plasminogen activators associated with these endothelial cells, and eventually differentiate into

new vasculature [7, 11]. Finally, granulation tissue begins to form in the wound bed around four days after injury [5]. Fibroblasts, stimulated by the presence of PDGF, TGF-β1, and FGF, begin to replace the provisional fibrin matrix in the wound bed with type III collagen and ECM molecules like fibronectin, glycosaminoglycans (GAGs), and proteoglycans [7, 8]. Because angiogenesis is still occurring when this granulation tissue forms, the developing tissue is highly vascularized and presents clinically with a characteristic red color [7].

The final phase of wound healing involves remodeling and reorganization of the granulation tissue into a mature scar. This stage typically begins about two to three weeks after injury and may last for several months [8]. Fibroblasts begin to differentiate into myofibroblasts, contractile cells which are characterized by a high expression of alpha-smooth muscle actin (α-SMA) [8]. MMPs secreted by fibroblasts, macrophages, and the other remaining cell types remodel the matrix into mature scar tissue [8]. Notably, collagen fibers found in this mature scar tissue are organized into bundles oriented parallel to the skin surface instead of the normal basket-weave orientation of uninjured skin. As collagen reorganization continues, crosslinks are formed between adjacent collagen bundles resulting in an increase in the scar's tensile strength [8]. However, at maximum, the scar only regains about 70% of its pre-injured mechanical strength [8].

Molecular and Cellular Basis of Hypertrophic Scar

As demonstrated, the normal wound healing process involves quite a delicate balance of cellular and molecular components. Though it appears that redundancies exist to prevent minor aberrations from completely disturbing this mechanism, larger disruptions typically lead to excessive scarring upon repair. Hypertrophic scar (HTS) is a fibroproliferative disorder of the

skin that often occurs after surgery, trauma, burn injury or excessive dermal inflammation. HTS presents clinically as a raised, red, itchy, and firm scar lesion that forms within the confines of an injury site [12] **(Figure 1.3)**. They usually appear about 4 to 8 weeks after initial injury, reach peak growth after 6 months, and then gradually remodel over time into normal scar [13]. HTS are often highly contractile in nature, limiting a patient's mobility and range of motion [14]. Moreover, these scars can be cosmetically deforming, thereby affecting a patient's quality of life on a psychological level as well [14].

The development of HTS is unique to humans, with females being at higher risk for developing HTS after burn injury than males [15, 16]. As a whole, HTS has an incidence varying from 32% to 77% and is generally more prevalent in lesions caused by burn injury, with a frequency as high as 91% post-burn [15-17]. Though HTS is more likely to occur in younger patients, it appears to manifest itself more rapidly in older individuals [16]. While fibrotic disorders like HTS occur in all races, more than 75% of non-white individuals develop HTS post-burn, indicating skin pigmentation as a significant risk factor [18]. A review of post-surgery HTS incidence in Chinese patients indicated almost 75% HTS occurrence and suggested a higher incidence rate post-burn, further supporting skin pigmentation as an important indicator of HTS risk [19]. Moreover, certain anatomical sites show a preference for developing HTS. HTS frequently occurs on areas of the body with high tension and frequent motion – such as the neck, wrists, elbows, knees, and digits – whereas anatomical sites like the palms, soles, genitalia, mucous membranes, eyelids, and cornea appear to be less affected [20]. Hypertrophic scar incidence also appears to be highly related to the depth of injury. A study by Dunkin, et al. found a critical depth for HTS by using a novel experimental jig to create a linear dermal scratch wound with varying depth – from no injury to full-thickness injury – within the same wound

lesion [21]. The threshold depth beyond which the resulting scar became hypertrophic in the patients was determined to be 0.56 ± 0.03 mm, or 33% of the lateral hip thickness [21]. Another similar study using this linear wound scratch model in burn patients also confirmed this threshold depth behavior for HTS incidence [22]. The speed at which wounds re-epithelialize after injury is known to dictate HTS formation, with burn wounds taking longer than two weeks to re-epithelialize showing an increased risk for HTS [23].

Histologically, HTS tissue contains whorled nodules of collagen in the dermis which gradually disappear during scar maturation as the collagen chains reorient themselves parallel to the skin surface [24, 25]. HTS tissue exhibits a reduced distance between adjacent collagen bundles as compared to normal skin tissue, indicating an increased density of collagen [26]. In addition, the ratios of different collagen types are altered in HTS. While normal skin and mature scar have about 80% type I collagen, 10-15% type III collagen and minimal amounts of type V collagen, HTS tissue contains about 33% type III collagen and up to 10% type V collagen [27]. Collagen III and V have both been shown to modify type I collagen fibril diameter, providing one explanation for the thinner collagen fibrils seen in HTS [28]. Also, an increased density of blood vessels exists within HTS lesions, with blood vessels organized perpendicular to the skin surface [29]. Similar to normal wound healing, skin appendages like sebaceous glands, hair follicles, and rete ridges are typically absent from HTS tissue.

Within their tissue structure, HTS lesions contain a high density of cells – particularly fibroblasts. The total cell number found in HTS tissue peaks during the immature phases of wound healing and then gradually declines as the tissue remodels into a mature scar [30]. HTS fibroblasts in immature scar lesions also exhibit an abnormal phenotype when compared to fibroblasts present in normal skin. These fibroblasts show a significantly decreased mRNA

expression of MMP-1, resulting in decreased collagenase protein levels as compared to site-matched normal fibroblasts from the same patient [31]. Moreover, HTS fibroblasts also express higher levels of TGF-β1, and its downstream effector connective tissue growth factor (CTGF), which concurrently work to stimulate excessive production of fibronectin, collagen types I and III, as well as the production of tissue inhibitors of matrix metalloproteinases (TIMPs) [31, 32]. Another byproduct of the elevated CTGF levels is the increase in number and proliferative capacity of myofibroblasts found in HTS tissue [24, 32]. These differentiated fibroblasts promote additional synthesis of ECM and contain vast amounts of α-SMA and microfilament bundles, contributing to the contractile behavior seen in HTS tissue clinically [24]. Furthermore, myofibroblasts in HTS have lower basal apoptotic rates and express higher levels of the anti-apoptotic marker B-cell-lymphoma-2 than the fibroblasts and myofibroblasts of normal skin, thereby promoting the hypercellularity of HTS tissue [33].

Furthermore, HTS fibroblasts show a prolonged expression of TGF-β receptors I and II (abbreviated TGFBRI and TGFBRII, respectively) on the cell surface, which provides TGF-β1 with a mechanism for autocrine positive feedback [34]. TGF-β1 binding to TGFBRI and TGFBRII initiates an important signal transduction pathway involving the intracellular SMAD regulatory proteins [13]. TGF-β1 initially binds to TGFBRII and then dimerizes with TGFBRI, resulting in the phosphorylation of one of five receptor-regulated-SMADs (R-SMADs). Phosphorylated R-SMADs have a high affinity for and bind to SMAD 4, forming a complex which enters the nucleus and functions as a controller of genetic expression. Of particular importance is R-SMAD 3, which has been shown to be the predominantly phosphorylated R-SMAD in HTS fibroblasts. Interestingly, a recent study involving siRNA inhibition of TGFBRI expression in HTS fibroblasts significantly suppressed cellular proliferation, decreased mRNA

levels of collagen I, collagen III, fibronectin and CTGF and reduced collagen I and fibronectin protein expression [35].

Prolonged duration and increased severity of inflammation in burn patients have also been shown to be reliable predictors of HTS formation [36]. $CD4^+$ helper T cells show an increased presence in HTS dermal tissue, as compared to normal skin [37]. $CD4^+$ T lymphocytes are capable of transitioning into either a Th1 or a Th2 sub-type, each having a unique cytokine expression profile: Th1 cells express anti-fibrotic cytokines (e.g. IL-2, IL-12 and interferon (IFN)-γ), while Th2 cells express pro-fibrotic cytokines (e.g. IL-4, IL-5, IL-10 and IL-13) [38, 39]. Moreover, Th1 cells induce fibroblast apoptosis and activate nitric oxide synthase in order to promote collagenase activity, further supporting their anti-fibrotic role, while Th2 cells induce ECM production and upregulation of procollagens I, III and V and TIMP-1, further supporting their pro-fibrotic role [38, 40]. A study of cytokines in the serum of burn patients with HTS has shown elevated levels of IL-4 and IL-10 with decreased levels of IL-12 and an absence of IFN-γ, implicating an elevated Th2 and suppressed Th1 presence in HTS [41]. Another study found an increased frequency of $CD4^+$/TGF-β^+ cells in the peripheral blood of burn patients with HTS, suggesting that Th2 cells may influence dermal fibroblasts towards pro-fibrotic differentiation and behavior [37].

Research suggests that bloodborne cells known as fibrocytes exist in higher levels in HTS tissue and contribute to HTS development [42]. These cells, which only make up about 0.1 to 0.5% of the peripheral blood mononuclear cells in normal circulation, account for about 10% of the cells infiltrating acute wounds and express collagens I and III, CD13, CD34, and the bone-marrow-derived surface marker CD45 [43]. Fibrocytes have been implicated as synthesizers of ECM and collagenase, as antigen-presenting cells responsible for priming naïve T cells, and as

stimulators of dermal fibroblasts towards pro-fibrotic behavior through paracrine signaling of cytokines like TGF-β1, TNF-α, IL-6, and IL-8 [36, 44]. They can also promote the differentiation of dermal fibroblasts into myofibroblasts, further supporting their pro-fibrotic role in HTS development [44].

Mast cells have also been implicated in HTS development, due to their increased presence in HTS tissue [45]. Since mast cells contribute to the immune response by releasing a number of mediators including histamine, which causes vasodilation and the itchiness associated with allergies, their presence in HTS tissue helps to explain the pruritic behavior of HTS lesions. Some proinflammatory mast cell functions in HTS are the result of prostanoid and leukotriene release [45]. Mast cells have also been implicated in promoting pro-fibrotic behavior in skin fibroblasts, in part via gap-junction mediated communication [46].

Chemokines, small 8-10 kDa proteins that induce local chemotaxis after injury, are also present in HTS, particularly those from the CXC and CC sub-families [47]. CXCR4 is a unique CXC chemokine receptor because it binds exclusively to stromal-cell-derived factor (SDF)-1. This chemokine pathway is important for recruiting bone-marrow-derived cells and stimulating angiogenesis [47]. As such, increased SDF-1 was found in HTS tissue and burn patient serum, and is thought to contribute to HTS pathogenesis by recruiting bone-marrow-derived cells to the injury site, where they then differentiate into fibrocytes and myofibroblasts [47]. An important CC chemokine involved in HTS is monocyte chemotactic protein (MCP)-1. MCP-1 is secreted by the cells involved in normal wound healing, in order to recruit monocytes and T cells to the injury site [48]. MCP-1 is found to be upregulated in HTS fibroblasts, where it stimulates collagen overproduction and increases endogenous TGF-β expression via Th2 polarization [48].

Non-collagen ECM Modifications during HTS

As a consequence of changes in the molecular expression of HTS fibroblasts, the non-collagenous ECM environment also becomes altered. Structural changes in addition to the collagen modifications noted above are present, including a significant reduction of elastin and fibrillin-1 in HTS tissue [49]. On a molecular level, a two-fold increase in the total GAG content has been found in scar tissue [50]. In particular, this GAG increase is attributed to an elevated expression of the sulfated GAGs – particularly dermatan-sulfate, chondroitin-sulfate, and heparin-sulfate – as opposed to the non-sulfated GAG hyaluronic acid (HA) [50]. Moreover, there appears to be an increase in GAG chain size, especially dermatan-sulfate chains, in addition to the increased quantity in HTS tissue [51]. Taken together, this data suggests that a modified level of proteoglycans exist in HTS tissue. Though quantitatively minor as compared to collagen, increased proteoglycan content helps to explain the characteristic firmness of HTS lesions because proteoglycans facilitate ECM swelling by attracting water and fluids to the scar lesion.

One proteoglycan of note which is modified in HTS is versican, a large chondroitin-sulfate proteoglycan. Belonging to the lectican protein family, versican is named for its multiple protein-binding motifs which give it functional versatility [52]. Structurally, versican has a 400kDa core protein consisting of four major domains: two terminal globular domains (G1 and G3) and two central GAG-attachment regions (GAG-α and GAG-β) [52]. The G1 domain serves as a functional HA-binding region, allowing for the formation and stabilization of large, highly-hydrated collagen-HA-versican networks [52]. As a result, versican has a near-cartilage-like phenotype similar to aggrecan and is normally found in many fibrocartilage tissues of the body. These networks are important for maintaining a tissue's viscoelasticity, for sensing the local mechanical microenvironment in the tissue in order to regulate tissue metabolism, and for

influencing cellular behavior through G3-mediated interactions with cell-surface receptors [52]. While nearly absent in normal skin tissue, versican is present in elevated levels throughout the connective tissue of HTS [53]. Versican disrupts the proper formation of collagen bundles by positioning itself between individual fibrils and expanding the ECM network, allowing for increased cellular migration during wound healing [52, 53]. In HTS, elevated versican levels are thought to give rise to the increased scar volume seen clinically [53]. Moreover, overexpression of versican may stimulate the proliferation of fibroblasts, due to its role in regulating growth control and differentiation [54].

Proteoglycans from the small leucine-rich proteoglycan (SLRP) family are also of particular importance to HTS. SLRPs are named for the presence of multiple leucine-rich repeat motifs on their core proteins. Along with cartilage and the cornea, skin tissue has one of the highest localizations of this proteoglycan family in the body [52]. SLRPs are responsible for a variety of roles in the skin – namely the development, maintenance, organization, and remodeling of the ECM [52]. Moreover, SLRPs can modulate the activity of various growth factors and play a role in influencing cellular behavior and growth through autocrine and paracrine signaling [54]. Many of the SLRPs interact directly with all three isoforms of TGF-β, indicating their importance in the process of fibrosis [55].

Decorin (DCN) is arguably the most important SLRP involved in HTS. DCN consists of a 36kDa core protein with 12 leucine-rich repeat regions and one chondroitin-sulfate or dermatan-sulfate GAG chain bound near its N-terminus. DCN's core protein folds into a horseshoe-shaped configuration which consists of two individual collagen-binding sites on the concave face that are located on leucine-rich repeat 10 and between leucine-rich repeats 3 and 4 [56]. Double-staining strategies and immunoelectron microscopy have identified that DCN binds

prominently to the *d* and *e* bands on type I collagen, both of which contain a similar 11-amino-acid motif that is not present elsewhere in collagen types I-III [56]. Though it was initially postulated that DCN binds to only one collagen molecule using the concave face of its core protein, recent molecular modeling suggests that individual DCN molecules can interact with four to six collagen molecules at one time [56].

DCN is involved in delaying the lateral assembly of collagen fibrils during fibrillogenesis, a key role that was elucidated through the use of DCN knockout mice [57]. Transmission electron microscopy from DCN knockout mice showed a highly-varied and irregular fibril diameter as compared to the wild type, which was thought to be the result of uncontrolled lateral fusion of thick and thin fibrils during fibrillogenesis [57] **(Figure 1.4)**. In addition, the interfibrillar spacing between fibrils had a distribution that was looser and more disorganized [57]. Moreover, DCN knockout mice had unusually lax skin displaying a reduced tensile strength and ductility [57]. DCN also plays an important role as an antagonist of TGF-β1 activity [58]. DCN has a unique TGF-β1 binding site located on its protein core, which allows for saturation with TGF-β1 even when bound to type I collagen [59]. As such, DCN is not thought to antagonize TGF-β1 through formation of a DCN/TGF-β complex, but rather by sequestering it in the ECM and preventing it from binding to its receptors on the cell surface [60]. DCN also contains a specific binding site for CTGF on its core protein, further supporting its role as an antagonist of TGF-β1 activity [61]. Additionally, DCN binds to and modulates the activities of the EGF receptor, the IGF-1 receptor, and the hepatocyte growth factor receptor Met, indicating a prominent role in cell signaling [62-64].

Interestingly, HTS tissue was found to have a 75% reduction in DCN content as compared to normal skin tissue [51]. DCN levels in HTS tissue were studied over time in burn

patients and were found to be reduced for the first year after injury, then elevated for the next two years, and finally found in normal levels from year three onward [65]. This delayed appearance is abnormal when compared to normal wound healing, where abundant DCN levels are found within a couple of months after wounding, suggesting that this behavior plays a key role in HTS development [65]. Moreover, a recent study indicates that serum levels of DCN in burn patients may be predictive of HTS, further implicating its role in HTS development [66].

Two other SLRPs involved in HTS are biglycan and fibromodulin. Biglycan is structurally similar to DCN, consisting of a 38kDa core protein with 12 leucine-rich repeats and two chondroitin-sulfate/dermatan-sulfate chains near its N-terminus [52]. Recent studies have implicated biglycan as a danger-associated molecular pattern signaling molecule that is involved in the innate immune system [67]. After injury, biglycan is cleaved from the ECM and interacts with Toll-like receptor (TLR)-2 and -4 on macrophages, triggering an inflammatory response [67]. Moreover, macrophages can synthesize their own biglycan, resulting in autocrine and paracrine stimulation of inflammation [67]. Since biglycan is localized near the surfaces of cells and can bind TGF-β1 more strongly than DCN, it may also play a role in boosting the action of TGF-β1 in HTS [51, 55]. Notably, biglycan is found to be 6-fold higher in HTS tissue as compared to normal skin tissue [51]. On the other hand, fibromodulin is reduced in post-burn HTS [68]. Though similar to DCN and biglycan, fibromodulin has a 42kDa core protein with four N-linked oligosaccharide sites within its central leucine-rich region that are substituted with keratan-sulfate [52]. Fibromodulin also contains sulfated tyrosine residues on its N-terminal end which can interact with heparin-binding proteins [52]. Like DCN, fibromodulin is involved in delaying fibrillogenesis of collagen types I and II [52]. However, it is not as ubiquitous as

decorin and biglycan – fibromodulin is typically localized in cartilage, tendon, and sclera, though it is found in the epidermis and basement membrane of the skin [52, 55].

Current Prevention and Treatment Modalities for HTS after Burn Injury

The first line of defense against HTS is prevention of scarring. Since the re-epithelialization rate, the level of inflammation and depth of wound are key contributors to HTS, preventative steps directed towards improving these measures should be immediately applied. Preventative measures include debridement of dead tissue to avert infection, application of wound dressings often in conjunction with moisturizing creams or moisture-retaining silicone gel to avoid dehydration, and splinting or stretching of the wound and additional physical treatments like massaging and physiotherapy to hinder contraction [69]. Some clinicians also make use of scanning laser doppler or thermography technologies in order to establish wound depth and to determine which wounds need invasive treatments, like skin graft surgery, earlier in the treatment regimen in order to counter HTS development [36].

Upon wound closure, non-invasive treatment modalities like pressure garments and silicone gel sheeting are applied in order to reduce HTS. Pressure garments are utilized while the scar is still active, usually for at least 23 hours a day, and continue to be used until the scar matures [27]. These garments, which apply compressions exceeding capillary pressure – usually around 24-30 mmHg – are thought to enhance ECM remodeling and reduce contracture by stimulating an increased expression of MMP-9 and increasing myofibroblast apoptosis [27]. Despite the improved clinical features and reduced scar itching and pain, patient compliance is often low due to extreme discomfort and high cost [69]. Silicone-based products have been shown to improve scar elasticity, pigmentation, and vascularity and are recommended as the

"gold standard" for HTS prevention and treatment in the most recent guidelines [69]. The major mechanism of action is widely accepted to be the occlusion and hydration of the stratum corneum, thus preventing transepidermal water loss from the re-epithelialized wound tissues [69]. However, since HTS tissue is hyper-hydrated, increasing hydration might make the tissue more susceptible to scar formation since it would thicken the matrix and render it stiffer. Therefore, an alternative mechanism of action has been proposed, since the elevated scar surface temperature after application of silicone gel sheeting substantially increases MMP activity in the wound, thus enhancing its tissue remodeling capability [70].

A supplementary, second-line therapy regimen of injection-based treatment is recommended for patients with continuing hypertrophy after six months of the above first-line therapies [69]. Intralesional injections of triamcinolone acetonide, a synthetic corticosteroid, are the most commonly used, with a recommended dosage of 40 mg diluted to less than 20mg/ml every two to four weeks [69]. These injections are thought to work by suppressing inflammation, increasing collagenase production and inhibiting growth factors like TGF-β1 and IGF-1 [27]. Due to side effects like subcutaneous tissue atrophy and hypopigmentation, these injections should be confined to the papillary dermis [69]. 5-fluorouracil may also be injected into the lesion, either alone or in combination with corticosteroids. This pyramidine analog has an anti-metabolite activity and works by targeting the rapidly proliferating and highly active fibroblasts in HTS, resulting in softer, flatter scars with a decreased lesion size [27].

New information about the inflammatory mechanisms involved in HTS has led to the development of injection-based therapies involving IFNs and chemokines. IFNs are anti-fibrotic cytokines which are involved in reducing collagen and GAG expression by fibroblasts and normalizing their collagenase activity [27]. Two IFNs, IFN-α2b and IFN-γ, are particularly

important for HTS as they both show antagonistic behavior towards TGF-β1 by reducing its mRNA and protein expression in HTS fibroblasts [71]. Treatment of dermal fibroblasts with these IFNs resulted in a marked decrease in dermal fibroblast proliferation and type I collagen mRNA and protein secretion, with IFN-α2b also improving collagenase activity [72]. In addition, IFN-α2b treatment *in vitro* showed an increase in fibroblast and myofibroblast apoptosis, thus reducing their total numbers in culture [30]. As such, clinical trials involving HTS patients who were subcutaneously injected with IFN-α2b showed a normalization of TGF-β levels with no recurrence after stopping treatment as well as improved scar color and overall assessment [73]. Notably, intralesional injections showed minimal response, suggesting a systemic delivery of IFN-α2b is needed to resolve HTS [36]. Chemokine receptor antagonist CTCE-9908, which binds to CXCR4 and blocks the SDF-1/CXCR4 pathway, has also shown promise as a new HTS therapy [74]. Subcutaneous injections of the antagonist into a nude mouse HTS model showed significantly improved scar characteristics – decreased thickness, contraction, cellularity and vascularity – with a reduction in fibrocyte precursor migration, downregulation of collagen I and TGF-β1 and increased levels of decorin [74].

Surgical scar revision is recommended for patients with HTS after 12 months of treatment, although those with functional impairments or severe injury may be considered for surgical treatment earlier [69]. In burn treatment, for example, an autologous skin graft is often used before the aforementioned preventative and injection-based treatments in order to close the wound and reestablish the skin's barrier function. Most commonly, this involves harvesting skin from an unaffected site on the body using a dermatome. Unfortunately, this leads to donor-site morbidity, as dermatome slices contain the epidermis and part of the dermis thus simulating a second-degree burn [75]. In patients with extensive burn wounds, there may not be enough

healthy skin for an autologous graft, in which case allografts can be used from human cadavers [75]. However, a host of issues exist with allografts including risk of viral transmission and graft rejection by the patient's immune system [75]. Once HTS has formed, a Z-plasty scar revision surgery can be carried out in order to relieve tension and contracture in the scar, thus promoting collagen remodeling [36]. Additionally, the scar tissue can be completely excised as HTS has a low post-excisional recurrence rate, though this step may not be necessary in some patients due to the ability of HTS to remodel into mature scar over time [13].

Recently, laser therapy has been used alone or in conjunction with surgery to further promote HTS revision. The established standard used to improve the characteristics of immature HTS is currently a flash-lamp pulsed dye laser emitting 585 nm or 595 nm wavelengths at low to medium fluence (about 4-8 J/cm^2), a 7 or 10 mm spot size, and a short pulse duration of approximately 0.45 to 1.50 milliseconds [76]. These treatments, which are repeated at 1- to 2-month intervals, work by selective photothermolysis of the small blood vessels in HTS tissue – thereby promoting an ischemic environment – and have been effective at reducing erythema and pruritus but not scar thickness or contour [76]. Lately, a shift towards fractional CO_2 laser therapy for HTS treatment has been noted [76]. This laser emits wavelengths of 10,600 nm in order to target intracellular water, thus resulting in non-specific vaporization of scar tissue [76]. Fractional CO_2 lasers create ablative columns in the HTS tissue, known as microthermal treatment zones, which are 0.08-4.0 mm deep and have diameters of 60-250 μm surrounded by a thermal coagulation layer around 50-150 μm thick [76]. This treatment modality shows improvements in HTS tissue pliability, texture, erythema, thickness, and pigmentation [76-78]. On a biological level, fractional CO_2 therapy is thought to work by normalizing the collagen fibrillogenesis-collagenolysis cycle to improve dermal architecture, releasing mechanical tension

in the scar tissue to alleviate contracture, and modulating the growth factor and cytokine expression of dermal fibroblasts – notably inhibiting TGF-β1 secretion [76, 77, 79].

Tissue-engineered skin products have also improved patient outcomes in recent years, with increased survival rates seen in patients with greater than 60% total body surface area (TBSA) burned who were treated with skin substitutes and excellent/good outcomes reported for neck contracture in 27 out of 28 burn patients treated with a dermal substitute/skin graft combination [80, 81]. Tissue-engineered skin substitutes came into being following the advent of serial subculture of keratinocytes in 1975 [82]. Not long after, keratinocytes from burn patients were cultured into epithelial sheets, known as cultured epithelial autografts (CEAs), in order to assist the treatment of extensive third-degree burns [83]. However, CEAs have suffered from fragility (making them difficult for the physician to handle and graft), high cost, lengthy production times, and a varied "take" – the adherence and integration of a graft into the recipient's skin [75]. Nevertheless, many commercial CEA products have come to market - Epicel™ , MySkin™, and EpiSkin™ – some of which attempt to improve wound engraftment using a dermal substitute like silicone, hydrogel, fibrin, or decellularized collagen scaffolds [84-86]. Recently, sprayed epithelial products like CellSpray™ and ReCell™ have been developed [86]. These keratinocyte suspensions reduce the culture time needed before clinical use and increase cell proliferation, minimize enzymatic degradation of cell-surface proteins, and produce a more robust epithelial layer [86].

In addition to epidermal replacements, numerous dermal substitutes have been created in order to replicate the dermis in full-thickness wounds and promote re-epithelialization, revascularization, and restoration of an appropriate growth factor and cytokine profile [87]. Many of these products are simply decellularized collagen matrix from either human

(AlloDerm™, SureDerm™, KaroDerm™), porcine (Permacol™, EZDerm™, OASIS Wound Matrix™) or bovine (Integra DRT™, MatriDerm™, PriMatrix™) sources [84, 86]. Since these matrices are acellular, they must recruit their own cells and growth factors from the underlying wound bed. Other dermal replacements, like Dermagraft™ and TransCyte™, are embedded with allogeneic cells that express growth factors, cytokines, and inflammatory mediators into the wound bed upon engraftment to stimulate a natural wound healing response [87]. Although immune rejection is an inherent risk to the efficacy of these products, clinically it seems to be a negligible issue [87].

Advances in tissue engineering have led to the development of commercially-available bi-layered skin substitutes that are composed of both keratinocytes and fibroblasts, such as Apligraf™ and Orcel™ [84]. The co-culture of keratinocytes with fibroblasts in these skin substitutes promotes the formation of a basement membrane between the epidermal and dermal layers of the product, encouraging increased epidermal attachment [85]. While they may seem ideal as a replacement for split-thickness skin grafts, these products are generally used on a temporary basis as biological wound dressings due to their limited lifespan and high cost [84, 85]. Other bi-layered skin substitutes, like PermaDerm™, PolyActive™ , and the TissueTech Autograft System™ have improved upon the above products by incorporating autologous keratinocytes and fibroblasts from the patient into their scaffolds, although their efficacy, cost and ease of use are still not ideal [84]. Notably, PolyActive™ and the TissueTech Autograft System™ use non-collagen matrix materials, with PolyActive™ using a synthetic polyethylene oxide terephthalate/polybutylene terephthalate block co-polymer and the TissueTech Autograft System™ incorporating its cells into a HA ester matrix [84].

Despite the utility of tissue-engineered skin products, especially after thermal injury, there are still a few drawbacks that prevent these products from completely replacing allografts and autografts in burn therapy. A recent multi-center study of skin substitute effectiveness in burn patients showed only an average take of 49%, while another study reported almost negligible take at 2 weeks, suggesting that the harsh burn wound environment may present a significant challenge to engraftment of skin substitutes [88, 89]. Decreased take may also be due to the inadequate revascularization rates plaguing current skin substitutes [84]. Other problems include varied consistency, loss of sensation because of insufficient innervation, and the formation of scar at the graft margins [84, 85]. Furthermore, hypopigmentation due to the absence of melanocytes and the lack of various skin appendages, like sweat glands and hair follicles, in these products are not only aesthetically disfiguring but also functionally limiting [84, 85] **(Figure 1.5)**. Current research is attempting to overcome some of these limitations and improve the efficacy of tissue-engineered skin.

Development of Scaffolds for Tissue-engineered Skin

The collagen-glycosaminoglycan (CGAG) matrix was first developed by Yannas and Burke in 1980 and has since become the gold-standard scaffold material used for skin tissue engineering [90]. Slight modifications have been made over time to this formula in order to improve or modulate certain components of the end product, but in general the procedure remains the same [91]. Briefly, type I collagen from bovine tendon or hide is mixed with acetic acid at 4^{o}C using a high speed blender. This mixture is then blended at 4^{o}C with chondroitin-6-sulfate from shark cartilage in order to form a CGAG suspension. The suspension is then degassed under vacuum to remove any air, poured into a casting tray and then freeze-dried in order to remove water, thus leaving behind a highly porous matrix. The matrix can then be

crosslinked in order to improve its mechanical properties and may subsequently be seeded with cells in certain applications.

One of the most common adjustments made to this procedure is changing the parameters used for freeze-casting and lyophilization in order to fine-tune the matrix pore size for the application at hand. Matrix pore size has been well documented in the literature to modify cellular attachment, proliferation and expression behavior and ideal pore size varies from cell-type-to-cell-type [92-94]. Furthermore, the cells which are eventually seeded onto the matrices also tend to modulate the pore size of their matrix [95]. A pore size ranging from 20-120μm has been determined to be the most ideal for creating tissue-engineered skin [96]. Recent studies have determined that the cooling rate used during the freeze-cast process determines the heterogeneity of the CGAG matrix, with a cooling rate of 0.9ºC/min yielding a matrix with the most equiaxial and least-varied pore size [97]. Moreover, the final freezing temperature also influences pore size, with colder freezing temperatures leading to reduced pore sizes up to a plateau around -50ºC [98]. By including annealing steps during the freeze-dry process, in which the substrate is increased in temperature after freezing in order to increase ice crystal growth rate, pore sizes ranging from 85 to 325 μm were able to be created in the CGAG substrate, thus proving its versatility for a variety of applications [98]. Alternate methods for cooling matrices prior to freeze-drying also exist, like submersion in an ethanol bath or, more recently, controlled-rate freezing using a gaseous-phase liquid nitrogen freezing chamber, and can enable even smaller pore sizes down to about 25 μm [99].

Another frequently adjusted procedure is the crosslinking step following matrix creation. As a natural material, collagen has limitations to its mechanical integrity. These mechanical properties can be increased by varying the degree of crosslinking – the number of covalent bonds

between the amino acids on adjacent collagen molecules – thus preventing collagen fibers from sliding past one another under stress [100]. Dehydrothermal treatment (DHT) is a commonly used crosslinking method for CGAG matrices and involves subjecting the substrate to a temperature above 90^{o}C under vacuum pressure in order to promote condensation reactions between neighboring collagen molecules [100]. Increased DHT temperature and duration were reported to increase the compressive properties of the CGAG matrix up to two-fold and the tensile strength up to 3.8-fold, while only increased DHT temperature was found to affect crosslink density [100]. Notably, the high temperature and long duration of DHT resulted in collagen denaturation, which was positively correlated with tensile strength [100]. While denaturation seems like it would be detrimental to CGAG function, it is actually shown to improve fibroblast permeability and matrix affinity [101]. Another method of physical crosslinking is via ultraviolet (UV) irradiation [102]. Crosslinks in this method are formed between free radicals generated on the aromatic amino acid side chains of the collagen molecule [102]. Overall, UV irradiation seems to exhibit a similar outcome to DHT, although it results in a less denatured end-product [102].

Chemical crosslinking is also a fairly popular method to increase the mechanical properties of CGAG matrices. The two most commonly used chemical crosslinking agents are gluteraldehyde (GA) and 1-ethyl-3-(3-dimethyl aminopropyl) carbodiimide hydrochloride (EDC) [103]. GA crosslinks collagen molecules by forming a chemical “bridge” between adjacent molecules, whereas EDC directly links together the collagen fibers [103]. While these modalities both result in improved mechanical properties, EDC is preferred over GA as EDC shows stronger resistance to enzymatic degradation and GA exhibits a gradual cytotoxic effect [103]. Finally, biological crosslinking via transglutaminase (TG) has recently attracted great interest

[103]. Due to its biological characteristic, it is an inherently safer process. Additionally, TG has been shown to modulate VEGF and fibronectin levels, as well as recruit endothelial cells, suggesting that it may result in better revascularization [103].

The rise of synthetic materials for dermal engineering has also led to alternative methods for making 3D matrices, notably electrospinning. Electrospinning uses a voltage gradient in order to deposit a suspension of matrix solution onto a collection vehicle in a controlled manner, allowing for a highly-tunable fiber diameter and orientation (random or parallel). Coaxial electrospinning allows for the production of synthetic fibers with a continuous shell coating of bioactive polymer, thus improving cellular adhesion and proliferation, while retaining the ability to tune scaffold mechanics [104]. Furthermore, electrospinning also offers an ideal way to incorporate elastin fibers into tissue-engineered skin substitutes, which may allow for improved pliability of regenerated skin and provides a tool for combating the increased skin contracture seen in recovering burn patients [105]. Recently developed electrospun scaffolds containing 80% human tropoelastin and 20% type I collagen supported fibroblast infiltration, collagen deposition, and angiogenesis and behaved similarly to Integra^{TM} in a subcutaneous implantation model [105]. Moreover, electrospun scaffolds provide another means for delivering drugs and growth factors into healing wound sites. A recent study using acid-responsive, ibuprofen-loaded polylactic acid scaffolds in an *in vivo* rat wound model attenuated inflammation and reportedly accelerated wound healing [106]. The ratios of collagen I:collagen III and TGF-β1:TGF-β3 were reduced, while the MMP:TIMP ratio was increased, in addition to a regulated collagen, α-SMA, and basic FGF expression profile [106]. Another electrospun scaffold containing collagen, HA, and gelatin with pro-angiogenic growth factors loaded to allow for staged-release – with basic FGF and endothelial growth factor released first, followed later by VEGF and PDGF – showed

accelerated wound closure and enhanced maturation of newly-formed wound vasculature, providing a potential solution to the reduced angiogenesis seen in currently available tissue-engineered skin substitutes [107].

Tissue-engineered Skin as an *in vitro* Dermal Model

Though the field of tissue-engineering is colloquially thought of as a means for providing new medical therapies, the same principles used for generating tissue-engineered constructs can help generate new *in vitro* models for cell culture. As one of the oldest tissue-engineered organs, tissue-engineered skin has been used as an *in vitro* model for studying a variety of disorders, including melanoma, psoriasis, bacterial infection, and fibrosis [108-111]. Due to European Union regulations encouraging reducing animal model usage and banning cosmetic testing on animals, tissue-engineered skin models are also being used as tool to optimize and develop new pharmaceutical formulations [112].

In addition, tissue-engineered skin models have been used to better understand the epithelial-mesenchymal interactions involved in normal and diseased skin tissue. One of the first discoveries that organotypic culture models helped to uncover was the paracrine signaling cross-talk between fibroblasts and keratinocytes. A 1993 study by Smola, et al. found that the presence of keratinocytes stimulated the expression of KGF, IL-6, and granulocyte-macrophage colony-stimulating factor in fibroblasts, an effect which contributed to the proper proliferation behavior of keratinocytes in culture and which could not be replicated using conditioned medium or by adding growth factors to the medium [113]. Follow up studies identified IL-1 as the stimulatory factor being secreted by keratinocytes, demonstrating the presence of a double-paracrine signaling loop between keratinocytes and fibroblasts [114]. Indeed, neutralization of IL-1α, IL-

1β, and the IL-1 receptor significantly reduced keratinocyte proliferation by blocking the production of KGF by fibroblasts [114].

Another area of epidermal-mesenchymal interaction research involves trying to understand the influence of the dermis on epidermal differentiation during and after development. Many studies involving cross-recombined epithelial specimens from different animal species were carried out in the 1970s and 1980s in order to elucidate whether the adult epithelial phenotype is intrinsic to the epithelium or can be modified by the sub-epithelial tissue [115]. Tissue-engineered skin models are being used in order to explore these behaviors in humans, indicating that the epithelial phenotype and keratin expression of epithelial cells can be modified by the underlying fibroblasts of the dermis [116, 117].

In vitro tissue-engineered skin models have also been used to explore the heterogeneous behavior of papillary and reticular fibroblasts. In addition to the differences in collagen architecture noted above, these sub-populations of fibroblasts display differences in their protein expression. Fibroblasts from the reticular dermis produce more collagen and less collagenase, less decorin and more versican, and more TGF-β1 and α-SMA as compared to papillary fibroblasts, strongly suggesting that they contribute to the development of HTS [118]. Reticular fibroblasts grown in 3D collagen matrices resulted in the formation of stiffer, more contracted matrices than those made using papillary fibroblasts [119]. When grown together with keratinocytes in an organotypic skin model, constructs created using reticular fibroblasts resulted in the formation of an epidermis with poorer barrier function and a more fragile basement membrane than those made using papillary fibroblasts [120, 121]. Interestingly, the presence of normal keratinocytes beneficially influenced the expression profile of reticular fibroblasts, resulting in reductions to TGF-β1 and CTGF and increases in MMP-1 [122]. Normal

keratinocytes co-cultured with reticular fibroblasts generated matrices that were less contracted, had lower numbers of myofibroblasts, and lower expression of matrix crosslinking factors [95].

Although the above evidence suggests a strictly beneficial impact of keratinocytes on fibroblasts, keratinocytes from fibrotic tissue may act to exacerbate dermal fibrosis. Using an *in vitro* tissue-engineered skin model, Bellemare, et al. showed that keratinocytes harvested from HTS tissue sent more pro-fibrotic signals to dermal fibroblasts than normal skin keratinocytes [123]. HTS keratinocytes induced the formation of a thicker dermis than normal skin keratinocytes, which may have been the result of elevated collagen secretion and decreased MMP-1 synthesis [123]. Moreover, dermal proliferation was enhanced, without an according reduction in apoptosis, when constructs were created using HTS keratinocytes instead of those from normal skin [123]. The authors suggested that these effects may stem from the modulated growth factor and cytokine profile of HTS keratinocytes, including over-secretion of TGF-β1, PDGF, FGF, and TNF-α [123]. Additionally, IL-1α has been found to be decreased in HTS keratinocytes, perhaps contributing to abnormal keratinocyte proliferation and differentiation behavior while simultaneously impacting ECM turnover and dermal cell number [123, 124]. Increased TIMP-1 levels have also been found in HTS keratinocytes, further implicating their role in perpetuating dermal fibrosis [125].

Adenovirus-mediated Gene Therapy

Despite the utility of the above HTS treatments, scarring after burn injury continues to be a significant cause of patient morbidity and presents a major clinical challenge for medical providers. Burn patients require prolonged rehabilitation and treatment regimens, with patients who were employed prior to their burn injury enduring a mean time off from work of about 10

weeks – a value which increases further as the TBSA burned goes up [126]. Rehabilitation time is also highly dependent on the site of injury, with patients suffering from hand burns needing a mean time of 19 weeks to return to work [126]. Current therapies have reduced this value from the average 12.7 weeks off work reported in 1987, but there is clearly still room for improvement with respect to HTS treatment [127]. Recent advances in adenoviral gene therapy appear to provide promising new solutions to the HTS problem.

To date, more than 50 serotypes of adenovirus have been discovered, which have been sub-classified into seven species (A-G) on the basis of DNA homology, their ability to agglutinate red blood cells, and their oncogenicity in rodents [128]. However, most studies on adenoviruses have been carried out using serotypes 2 and 5 from species group C [129]. Human adenoviruses are typically associated with diseases of the respiratory system, eyes, and gastrointestinal tract, though they can also cause disease in the urinary tract, liver, and tonsils/adenoids [128]. Structurally, the adenovirus virion consists of a 90nm icosahedral-shaped, non-enveloped protein shell surrounding a double-stranded DNA strand roughly 36 kb in length [128]. The protein shell, or capsid, is mainly made up of three main proteins: hexon proteins, penton base proteins, and fiber proteins. Hexon proteins make up the facets of the viral capsid, with minor components like protein IIIa, protein VI, protein VIII, and protein IX working like a glue to keep them together [129]. Each of the 12 capsid vertices consists of a penton base, which serves as an anchor for the protruding fiber proteins.

Species C adenoviruses typically use the coxsackievirus and adenovirus receptor (CAR) in order to enter host cells. These transmembrane proteins have an extracellular domain with a high affinity for the knob region of adenoviral fiber proteins. Once bound to a CAR on the host cell, an RGD motif on the adenoviral penton base protein binds to an α_v integrin, triggering an

internalization signaling cascade which results in clathrin-mediated endocytosis of the virus [130]. Once inside the cell, protein VI is released from the viral capsid, destroying the endosomal membrane and resulting in the release of the virus into the cytoplasm [130]. The virion then associates with dynein motor proteins and is trafficked to the nuclear pore complex via microtubules [130]. Proteins on the nuclear pore complex stimulate the disassembly of the viral capsid, allowing the viral genome to be imported into the nucleus [130].

Once the viral genome has entered the nucleus, the E1 region is transcribed, producing proteins that function to activate the other adenoviral early transcription units (E2, E3, and E4) [129]. The E2 region encodes proteins needed for replicating the viral genome [129]. The E3 region encodes proteins involved in preventing the activation of the immune system against the virus-infected cell as well as preventing the induction of apoptosis [129]. The E4 regions encodes proteins that play a role in cell cycle control [129]. Once the products of the early genes have been produced and the viral DNA has been replicated, late phase genes are expressed and work to package the replicated DNA into new viral particles [129]. These newly-assembled viruses are then released from the host cell via virally-induced lysis.

Adenoviral vectors have many features which make them a popular choice for gene therapy: they are relatively easy to grow to a high concentration (known as a titer), they allow for the insertion of a large transgene of interest, they can transduce both dividing and non-dividing cells, and the viral genome does not incorporate into the genome of the host cell [129]. As such, adenoviruses are the most commonly used viral vector in gene therapy clinical trials, with over 500 clinical trials initiated as of February 2016 (~22% of all gene therapy clinical trials) [131]. The vast majority of these trials are using adenoviral vectors as a cancer therapy, though many

are also used to treat cardiovascular diseases like angina, ischemia, and artery diseases [128]. Adenoviral vectors are also being tested clinically for used as vaccines or to treat infection [128].

In order to use adenoviruses as a gene therapy vector, modifications are made to the adenoviral genome structure in order to make them safe for use. Because the E1 region is necessary for adenoviral replication, replication-incompetent adenoviruses are created by replacing the E1 region with the transgene of interest. This simultaneously renders the adenoviral non-oncogenic, as the E1 region also encodes the oncogenic transforming functions of the adenovirus [129]. This also allows scientists to have more control over the life cycle of the adenovirus, as adenoviral vectors must be propagated in an E1-containing cell line such as the human embryonic kidney (HEK) 293 cell line. Occasionally, recombination during viral propagation can lead to the formation of replication-competent progeny, so viral stocks must be assayed prior to use [129]. Cell lines like PER.C6 and 911 have been created in order to minimize this problem [129]. Another common modification to the adenoviral genome is the removal of the E3 region, which allows up to 8.2kb for transgene insertion when combined with the E1 deletion [129]. However, this eliminates the ability of the virus to diminish the host's immune response, which is more of a problem for *in vivo* studies as opposed to *in vitro* studies [129]. Moreover, E1-/E3-deleted adenoviral vectors administered systemically tend to be sequestered to the liver because of non-targeted binding to host blood coagulation factors, leading to a poor clinical effect [128]. As such, a concerted effort is being made to eliminate these issues using "gutless" second-generation adenoviral vectors lacking all viral structural genes, coating viral vectors with polyethylene glycol, and using adenoviral serotypes that do not promote an immune response [128].

Interestingly, adenoviral delivery of DCN is being explored as a therapeutic for a variety of pathological conditions. Adenoviral-DCN delivered systemically post-myocardial infarction in mice lead to reduced fibrosis in infarcted and non-infarcted areas of the ventricular wall [132]. Additionally, adenoviral-DCN mediated the effects of pulmonary fibrosis in both TGF-β1-treated and bleomycin-treated mouse models, resulting in normalized lung histology and reductions of hydroxyproline and TGF-β1 protein levels in bronchoalveolar lavage samples [133, 134]. Adenoviral-DCN also had anti-renal fibrosis and anti-albuminuria effects in a streptozocin-induced model of diabetic nephropathy via reductions in TGF-β1 and phosphorylated SMAD3 levels [135]. Furthermore, the matrix remodeling effects after adenoviral-DCN delivery are being taken advantage of in order to improve oncolytic therapy, allowing for a more complete dispersion of cancer therapeutics in tumor tissue [136].

Research Problem and Hypothesis

Recently in our lab, adenoviral-DCN treatment has been explored as a gene therapy for HTS. In a preliminary study by Kwan, et al., deep dermal fibroblasts were treated with adenoviral DCN and seeded in a CGAG matrix in order to determine whether or not their remodeling behavior would become more like that of superficial fibroblasts [137]. Upon treatment, adenoviral-DCN-treated deep dermal fibroblasts showed a maximal fiber thickness that was similar to superficial fibroblasts as well as an improved collagen matrix morphology [137]. Moreover, adenoviral-DCN treatment of deep dermal fibroblasts did not influence cellular proliferation or adhesion, though it did reduce cell migration in the CGAG matrix [137]. It was also determined that a multiplicity of infection (MOI) of 500 for 12-24 hours was needed for optimal transduction of these fibroblasts [27]. As a whole, these results suggest that adenoviral-

DCN treatment may have the potential to improve HTS by promoting regeneration rather than fibrosis.

Therefore, the aim of this research project was to use an *in vitro* tissue-engineered skin model to further explore the matrix remodeling effects after adenoviral-DCN treatment. In contrast to the study by Kwan, et al., this project uses site-matched fibroblasts harvested from normal skin and HTS tissue for experimentation instead of superficial and deep dermal fibroblasts. The specific aims of this project were to: 1) generate CGAG matrices that had pore characteristics which were optimal for the creation of tissue-engineered skin, 2) ensure that adenoviral-DCN treatment had minimal effects on HTS fibroblast viability, 3) evaluate matrix remodeling of tissue-engineered skin models created using HTS fibroblasts after adenoviral-DCN treatment by measuring matrix contraction, collagen orientation, and collagen packing density, and 4) assess the gene and protein expression of major molecular factors involved in HTS development after adenoviral-DCN treatment. The overall hypothesis of this project was that adenoviral-DCN treatment of HTS fibroblasts would result in anti-fibrotic matrix remodeling behavior and gene/protein expression, thus supporting the findings from Kwan, et al. and suggesting a new therapeutic for HTS.

Figures

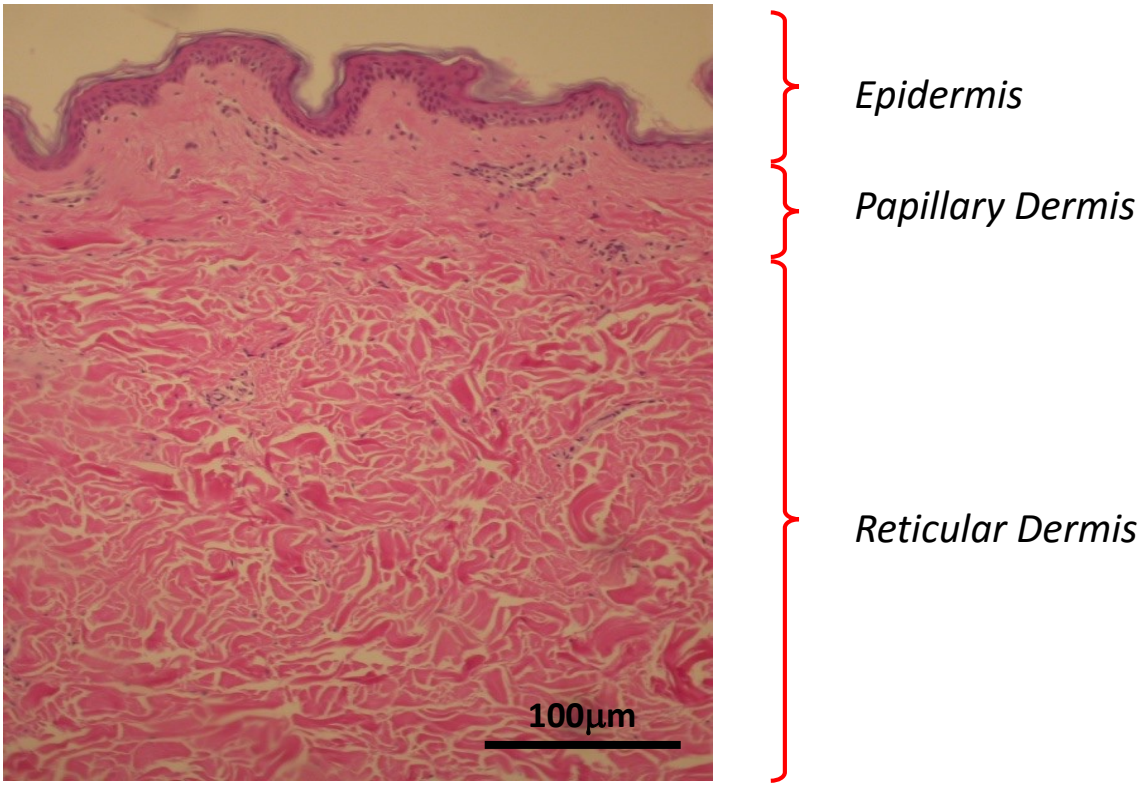

Figure 1.1. Hematoxylin and eosin stained histological section of human normal skin tissue.

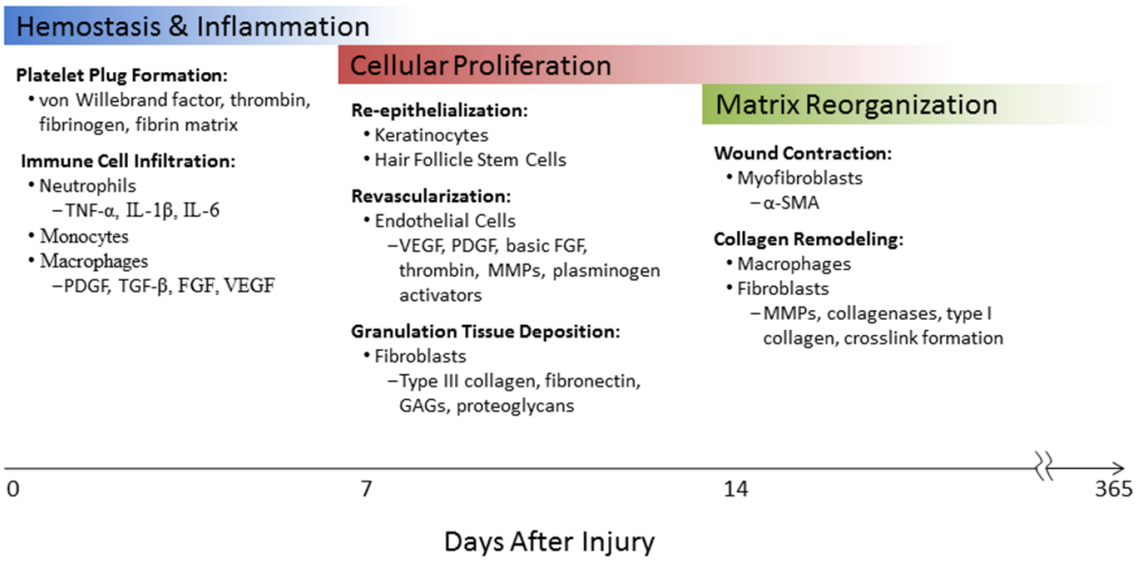

Figure 1.2. Cellular and molecular components involved in the normal wound healing process. (adapted from Sanon, S., Hart, D.A., Tredget, E.E., Molecular and cellular biology of wound healing and skin regeneration, in Skin tissue engineering and regenerative medicine, M.Z. Albanna, J.H. Holmes, Editors. 2016, Elsevier. p. 19-47).

Figure 1.3. Hypertrophic scars on a 12-year-old male, 29 months after burn injury to the face and trunk. Raised, erythematous lesions displaying contracture are evident. (adapted from Sanon, S., Hart, D.A., Tredget, E.E., Molecular and cellular biology of wound healing and skin regeneration, in Skin tissue engineering and regenerative medicine, M.Z. Albanna, J.H. Holmes, Editors. 2016, Elsevier. p. 19-47).

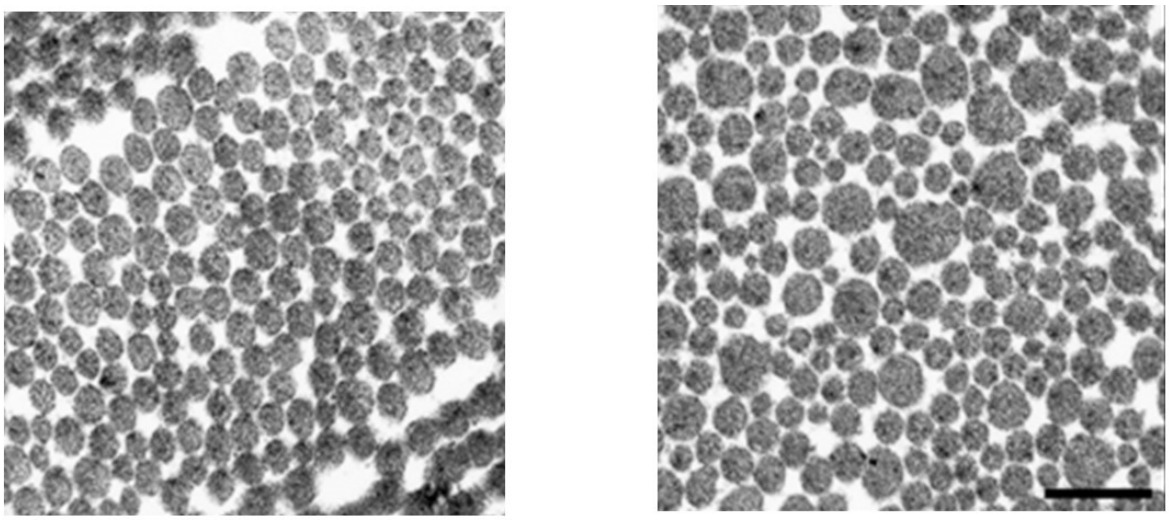

Figure 1.4. Decorin knockout mice have a highly-varied and irregular collagen organization as compared to wild-type mice. Scale bar = 500 nm. (adapted from Reed, C.C. and Iozzo, R.V., The role of decorin in collagen fibrillogenesis and skin homeostasis. Glycoconj J, 2002. **19**(4-5): p. 249-255).

Figure 1.5. A 28-year-old male suffered injuries to 93% TBSA, with 85% TBSA full-thickness burns, after a closed space explosion. Autografts were administered to the patient's back within the first week and the remaining 60% TBSA burned was covered with Integra^{TM}. Due to the extent of injury, 700cm^2 of cultured skin substitutes containing autologous keratinocytes and fibroblasts (Steven T. Boyce, University of Cincinnati, Shriners Hospitals for Children) were grafted over 11 procedures and allowed for successful resurfacing of 50% TBSA. High quality coverage was noted upon follow up 7 years post-injury, though hypopigmentation is clearly present. (adapted from Medina, A. and Tredget, E.E., Strategies to increase flap survival in nasal reconstruction in patients with deep panfacial burns. J Burn Care Res, 2013. 34(1): p. 42-47).

References

1. Alberts, B., Bray, D., Lewis, J., Raff, M., Roberts, K., and Watson, J.D., *Molecular biology of the cell*. Vol. 1st. 1983, New York, NY: Garland Publishing, Inc.
2. Eckhart, L., Lippens, S., Tschachler, E., and Declercq, W., *Cell death by cornification.* Biochimica et Biophysica Acta, 2013. **1833**(12): p. 3471-80.
3. Breitkreutz, D., Mirancea, N., and Nischt, R., *Basement membranes in skin: unique matrix structures with diverse functions?* Histochemistry and Cell Biology, 2009. **132**(1): p. 1-10.
4. Fenner, J. and Clark, R.A.F., *Anatomy, physiology, histology, and immunohistochemistry of human skin*, in *Skin Tissue Engineering and Regenerative Medicine*, M.Z. Albanna and J.H. Holmes, Editors. 2016, Elsevier. p. 1-17.
5. Wu, Y. and Tredget, E.E., *Pathology of tissue regeneration repair: skin regeneration*, in *Pathobiology of human disease*, L.M. McManus and R.N. Mitchell, Editors. 2014, Elsevier: San Diego, CA. p. 558-66.
6. Leeson, C.R. and Leeson, T.S., *Histology*. Vol. 3rd. 1976, Philadelphia, PA: W.B. Saunders Company.
7. Reinke, J.M. and Sorg, H., *Wound repair and regeneration.* European Surgical Research, 2012. **49**(1): p. 35-43.
8. Clark, R.A.F. and Singer, A.J., *Wound repair: basic biology to tissue engineering*, in *Principles of tissue engineering*, R.P. Lanza, R. Langer, and J. Vacanti, Editors. 2000, Academic Press: San Diego, CA. p. 857-78.
9. Levy, V., Lindon, C., Zheng, Y., Harfe, B.D., and Morgan, B.A., *Epidermal stem cells arise from the hair follicle after wounding.* FASEB Journal, 2007. **21**(7): p. 1358-66.

10. Ito, M., Liu, Y., Yang, Z., Nguyen, J., Liang, F., Morris, R.J., and Cotsarelis, G., *Stem cells in the hair follicle bulge contribute to wound repair but not to homeostasis of the epidermis.* Nature Medicine, 2005. **11**(12): p. 1351-4.

11. Brodsky, S., Chen, J., Lee, A., Akassoglou, K., Norman, J., and Goligorsky, M.S., *Plasmin-dependent and -independent effects of plasminogen activators and inhibitor-1 on ex vivo angiogenesis.* American Journal of Physiology: Heart and Circulatory Physiology, 2001. **281**(4): p. 1784-92.

12. Tredget, E.E., *Pathophysiology and treatment of fibroproliferative disorders following thermal injury.* Annals of the New York Academy of Sciences, 1999. **888**: p. 165-82.

13. Gauglitz, G.G., Korting, H.C., Pavicic, T., Ruzicka, T., and Jeschke, M.G., *Hypertrophic scarring and keloids: pathomechanisms and current and emerging treatment strategies.* Molecular Medicine, 2011. **17**(1-2): p. 113-25.

14. Bock, O., Schmid-Ott, G., Malewski, P., and Mrowietz, U., *Quality of life of patients with keloid and hypertrophic scarring.* Archives for Dermatological Research. Archiv für Dermatologische Forschung, 2006. **297**(10): p. 433-8.

15. Lawrence, J.W., Mason, S.T., Schomer, K., and Klein, M.B., *Epidemiology and impact of scarring after burn injury: a systematic review of the literature.* Journal of Burn Care & Research, 2012. **33**(1): p. 136-46.

16. Gangemi, E.N., Gregori, D., Berchialla, P., Zingarelli, E., Cairo, M., Bollero, D., Ganem, J., Capocelli, R., Cuccuru, F., Cassano, P., Risso, D., and Stella, M., *Epidemiology and risk factors for pathologic scarring after burn wounds.* Archives of Facial Plastic Surgery, 2008. **10**(2): p. 93-102.

17. Lewis, W.H.P. and Sun, K.K.Y., *Hypertrophic scar: a genetic hypothesis.* Burns, 1990. **16**(3): p. 176-8.

18. Bombaro, K.M., Engrav, L.H., Carrougher, G.J., Wiechman, S.A., Faucher, L., Costa, B.A., Heimbach, D.M., Rivara, F.P., and Honari, S., *What is the prevalence of hypertrophic scarring following burns?* Burns, 2003. **29**(4): p. 299-302.

19. Li-Tsang, C.W.P., Lau, J.C.M., and Chan, C.C.H., *Prevalence of hypertrophic scar formation and its characteristics among the Chinese population.* Burns, 2005. **31**(5): p. 610-6.

20. Niessen, F.B., Spauwen, P.H., Schalkwijk, J., and Kon, M., *On the nature of hypertrophic scars and keloids: a review.* Plastic and Reconstructive Surgery, 1999. **104**(5): p. 1435-58.

21. Dunkin, C.S.J., Pleat, J.M., Gillespie, P.H., Tyler, M.P.H., Roberts, A.H.N., and McGrouther, D.A., *Scarring occurs at a critical depth of skin injury: Precise measurement in a graduated dermal scratch in human volunteers.* Plastic and Reconstructive Surgery, 2007. **119**(6): p. 1722-32.

22. Honardoust, D., Varkey, M., Marcoux, Y., Shankowsky, H.A., and Tredget, E.E., *Reduced decorin, fibromodulin, and transforming growth factor-beta3 in deep dermis leads to hypertrophic scarring.* Journal of Burn Care & Research, 2012. **33**(2): p. 218-27.

23. Deitch, E.A., Wheelahan, T.M., Rose, M.P., Clothier, J., and Cotter, J., *Hypertrophic burn scars: analysis of variables.* The Journal of Trauma, 1983. **23**(10): p. 895-8.

24. Ehrlich, H.P., Desmouliere, A., Diegelmann, R.F., Cohen, I.K., Compton, C.C., Garner, W.L., Kapanci, Y., and Gabbiani, G., *Morphological and immunochemical differences*

between keloid and hypertrophic scar. American Journal of Pathology, 1994. **145**(1): p. 105-13.

25. Linares, H.A., Kischer, C.W., Dobrkovsky, M., and Larson, D.L., *The histiotypic organization of the hypertrophic scar in humans.* Journal of Investigative Dermatology, 1972. **59**(4): p. 323-31.

26. Verhaegen, P.D., van Zuijlen, P.P., Pennings, N.M., van Marle, J., Niessen, F.B., van der Horst, C.M., and Middelkoop, E., *Differences in collagen architecture between keloid, hypertrophic scar, normotrophic scar, and normal skin: An objective histopathological analysis.* Wound Repair and Regeneration, 2009. **17**(5): p. 649-56.

27. Kwan, P., Hori, K., Ding, J., and Tredget, E.E., *Scar and contracture: biological principles.* Hand Clinics, 2009. **25**(4): p. 511-28.

28. Kischer, C.W., *Collagen and dermal patterns in the hypertrophic scar.* The Anatomical Record, 1974. **179**(1): p. 137-45.

29. Lee, J.Y.Y., Yang, C.C., Chao, S.C., and Wong, T.W., *Histopathological differential diagnosis of keloid and hypertrophic scar.* American Journal of Dermatopathology, 2004. **26**(5): p. 379-84.

30. Nedelec, B., Shankowsky, H., Scott, P.G., Ghahary, A., and Tredget, E.E., *Myofibroblasts and apoptosis in human hypertrophic scars: The effect of interferon-α2b.* Surgery, 2001. **130**(5): p. 798-808.

31. Ghahary, A., Shen, Y.J., Nedelec, B., Wang, R., Scott, P.G., and Tredget, E.E., *Collagenase production is lower in post-burn hypertrophic scar fibroblasts than in normal fibroblasts and is reduced by insulin-like growth factor-1.* Journal of Investigative Dermatology, 1996. **106**(3): p. 476-81.

32. Penn, J.W., Grobbelaar, A.O., and Rolfe, K.J., *The role of the TGF-beta family in wound healing, burns and scarring: a review.* International Journal of Burns and Trauma, 2012. **2**(1): p. 18-28.

33. Moulin, V., Larochelle, S., Langlois, C., Thibault, I., Lopez-Valle, C.A., and Roy, M., *Normal skin wound and hypertrophic scar myofibroblasts have differential responses to apoptotic inductors.* Journal of Cellular Physiology, 2004. **198**(3): p. 350-8.

34. Schmid, P., Itin, P., Cherry, G., Bi, C., and Cox, D.A., *Enhanced expression of transforming growth factor-beta type I and type II receptors in wound granulation tissue and hypertrophic scar.* American Journal of Pathology, 1998. **152**(2): p. 485-93.

35. Wang, Y.W., Liou, N.H., Cherng, J.H., Chang, S.J., Ma, K.H., Fu, E., Liu, J.C., and Dai, N.T., *siRNA-targeting transforming growth factor-beta type I receptor reduces wound scarring and extracellular matrix deposition of scar tissue.* Journal of Investigative Dermatology, 2014. **134**(7): p. 2016-25.

36. Tredget, E.E., Levi, B., and Donelan, M.B., *Biology and principles of scar management and burn reconstruction.* Surgical Clinics of North America, 2014. **94**(4): p. 793-815.

37. Wang, J., Jiao, H., Stewart, T.L., Shankowsky, H.A., Scott, P.G., and Tredget, E.E., *Increased TGF-beta-producing CD4+ T lymphocytes in postburn patients and their potential interaction with dermal fibroblasts in hypertrophic scarring.* Wound Repair and Regeneration, 2007. **15**(4): p. 530-9.

38. Wynn, T.A., *Fibrotic disease and the T(H)1/T(H)2 paradigm.* Nature Reviews: Immunology, 2004. **4**(8): p. 583-94.

39. Mosmann, T.R. and Coffman, R.L., *TH1 and TH2 cells: different patterns of lymphokine secretion lead to different functional properties.* Annual Review of Immunology, 1989. **7**: p. 145-73.

40. Armour, A., Scott, P.G., and Tredget, E.E., *Cellular and molecular pathology of HTS: basis for treatment.* Wound Repair and Regeneration, 2007. **15 Suppl 1**: p. S6-17.

41. Tredget, E.E., Yang, L., Delehanty, M., Shankowsky, H., and Scott, P.G., *Polarized Th2 cytokine production in patients with hypertrophic scar following thermal injury.* Journal of Interferon & Cytokine Research, 2006. **26**(3): p. 179-89.

42. Yang, L., Scott, P.G., Dodd, C., Medina, A., Jiao, H., Shankowsky, H.A., Ghahary, A., and Tredget, E.E., *Identification of fibrocytes in postburn hypertrophic scar.* Wound Repair and Regeneration, 2005. **13**(4): p. 398-404.

43. Bucala, R., Spiegel, L.A., Chesney, J., Hogan, M., and Cerami, A., *Circulating fibrocytes define a new leukocyte subpopulation that mediates tissue repair.* Molecular Medicine, 1994. **1**(1): p. 71-81.

44. Wang, J.F., Jiao, H., Stewart, T.L., Shankowsky, H.A., Scott, P.G., and Tredget, E.E., *Fibrocytes from burn patients regulate the activities of fibroblasts.* Wound Repair and Regeneration, 2007. **15**(1): p. 113-21.

45. Wilgus, T.A. and Wulff, B.C., *The importance of mast cells in dermal scarring.* Advances in Wound Care, 2014. **3**(4): p. 356-65.

46. Foley, T.T. and Ehrlich, H.P., *Through gap junction communications, co-cultured mast cells and fibroblasts generate fibroblast activities allied with hypertrophic scarring.* Plastic and Reconstructive Surgery, 2013. **131**(5): p. 1036-44.

47. Ding, J., Hori, K., Zhang, R., Marcoux, Y., Honardoust, D., Shankowsky, H.A., and Tredget, E.E., *Stromal cell-derived factor 1 (SDF-1) and its receptor CXCR4 in the formation of postburn hypertrophic scar (HTS).* Wound Repair and Regeneration, 2011. **19**(5): p. 568-78.

48. Wang, J., Hori, K., Ding, J., Huang, Y., Kwan, P., Ladak, A., and Tredget, E.E., *Toll-like receptors expressed by dermal fibroblasts contribute to hypertrophic scarring.* Journal of Cellular Physiology, 2011. **226**(5): p. 1265-73.

49. Amadeu, T.P., Braune, A.S., Porto, L.C., Desmouliere, A., and Costa, A.M.A., *Fibrillin-1 and elastin are differentially expressed in hypertrophic scars and keloids.* Wound Repair and Regeneration, 2004. **12**(2): p. 169-74.

50. Kozma, E.M., Olczyk, K., Glowacki, A., and Bobinski, R., *An accumulation of proteoglycans in scarred fascia.* Molecular and Cellular Biochemistry, 2000. **203**(1-2): p. 103-12.

51. Scott, P.G., Dodd, C.M., Tredget, E.E., Ghahary, A., and Rahemtulla, F., *Chemical characterization and quantification of proteoglycans in human post-burn hypertrophic and mature scars.* Clinical Science (London, England: 1979), 1996. **90**(5): p. 417-25.

52. Smith, M.M. and Melrose, J., *Proteoglycans in normal and healing skin.* Advances in Wound Care, 2015. **4**(3): p. 152-73.

53. Scott, P.G., Dodd, C.M., Tredget, E.E., Ghahary, A., and Rahemtulla, F., *Immunohistochemical localization of the proteoglycans decorin, biglycan and versican and transforming growth factor-beta in human post-burn hypertrophic and mature scars.* Histopathology, 1995. **26**(5): p. 423-31.

54. Kresse, H. and Schonherr, E., *Proteoglycans of the extracellular matrix and growth control.* Journal of Cellular Physiology, 2001. **189**(3): p. 266-74.

55. Hildebrand, A., Romaris, M., Rasmussen, L.M., Heinegard, D., Twardzik, D.R., Border, W.A., and Ruoslahti, E., *Interaction of the small interstitial proteoglycans biglycan, decorin and fibromodulin with transforming growth factor beta.* Biochemical Journal, 1994. **302 (Pt 2)**(Pt 2): p. 527-34.

56. Orgel, J.P., Eid, A., Antipova, O., Bella, J., and Scott, J.E., *Decorin core protein (decoron) shape complements collagen fibril surface structure and mediates its binding.* PloS One, 2009. **4**(9): p. e7028.

57. Danielson, K.G., Baribault, H., Holmes, D.F., Graham, H., Kadler, K.E., and Iozzo, R.V., *Targeted disruption of decorin leads to abnormal collagen fibril morphology and skin fragility.* Journal of Cell Biology, 1997. **136**(3): p. 729-43.

58. Yamaguchi, Y., Mann, D.M., and Ruoslahti, E., *Negative regulation of transforming growth factor-beta by the proteoglycan decorin.* Nature, 1990. **346**(6281): p. 281-4.

59. Schonherr, E., Broszat, M., Brandan, E., Bruckner, P., and Kresse, H., *Decorin core protein fragment Leu155-Val260 interacts with TGF-beta but does not compete for decorin binding to type I collagen.* Archives of Biochemistry and Biophysics, 1998. **355**(2): p. 241-8.

60. Markmann, A., Hausser, H., Schonherr, E., and Kresse, H., *Influence of decorin expression on transforming growth factor-beta-mediated collagen gel retraction and biglycan induction.* Matrix Biology, 2000. **19**(7): p. 631-6.

61. Vial, C., Gutierrez, J., Santander, C., Cabrera, D., and Brandan, E., *Decorin interacts with connective tissue growth factor (CTGF)/CCN2 by LRR12 inhibiting its biological activity.* Journal of Biological Chemistry, 2011. **286**(27): p. 24242-52.

62. Goldoni, S., Humphries, A., Nystrom, A., Sattar, S., Owens, R.T., McQuillan, D.J., Ireton, K., and Iozzo, R.V., *Decorin is a novel antagonistic ligand of the Met receptor.* Journal of Cell Biology, 2009. **185**(4): p. 743-54.

63. Iozzo, R.V., Buraschi, S., Genua, M., Xu, S.Q., Solomides, C.C., Peiper, S.C., Gomella, L.G., Owens, R.C., and Morrione, A., *Decorin antagonizes IGF receptor I (IGF-IR) function by interfering with IGF-IR activity and attenuating downstream signaling.* Journal of Biological Chemistry, 2011. **286**(40): p. 34712-21.

64. Iozzo, R.V., Moscatello, D.K., McQuillan, D.J., and Eichstetter, I., *Decorin is a biological ligand for the epidermal growth factor receptor.* Journal of Biological Chemistry, 1999. **274**(8): p. 4489-92.

65. Sayani, K., Dodd, C.M., Nedelec, B., Shen, Y.J., Ghahary, A., Tredget, E.E., and Scott, P.G., *Delayed appearance of decorin in healing burn scars.* Histopathology, 2000. **36**(3): p. 262-72.

66. Kwan, P.O., Ding, J., and Tredget, E.E., *Serum decorin, IL-1beta, and TGF-beta predict hypertrophic scarring postburn.* Journal of Burn Care & Research, 2015.

67. Iozzo, R.V. and Schaefer, L., *Proteoglycans in health and disease: novel regulatory signaling mechanisms evoked by the small leucine-rich proteoglycans.* FEBS Journal, 2010. **277**(19): p. 3864-75.

68. Honardoust, D., Varkey, M., Hori, K., Ding, J., Shankowsky, H.A., and Tredget, E.E., *Small leucine-rich proteoglycans, decorin and fibromodulin, are reduced in postburn hypertrophic scar.* Wound Repair and Regeneration, 2011. **19**(3): p. 368-78.

69. Meaume, S., Le Pillouer-Prost, A., Richert, B., Roseeuw, D., and Vadoud, J., *Management of scars: updated practical guidelines and use of silicones.* European Journal of Dermatology, 2014. **24**(4): p. 435-43.

70. Musgrave, M.A., Umraw, N., Fish, J.S., Gomez, M., and Cartotto, R.C., *The effect of silicone gel sheets on perfusion of hypertrophic burn scars.* The Journal of Burn Care & Rehabilitation, 2002. **23**(3): p. 208-14.

71. Tredget, E.E., Wang, R., Shen, Q., Scott, P.G., and Ghahary, A., *Transforming growth factor-beta mRNA and protein in hypertrophic scar tissues and fibroblasts: antagonism by IFN-alpha and IFN-gamma in vitro and in vivo.* Journal of Interferon & Cytokine Research, 2000. **20**(2): p. 143-51.

72. Ghahary, A., Shen, Y.J., Nedelec, B., Scott, P.G., and Tredget, E.E., *Interferons gamma and alpha-2b differentially regulate the expression of collagenase and tissue inhibitor of metalloproteinase-1 messenger RNA in human hypertrophic and normal dermal fibroblasts.* Wound Repair and Regeneration, 1995. **3**(2): p. 176-84.

73. Tredget, E.E., Shankowsky, H.A., Pannu, R., Nedelec, B., Iwashina, T., Ghahary, A., Taerum, T.V., and Scott, P.G., *Transforming growth factor-beta in thermally injured patients with hypertrophic scars: effects of interferon alpha-2b.* Plastic and Reconstructive Surgery, 1998. **102**(5): p. 1317-28; discussion 29-30.

74. Ding, J., Ma, Z., Liu, H., Kwan, P., Iwashina, T., Shankowsky, H.A., Wong, D., and Tredget, E.E., *The therapeutic potential of a C-X-C chemokine receptor type 4 (CXCR-4)*

antagonist on hypertrophic scarring in vivo. Wound Repair and Regeneration, 2014. **22**(5): p. 622-30.

75. Atiyeh, B.S., Hayek, S.N., and Gunn, S.W., *New technologies for burn wound closure and healing - Review of the literature.* Burns, 2005. **31**(8): p. 944-56.

76. Anderson, R.R., Donelan, M.B., Hivnor, C., Greeson, E., Ross, E.V., Shumaker, P.R., Uebelhoer, N.S., and Waibel, J.S., *Laser treatment of traumatic scars with an emphasis on ablative fractional laser resurfacing: consensus report.* JAMA Dermatology, 2014. **150**(2): p. 187-93.

77. Choi, J.E., Oh, G.N., Kim, J.Y., Seo, S.H., Ahn, H.H., and Kye, Y.C., *Ablative fractional laser treatment for hypertrophic scars: comparison between Er:YAG and CO2 fractional lasers.* Journal of Dermatological Treatment, 2014. **25**(4): p. 299-303.

78. Connolly, K.L., Chaffins, M., and Ozog, D., *Vascular patterns in mature hypertrophic burn scars treated with fractional CO2 laser.* Lasers in Surgery and Medicine, 2014. **46**(8): p. 597-600.

79. Makboul, M., Makboul, R., Abdelhafez, A.H., Hassan, S.S., and Youssif, S.M., *Evaluation of the effect of fractional CO2 laser on histopathological picture and TGF-beta1 expression in hypertrophic scar.* Journal of Cosmetic Dermatology, 2014. **13**(3): p. 169-79.

80. Lamy, J., Yassine, A.H., Gourari, A., Forme, N., and Zakine, G., *The role of skin substitutes in the surgical treatment of extensive burns covering more than 60 % of total body surface area. A review of patients over a 10-year period at the Tours University Hospital.* Annales de Chirurgie Plastique et Esthétique, 2013.

81. Seo, D.K., Kym, D., and Hur, J., *Management of neck contractures by single-stage dermal substitutes and skin grafting in extensive burn patients.* Annals of Surgical Treatment and Research, 2014. **87**(5): p. 253-9.

82. Rheinwald, J.G. and Green, H., *Serial cultivation of strains of human epidermal keratinocytes: the formation of keratinizing colonies from single cells.* Cell, 1975. **6**(3): p. 331-43.

83. O'Connor, N.E., Mulliken, J.B., Banks-Schlegel, S., Kehinde, O., and Green, H., *Grafting of burns with cultured epithelium prepared from autologous epidermal cells.* Lancet, 1981. **1**(8211): p. 75-8.

84. Kamel, R.A., Ong, J.F., Eriksson, E., Junker, J.P., and Caterson, E.J., *Tissue engineering of skin.* Journal of the American College of Surgeons, 2013. **217**(3): p. 533-55.

85. Boyce, S.T. *Tissue engineering*. in *American Burn Association*. 2007. San Diego, CA.

86. Fang, T., Lineaweaver, W.C., Sailes, F.C., Kisner, C., and Zhang, F., *Clinical application of cultured epithelial autografts on acellular dermal matrices in the treatment of extended burn injuries.* Annals of Plastic Surgery, 2014. **73**(5): p. 509-15.

87. Catalano, E., Cochis, A., Varoni, E., Rimondini, L., and Azzimonti, B., *Tissue-engineered skin substitutes: an overview.* Journal of Artificial Organs, 2013. **16**(4): p. 397-403.

88. Gomez, C., Galan, J.M., Torrero, V., Ferreiro, I., Perez, D., Palao, R., Martinez, E., Llames, S., Meana, A., and Holguin, P., *Use of an autologous bioengineered composite skin in extensive burns: Clinical and functional outcomes. A multicentric study.* Burns, 2011. **37**(4): p. 580-9.

89. Nanchahal, J., Dover, R., and Otto, W.R., *Allogeneic skin substitutes applied to burns patients.* Burns, 2002. **28**(3): p. 254-7.

90. Yannas, I.V. and Burke, J.F., *Design of an artificial skin. I. Basic design principles.* Journal of Biomedical Materials Research, 1980. **14**(1): p. 65-81.

91. Chamberlain, L.J. and Yannas, I.V., *Preparation of collagen-glycosaminoglycan copolymers for tissue regeneration.* Methods in Molecular Medicine, 1999. **18**: p. 3-17.

92. Zeltinger, J., Sherwood, J.K., Graham, D.A., Mueller, R., and Griffith, L.G., *Effect of pore size and void fraction on cellular adhesion, proliferation, and matrix deposition.* Tissue Engineering, 2001. **7**(5): p. 557-72.

93. O'Brien, F.J., Harley, B.A., Waller, M.A., Yannas, I.V., Gibson, L.J., and Prendergast, P.J., *The effect of pore size on permeability and cell attachment in collagen scaffolds for tissue engineering.* Technology and Health Care, 2007. **15**(1): p. 3-17.

94. Salem, A.K., Stevens, R., Pearson, R.G., Davies, M.C., Tendler, S.J., Roberts, C.J., Williams, P.M., and Shakesheff, K.M., *Interactions of 3T3 fibroblasts and endothelial cells with defined pore features.* Journal of Biomedical Materials Research, 2002. **61**(2): p. 212-7.

95. Varkey, M., Ding, J., Tredget, E.E., and Wound Healing Research, G., *The effect of keratinocytes on the biomechanical characteristics and pore microstructure of tissue engineered skin using deep dermal fibroblasts.* Biomaterials, 2014. **35**(36): p. 9591-8.

96. Yannas, I.V., Lee, E., Orgill, D.P., Skrabut, E.M., and Murphy, G.F., *Synthesis and characterization of a model extracellular matrix that induces partial regeneration of adult mammalian skin.* Proceedings of the National Academy of Sciences of the United States of America, 1989. **86**(3): p. 933-7.

97. O'Brien, F.J., Harley, B.A., Yannas, I.V., and Gibson, L., *Influence of freezing rate on pore structure in freeze-dried collagen-GAG scaffolds.* Biomaterials, 2004. **25**(6): p. 1077-86.

98. Haugh, M.G., Murphy, C.M., and O'Brien, F.J., *Novel freeze-drying methods to produce a range of collagen-glycosaminoglycan scaffolds with tailored mean pore sizes.* Tissue Engineering. Part C, Methods, 2010. **16**(5): p. 887-94.

99. Lloyd, C., Besse, J., and Boyce, S., *Controlled-rate freezing to regulate the structure of collagen-glycosaminoglycan scaffolds in engineered skin substitutes.* Journal of Biomedical Materials Research, Part B: Applied Biomaterials, 2014.

100. Haugh, M.G., Jaasma, M.J., and O'Brien, F.J., *The effect of dehydrothermal treatment on the mechanical and structural properties of collagen-GAG scaffolds.* Journal of Biomedical Materials Research, Part A, 2009. **89**(2): p. 363-9.

101. Koide, M., Osaki, K., Konishi, J., Oyamada, K., Katakura, T., Takahashi, A., and Yoshizato, K., *A new type of biomaterial for artificial skin: dehydrothermally cross-linked composites of fibrillar and denatured collagens.* Journal of Biomedical Materials Research, 1993. **27**(1): p. 79-87.

102. Weadock, K.S., Miller, E.J., Keuffel, E.L., and Dunn, M.G., *Effect of physical crosslinking methods on collagen-fiber durability in proteolytic solutions.* Journal of Biomedical Materials Research, 1996. **32**(2): p. 221-6.

103. Yang, H., Tan, Q., and Zhao, H., *Progress in various crosslinking modification for acellular matrix.* Chinese Medical Journal, 2014. **127**(17): p. 3156-64.

104. Blackstone, B.N., Drexler, J.W., and Powell, H.M., *Tunable engineered skin mechanics via coaxial electrospun fiber core diameter.* Tissue Engineering. Part A, 2014. **20**(19-20): p. 2746-55.

105. Rnjak-Kovacina, J., Wise, S.G., Li, Z., Maitz, P.K., Young, C.J., Wang, Y., and Weiss, A.S., *Electrospun synthetic human elastin:collagen composite scaffolds for dermal tissue engineering.* Acta Biomaterialia, 2012. **8**(10): p. 3714-22.

106. Yuan, Z., Zhao, J., Chen, Y., Yang, Z., Cui, W., and Zheng, Q., *Regulating inflammation using acid-responsive electrospun fibrous scaffolds for skin scarless healing.* Mediators of Inflammation, 2014. **2014**: p. 858045.

107. Lai, H.J., Kuan, C.H., Wu, H.C., Tsai, J.C., Chen, T.M., Hsieh, D.J., and Wang, T.W., *Tailored design of electrospun composite nanofibers with staged release of multiple angiogenic growth factors for chronic wound healing.* Acta Biomaterialia, 2014. **10**(10): p. 4156-66.

108. Li, L., Fukunaga-Kalabis, M., and Herlyn, M., *The three-dimensional human skin reconstruct model: a tool to study normal skin and melanoma progression.* Journal of Visualized Experiments, 2011(54).

109. Jean, J., Lapointe, M., Soucy, J., and Pouliot, R., *Development of an in vitro psoriatic skin model by tissue engineering.* Journal of Dermatological Science, 2009. **53**(1): p. 19-25.

110. Shepherd, J., Douglas, I., Rimmer, S., Swanson, L., and MacNeil, S., *Development of three-dimensional tissue-engineered models of bacterial infected human skin wounds.* Tissue Engineering. Part C, Methods, 2009. **15**(3): p. 475-84.

111. Reijnders, C.M., van Lier, A., Roffel, S., Kramer, D., Scheper, R.J., and Gibbs, S., *Development of a full-thickness human skin equivalent In vitro model derived from TERT-immortalized keratinocytes and fibroblasts.* Tissue Engineering. Part A, 2015. **21**(17-18): p. 2448-59.

112. Flaten, G.E., Palac, Z., Engesland, A., Filipovic-Grcic, J., Vanic, Z., and Skalko-Basnet, N., *In vitro skin models as a tool in optimization of drug formulation.* European Journal of Pharmaceutical Sciences, 2015. **75**: p. 10-24.

113. Smola, H., Thiekotter, G., and Fusenig, N.E., *Mutual induction of growth factor gene expression by epidermal-dermal cell interaction.* Journal of Cell Biology, 1993. **122**(2): p. 417-29.

114. Maas-Szabowski, N., Shimotoyodome, A., and Fusenig, N.E., *Keratinocyte growth regulation in fibroblast cocultures via a double paracrine mechanism.* Journal of Cell Science, 1999. **112 (Pt 12)**: p. 1843-53.

115. Mackenzie, I.C. and Hill, M.W., *Connective tissue influences on patterns of epithelial architecture and keratinization in skin and oral mucosa of the adult mouse.* Cell and Tissue Research, 1984. **235**(3): p. 551-9.

116. Yamaguchi, Y., Itami, S., Tarutani, M., Hosokawa, K., Miura, H., and Yoshikawa, K., *Regulation of keratin 9 in nonpalmoplantar keratinocytes by palmoplantar fibroblasts through epithelial-mesenchymal interactions.* Journal of Investigative Dermatology, 1999. **112**(4): p. 483-8.

117. Okazaki, M., Yoshimura, K., Suzuki, Y., and Harii, K., *Effects of subepithelial fibroblasts on epithelial differentiation in human skin and oral mucosa: heterotypically*

recombined organotypic culture model. Plastic and Reconstructive Surgery, 2003. **112**(3): p. 784-92.

118. Wang, J., Dodd, C., Shankowsky, H.A., Scott, P.G., Tredget, E.E., and Wound Healing Research, G., *Deep dermal fibroblasts contribute to hypertrophic scarring.* Laboratory Investigation, 2008. **88**(12): p. 1278-90.

119. Varkey, M., Ding, J., and Tredget, E.E., *Differential collagen-glycosaminoglycan matrix remodeling by superficial and deep dermal fibroblasts: potential therapeutic targets for hypertrophic scar.* Biomaterials, 2011. **32**(30): p. 7581-91.

120. Sorrell, J.M. and Caplan, A.I., *Fibroblast heterogeneity: more than skin deep.* Journal of Cell Science, 2004. **117**(5): p. 667-75.

121. Varkey, M., Ding, J., and Tredget, E.E., *Superficial dermal fibroblasts enhance basement membrane and epidermal barrier formation in tissue-engineered skin: implications for treatment of skin basement membrane disorders.* Tissue Engineering. Part A, 2014. **20**(3-4): p. 540-52.

122. Varkey, M., Ding, J., and Tredget, E.E., *Fibrotic remodeling of tissue-engineered skin with deep dermal fibroblasts is reduced by keratinocytes.* Tissue Engineering. Part A, 2014. **20**(3-4): p. 716-27.

123. Bellemare, J., Roberge, C.J., Bergeron, D., Lopez-Valle, C.A., Roy, M., and Moulin, V.J., *Epidermis promotes dermal fibrosis: role in the pathogenesis of hypertrophic scars.* The Journal of Pathology, 2005. **206**(1): p. 1-8.

124. Niessen, F.B., Andriessen, M.P., Schalkwijk, J., Visser, L., and Timens, W., *Keratinocyte-derived growth factors play a role in the formation of hypertrophic scars.* Journal of Pathology, 2001. **194**(2): p. 207-16.

125. Simon, F., Bergeron, D., Larochelle, S., Lopez-Valle, C.A., Genest, H., Armour, A., and Moulin, V.J., *Enhanced secretion of TIMP-1 by human hypertrophic scar keratinocytes could contribute to fibrosis.* Burns, 2012. **38**(3): p. 421-7.

126. Brych, S.B., Engrav, L.H., Rivara, F.P., Ptacek, J.T., Lezotte, D.C., Esselman, P.C., Kowalske, K.J., and Gibran, N.S., *Time off work and return to work rates after burns: systematic review of the literature and a large two-center series.* The Journal of Burn Care & Rehabilitation, 2001. **22**(6): p. 401-5.

127. Engrav, L.H., Covey, M.H., Dutcher, K.D., Heimbach, D.M., Walkinshaw, M.D., and Marvin, J.A., *Impairment, time out of school, and time off from work after burns.* Plastic and Reconstructive Surgery, 1987. **79**(6): p. 927-34.

128. Arnberg, N., *Adenovirus receptors: implications for targeting of viral vectors.* Trends in Pharmacological Sciences, 2012. **33**(8): p. 442-8.

129. McConnell, M.J. and Imperiale, M.J., *Biology of adenovirus and its use as a vector for gene therapy.* Human Gene Therapy, 2004. **15**(11): p. 1022-33.

130. Kremer, E.J. and Nemerow, G.R., *Adenovirus tales: from the cell surface to the nuclear pore complex.* PLoS Pathogens, 2015. **11**(6): p. e1004821.

131. Edelstein, M. *Vectors used in gene therapy clinical trials*. Gene Therapy Clinical Trials Worldwide 2016 [cited 2016 May]; Available from: http://www.wiley.com//legacy/wileychi/genmed/clinical/.

132. Li, L., Okada, H., Takemura, G., Kosai, K., Kanamori, H., Esaki, M., Takahashi, T., Goto, K., Tsujimoto, A., Maruyama, R., Kawamura, I., Kawaguchi, T., Takeyama, T., Fujiwara, T., Fujiwara, H., and Minatoguchi, S., *Postinfarction gene therapy with adenoviral vector expressing decorin mitigates cardiac remodeling and dysfunction.*

American Journal of Physiology: Heart and Circulatory Physiology, 2009. **297**(4): p. H1504-13.

133. Kolb, M., Margetts, P.J., Galt, T., Sime, P.J., Xing, Z., Schmidt, M., and Gauldie, J., *Transient transgene expression of decorin in the lung reduces the fibrotic response to bleomycin.* American Journal of Respiratory and Critical Care Medicine, 2001. **163**(3 Pt 1): p. 770-7.

134. Kolb, M., Margetts, P.J., Sime, P.J., and Gauldie, J., *Proteoglycans decorin and biglycan differentially modulate TGF-beta-mediated fibrotic responses in the lung.* American Journal of Physiology: Lung Cellular and Molecular Physiology, 2001. **280**(6): p. L1327-34.

135. Zhang, Z., Wu, F., Zheng, F., and Li, H., *Adenovirus-mediated decorin gene transfection has therapeutic effects in a streptozocin-induced diabetic rat model.* Nephron Experimental Nephrology, 2010. **116**(1): p. e11-21.

136. Choi, I.K., Lee, Y.S., Yoo, J.Y., Yoon, A.R., Kim, H., Kim, D.S., Seidler, D.G., Kim, J.H., and Yun, C.O., *Effect of decorin on overcoming the extracellular matrix barrier for oncolytic virotherapy.* Gene Therapy, 2010. **17**(2): p. 190-201.

137. Kwan, P., Ding, J., and Tredget, E.E., *Decorin gene therapy alters deep dermal fibroblast behavior to mimic that of superficial dermal fibroblasts in remodeling collagen scaffold used for cultured skin substitutes.* Tissue Engineering. Part A, 2016 (submitted).

Chapter 2 : Effect of Adenovirus-mediated Decorin Gene Therapy on Fibrotic Remodeling in Tissue-engineered Skin

Introduction

As the outer covering of the human body, skin plays a key role in protecting the body from its surroundings and in maintaining homeostasis. Disruption of the skin structure, whether through injury or disease, initiates a process of wound healing in order to restore the skin's function. Abnormalities of this wound healing process can result in chronic wounding and/or the development of fibrosis. HTS is a fibroproliferative disorder of the skin that results in the development of elevated, painful, erythematous, and pruritic scars that form within the margins of the original wound. These lesions are particularly prevalent after burn injury, with an incidence typically greater than 70% post-burn [1, 2]. Moreover, HTS are often highly-contractile in nature, limiting patient mobility when formed over mobile regions of the body and leading to psychosocial impairment due to cosmetic disfigurement [3].

Although HTS pathogenesis is still not well understood, due to the complex interplay of molecular and cellular factors involved, TGF-β1 and its downstream effector CTGF have been implicated as key drivers of this disorder [4]. Primarily, these effects include ECM modulation, such as an increased deposition of matrix proteoglycans and collagen types I and III, as well as the suppressed expression of MMPs [5-7]. Histologically, this results in the accumulation of a disorganized ECM, consisting of whorled nodules of thin, densely-packed collagen bundles and elevated glycosaminoglycan content, thus facilitating the increased scar volume and turgidity seen clinically [8-11]. Additional effects of TGF-β1 include delayed apoptosis of α-SMA-

expressing myofibroblasts, which promotes contraction and hypercellularity, increased expression of fibronectin, and a significant reduction in DCN [10, 12, 13].

DCN, part of the small leucine-rich proteoglycan family, plays an important role in regulating the proper formation and orientation of collagen during fibrillogenesis [14]. Interestingly, DCN's core protein contains specific binding sites for TGF-β1 and CTGF, allowing it to serve as a natural antagonist of these growth factors by sequestering them in the ECM and preventing their binding to cell surface receptors [15, 16]. As such, DCN gene therapy has been explored as a treatment for a variety of fibrotic conditions, including pulmonary fibrosis, hepatic fibrosis, diabetic nephropathy, and post-infarction cardiac remodeling [17-20]. DCN has also proposed as a therapeutic for HTS, due to its ability to reduce TGF-β1-mediated collagen lattice contraction, downregulate TGF-β1 production, decrease cellular proliferation and collagen synthesis, and upregulate MMP expression [21-23].

Recently, our lab has explored adenovirus-mediated DCN gene therapy as a treatment for HTS. Upon treatment with an adenoviral-DCN vector, deep dermal fibroblasts – which naturally exhibit a hypertrophic-scar-like phenotype – showed improved collagen morphology and fiber thickness in a CGAG scaffold [24, 25]. Moreover, adenoviral-DCN treatment did not influence cellular proliferation or adhesion by deep dermal fibroblasts, though it did reduce cellular migration [25]. As such, the goal of this study was to further explore the matrix remodeling effects of adenoviral-DCN treatment using an *in vitro* tissue-engineered skin model. This model has been used previously by our lab to investigate the differential remodeling behavior of superficial and deep dermal fibroblasts *in vitro* [26-28]. Here, we hypothesize that adenoviral-DCN treatment of hypertrophic scar fibroblasts (HTS Fb) will result in anti-fibrotic effects,

including increased DCN protein levels, reduced contraction, normal-skin-like collagen orientation, and elevated gene expression of MMP-1.

Materials and Methods

Fibroblast Isolation, Expansion and Storage

The protocols for obtaining human tissue samples for fibroblast isolation were approved by the University of Alberta Hospital Health Research Ethics Board. Following informed consent, punch-biopsy specimens were acquired from the scar lesions of four patients at the University of Alberta Hospital Firefighters' Burn Treatment Unit who presented clinically with HTS **(Table 2.1)**. To account for the confounding effects of factors such as patient sex, patient age, scar age, and extent of burn injury, site-matched biopsies of normal skin from each patient were also acquired for use as a control for HTS samples.

Fibroblast isolation and culture from biopsy samples was performed as described previously [29]. Biopsy samples were minced into pieces smaller than 0.5mm in size, washed three times with sterile, high-glucose Dulbecco's Modified Eagle's Medium with L-glutamine (DMEM) (Thermo Fisher Scientific, Canada), and distributed into 100mm Petri dishes, four pieces to a dish. Sterile glass cover slips, attached to the Petri dishes using silicone grease, were used to immobilize tissue pieces. Fibroblast culture medium (DMEM, 10% fetal bovine serum (FBS) (PAA Laboratories, Canada), 1% antibiotic-antimycotic (Thermo Fisher Scientific, Canada)) was added and the dishes were incubated at 37ºC, 5% CO_2, and 95% relative humidity, with medium changes every 5 days. After 3 weeks, fibroblasts explanted from the tissue were harvested using 0.1%, 0.02% Trypsin/EDTA and moved to T-75 culture flasks. Fibroblasts were grown to at least passage 2 with medium changes every 2-3 days, sub-culturing at 90%

confluence with a splitting ratio of 1:4. Fibroblasts were cryopreserved for future use by suspending harvested cells in DMEM containing 20% FBS and 10% dimethyl sulfoxide (DMSO) (Sigma Aldrich, Canada), freezing to -80ºC in cryovials, and storing in liquid nitrogen tanks.

Keratinocyte Isolation, Expansion and Storage

The protocols for obtaining human tissue samples for keratinocyte isolation were approved by the University of Alberta Hospital Health Research Ethics Board. Following informed consent, keratinocytes were isolated from lower abdominal tissue specimens acquired from a patient who underwent elective abdominoplasty surgery **(Table 2.1)**. A dermatome (Padgett Instruments, United States) was used to tangentially section off the superficial layer (approximately 0.5mm) of the skin. This layer was treated overnight with 2.5U/ml Dispase II (Sigma Aldrich, Canada) at 4ºC in order to separate the epidermis from the superficial dermis. The epidermis was then minced into 1mm pieces, placed into a Falcon tube containing TrypLE Express (Thermo Fisher Scientific, Canada), and incubated for one hour in a 37ºC water bath. An equal volume of DMEM with 10% FBS was added to quench digestion and the solution was pipetted vigorously. The suspension was then passed through a 70µm cell strainer to remove any undigested tissue pieces. Keratinocytes were resuspended in keratinocyte culture medium (Epilife medium (Thermo Fisher Scientific, Canada), 1% Human Keratinocyte Growth Supplement (HKGS) (Thermo Fisher Scientific, Canada), 1% antibiotic-antimycotic), plated at a density of $4x10^4$ cells/cm^2 in T-150 culture flasks, and incubated at 37ºC, 5% CO_2, and 95% relative humidity, with medium changes every 2 days. At 75-80% confluence, cells were subcultured using TrypLE Express using a splitting ratio of 1:4. Passsage 2 keratinocytes were cryopreserved for future use by suspending harvested cells in keratinocyte freezing medium (9:1 FBS:DMSO), freezing to -80ºC in cryovials, and storing in liquid nitrogen tanks.

Preparation of CGAG Matrices

Freeze-dried, bovine type I collagen (Devro Pty. Ltd., Australia) was dissolved overnight at 4ºC in 215ml of 0.5M acetic acid (Sigma-Aldrich, Canada) at a concentration of 6.42mg/ml. The collagen solution was then transferred to an ice bath and homogenized at 15,000 rpm for one hour using a mechanical disperser (Ultra Turrax® T 25 with S25N-25F attachment, IKA, United States). Meanwhile, chondroitin-6-sulfate from shark cartilage (Sigma Aldrich, Canada) was dissolved at 4ºC in 35ml of 0.5M acetic acid at a concentration of 3.45mg/ml. The chondroitin-6-sulfate solution was then added dropwise to the collagen solution over three hours while continuing to homogenize at 15,000 rpm to yield a CGAG slurry containing 0.55% w/v type I collagen, 0.048% w/v chondroitin-6-sulfate. The CGAG slurry was then transferred to Falcon tubes and briefly centrifuged (up to 1,000 rpm). Foam was aspirated and the tubes were stored at 4ºC until further use.

Porous CGAG matrices were prepared using a freeze-cast, lyophilization methodology. CGAG slurry was degassed under vacuum for 2.5 hours at room temperature with a brief centrifuge (up to 1,000 rpm) midway through the degassing process. The degassed slurry was then dispensed into the casting apparatus – two stainless steel plates separated by a 1mm-thick rubber spacer. The casting apparatus was transferred to a refrigerated, circulating ethanol bath (Haake Pheonix II, Thermo Fisher Scientific, United States), frozen to -40ºC at a rate of 0.9ºC/min, then held at -40ºC for one hour. The casting apparatus was then opened and moved to the shelves of a freeze-dryer (Freezone 6 Plus, Labconco, United States) that had been pre-cooled to -40ºC. Matrices were lyophilized for 18 hours at a vacuum pressure of 0.070mbar while raising the temperature from -40ºC to 20ºC in a step-wise fashion as seen in **Table 2.2**. The highly-porous sheets were stored in a desiccator at room temperature until further use.

Prior to use for cell culture, the porous CGAG sheets were cut into 32mm discs and crosslinked via dehydrothermal treatment in a vacuum oven (APT.Line VD, Binder GmbH, Germany) for 24 hours. The vacuum oven was set to 140ºC with a vacuum pressure of 50mbar. Crosslinked matrix discs were stored in a desiccator at room temperature until further use.

CGAG Matrix Pore Size Measurement

Punch biopsies of crosslinked CGAG discs (n=3) were sputter-coated (Hummer 6.2, Anatech USA, United States) with gold-palladium for 2min at 15mA and imaged at a 10kV accelerating voltage using a scanning electron microscope (SEM) (S-4800 FEGSEM, Hitachi, Japan). Images of the scaffold cross-sections were taken at 50x magnification and the diameter of 50 pores per scaffold was measured using NIH Image J. Values were reported as mean pore diameter ± standard deviation.

Construction of Adenoviral Vectors for Experimentation

DCN- and green-fluorescent-protein (GFP)-expressing adenoviral vectors were created for experimentation using the AdMax system (Microbix Biosystems, Canada), as described in detail elsewhere [30]. Briefly, recombinant DCN or enhanced GFP expression cassettes were cloned into E1 shuttle plasmids containing a loxP recognition site and a murine cytomegalovirus promoter (pDC316). HEK293A cells were then cotransfected with either the DCN or enhanced GFP E1 shuttle plasmid and an E1,E3-deleted adenoviral genomic plasmid containing the Cre recombinase (pBHGloxΔE1,E3Cre). Expression of Cre recombinase in HEK293A cells resulted in the generation of replication-incompetent adenoviral vectors expressing either recombinant DCN (Ad5-DCN) or enhanced GFP (Ad5-GFP). Viral vectors were screened for the presence of the recombinant DCN or enhanced GFP genes, as well as the absence of the E1 replication

region, using quantitative polymerase chain reaction (PCR) (StepOnePlus, Applied Biosystems, United States). High-titer viral stocks were created by transducing HEK293A cells with virus and concentrating the cell culture supernatant. Viral titer, in plaque-forming units (PFU)/ml, was determined using a plaque-forming assay.

Cell Viability Assessment after Viral Transduction

HTS Fb were seeded in 24-well plates at a density of $0.5x10^5$ cells/well in fibroblast culture medium. After one hour, fibroblasts were exposed to either Ad5-DCN (n=18), Ad5-GFP (n=18), or no virus (n=18) for 18 hours at a MOI of 25. MOI is related to the viral titer by **Equation 2.1**:

$$Multiplicity\ of\ Infection\ (MOI) = \frac{Plaque\ Forming\ Units\ (PFU)}{\#\ of\ cells} \quad \textbf{(2.1)}$$

After 18 hours, virus-containing medium was removed, cells were washed twice with phosphate-buffered saline (PBS), and fresh fibroblast culture medium was added to wells. Cell viability was assessed at 24, 48, and 72 hours after viral infection using a MTT assay (n=6 per time point). Briefly, a yellow tetrazolium salt, 3-(4,5-dimethylthiozol-2-yl)-2,5-diphenyl tetrazolium bromide (Sigma-Aldrich, Canada), was added to culture wells at a concentration of 0.5mg/ml for 2 hours at 37ºC in the dark. Culture medium was removed and replaced with 700µl DMSO for 30min in order to dissolve the insoluble, purple formazan product. 200µl of supernatant was transferred to a 96-well plate and the absorbance was read at 540nm with a correction wavelength of 650nm using a microplate reader (Varioskan LUX, Thermo Fisher Scientific, United States). Values were reported as mean corrected absorbance ± standard error.

Cell Culture in the *in vitro* Tissue-engineered Skin Model

An *in vitro* tissue-engineered skin model was developed for this experiment by co-culturing fibroblasts with keratinocytes over 17 days in crosslinked CGAG scaffolds, as summarized in **Figure 2.1**. The procedure below was repeated using fibroblasts from each patient listed in **Table 2.1** independently, resulting in a total of 12 samples per experimental group. Fibroblasts from passage 2-5 and keratinocytes from passage 2 were used for all experiments.

HTS Fb and normal skin fibroblasts (NS Fb) were recovered from liquid nitrogen cryostorage and expanded to 90% confluence in T-75 culture flasks using fibroblast culture medium. 18 hours prior to seeding fibroblasts on CGAG scaffolds, viral supernatant containing either Ad5-DCN or Ad5-GFP was added to some of the HTS Fb-containing culture flasks at a MOI of 25. HTS Fb and NS Fb without any viral supernatant exposure were used as controls. Immediately prior to harvesting fibroblasts from culture flasks, crosslinked CGAG scaffolds were washed twice with PBS (30min each), washed twice with fibroblast culture medium (30min each), then placed in 6-well plates on top of biologically-inert filter paper (0.45µm MF membrane filters, Millipore Ltd., Canada). HTS Fb, HTS Fb+Ad5-GFP, HTS Fb+Ad5-DCN, or NS Fb were harvested from T-75 flasks using 0.05%, 0.01% Trypsin/EDTA and resuspended in a modified Green's Medium (3:1 DMEM:Ham's F12 with L-glutamine and HEPES (Thermo Fisher Scientific, Canada), 5µg/ml insulin (Sigma Aldrich, Canada), 0.5µg/ml hydrocortisone (Sigma Aldrich, Canada), 50µg/ml ascorbic acid-2-phosphate (Sigma Aldrich, Canada), 1µM isoproterenol (Sigma Aldrich, Canada), 10ng/ml epidermal growth factor (R&D Systems, United States), 1% antibiotic-antimycotic) containing 5% FBS. Fibroblasts were seeded dropwise onto scaffolds at a density of $2.5x10^5$ cells/cm^2 (n=3 per experimental group). Stainless steel tissue-

culture rings (2.25cm inner diameter) were used to maintain a consistent seeding area between scaffolds. Fibroblast-populated scaffolds were cultured in a submerged fashion in modified Green's Medium containing 5% FBS at 37°C, 5% CO_2, 95% relative humidity for four days, with daily medium changes.

Meanwhile, keratinocytes were recovered from liquid nitrogen cryostorage and expanded to 75-80% confluence in T-150 culture flasks using keratinocyte culture medium. On the fourth day after seeding fibroblasts on CGAG scaffolds, keratinocytes were harvested from T-150 culture flasks using TrypLE Express and resuspended in modified Green's Medium containing 1% FBS. Keratinocytes were seeded dropwise onto fibroblast-populated CGAG scaffolds at a density of $5.0x10^5$cells/cm^2. Scaffolds were co-cultured in a submerged fashion in modified Green's Medium containing 1% FBS at 37°C, 5% CO_2, 95% relative humidity for three days, with daily medium changes. One day after keratinocytes were seeded on the matrix, the stainless steel tissue culture rings were removed to allow matrix contraction to begin.

Three days after seeding keratinocytes, scaffolds were lifted to the air-liquid interface on a perforated, stainless steel platform in order to enable epidermal differentiation. Differentiation medium (modified Green's Medium with epidermal growth factor removed and 2µg/ml linoleic acid/bovine serum albumin (BSA) (Sigma Aldrich, Canada) added) was used as the culture medium for the remaining 10 days of co-culture, with daily medium changes. The *in vitro* tissue-engineered skin construct was assayed for further analysis as described below. Cell culture medium was collected on day 17 and stored at -20°C until further use.

Measurement of Contraction of Tissue-engineered Skin

Photographs of the tissue-engineered skin constructs were taken on culture days 7, 10, 14, and 17. Images were analyzed using NIH Image J in order to determine the area of the cell-seeded region for each CGAG scaffold. A ruler was present in each image in order to allow for scale standardization prior to image analysis. Values were reported as mean percent of original area ± standard error.

Quantification of Soluble DCN Expressed into the Culture Medium

Soluble DCN present in the medium on day 17 was quantified using a sandwich enzyme-linked immunosorbent assay (ELISA) specific for human DCN (DuoSet ELISA System, R&D Systems, United States), according to the manufacturer's protocol. The absorbance of colored product in each well was read at 450nm, with a correction wavelength of 550nm, using a microplate reader (THERMOmax, Molecular Devices, United States). A standard curve was created using seven known amounts of DCN and was used to convert absorbance values into concentration values, as described in the manufacturer's protocol. All wells were run in duplicate. DCN concentration was standardized using the total protein concentration of the medium, which was evaluated using a Bio-Rad Protein Assay (Bio-Rad Laboratories, United States) according to the manufacturer's protocol. Data was normalized to the HTS Fb experimental group and reported as mean fold change ± standard error.

Biopsy Preparation for Immunohistochemistry

6mm punch biopsies were taken from the center of each tissue-engineered skin construct on day 17 and fixed using Z-Fix (Anatech Ltd, United States) for 24 hours. Samples were then

processed into paraffin blocks, cut into 5μm slices, and mounted on glass slides by the Alberta Diabetes Institute HistoCore (University of Alberta, Canada).

Analysis of DCN Present in the Matrix

Histological sections were warmed at 60ºC for 20min, deparaffinized in two changes of xylene, and rehydrated in decreasing concentrations of ethanol. Tissue sections were blocked with 10% BSA (Sigma Aldrich, Canada) in PBS for one hour at room temperature, then incubated at 4ºC overnight with primary polyclonal goat anti-human DCN antibody (R&D Systems, United States) diluted 1:200 in 1% BSA. 1% BSA without any primary antibody was used as a negative control for each sample. Sections were then incubated at room temperature for one hour with a Texas-Red-conjugated rabbit anti-goat secondary antibody (Santa Cruz Biotechnology, United States) diluted 1:100 in 1% BSA. Specimens were mounted under glass cover slips using ProLong Gold (Thermo Fisher Scientific, Canada) and imaged at 20x magnification using fluorescent microscopy (Nikon Eclipse Ti, Nikon Instruments, Japan). Fluorescent intensity was evaluated using Nikon NIS-Elements BR software. Values were reported as mean fluorescent intensity/μm^2 ± standard error.

Quantification of Collagen Orientation and Packing Density

Histological sections were warmed at 60ºC for 20min, deparaffinized in two changes of xylene, and rehydrated in decreasing concentrations of ethanol. Sections were stained using picrosirius red dye (0.5g sirius red F3B (Sigma Aldrich, Canada) in 500ml 1.3% picric acid (Sigma Aldrich, Canada) in distilled H_2O) for one hour. Slides were washed in two changes of acidified water (0.5% acetic acid in distilled H_2O), dehydrated in three changes of 100% ethanol, and cleared in xylene. Specimens were mounted under glass cover slips using Permount (Thermo

Fisher Scientific, Canada) and imaged at 40x magnification using circularly polarized light (Nikon Eclipse 50i POL, Nikon Instruments, Japan) in order to visualize collagen fibers.

Image analysis was performed using the power-plot generated by means of the fast Fourier transform feature of NIH Image J (**Figure 2.2)**, as described elsewhere in detail [31]. Briefly, the collagen orientation index (COI) was calculated using **Equation 2.2**:

$$Collagen\ Orientation\ Index = 1 - (\frac{length}{width}\ ratio\ of\ zeroth\ order\ maximum) \quad \textbf{(2.2)}$$

This analysis results in values that range from 0 to 1, with "0" representing perfectly randomly-oriented tissue and "1" representing perfectly parallel-oriented tissue. The distance between the centers of collagen bundles (λ), also known as the collagen bundle packing index (CBPI), was calculated using **Equation 2.3**:

$$\lambda = image\ size\ \times \frac{1}{0.5d} \quad \textbf{(2.3)}$$

where *d* is the distance between centers of gravity of the first order maxima from the generated power-plot. Values were reported as COI or CBPI ± standard error.

Measurement of Collagen Production by Fibroblasts

The total collagen content in the medium on day 17 was determined by quantifying 4-hydroxyproline levels via liquid chromatography/mass spectrometry (LC/MS), as previously described [32]. For each experimental sample, total collagen present in the medium was precipitated on ice using acetonitrile. Precipitates were dried under vacuum, then hydrolyzed overnight at 110°C using 6N hydrochloric acid. A known amount of 4-hydroxyproline-d_3 was then added to the hydrolyzed precipitate for use as an internal standard. A 4:1 molar ratio of n-butanol:acetyl chloride was added to the samples for 30min at 110°C in order to form the n-butyl

ester derivatives of 4-hydroxyproline and 4-hydroxyproline-d_3. Residues were dried under vacuum and dissolved in 20% methanol, before being injected into a liquid chromatograph (Series 1100, Hewlett Packard, United States). 4-hydroxyproline and 4-hydroxyproline-d_3 derivatives were isolated on the column and further analyzed by a mass spectrometer (6130 Quadrupole LC/MS, Agilent Technologies, United States). 188^+ (4-hydroxyproline n-butyl ester) and 191^+ (4-hydroxyproline-d_3 n-butyl ester) ion peaks were measured using a mass-selective detection method and the ratio of the peak areas was used to quantify the level of 4-hydroxyproline in each sample. A standard curve was created using six known amounts of 4-hydroxyproline and was used to convert ratios into concentration values. 4-hydroxyproline concentration was standardized using the total protein concentration of the medium, which was evaluated using a Bio-Rad Protein Assay (Bio-Rad Laboratories, United States) according to the manufacturer's protocol. Data was normalized to the HTS Fb experimental group and reported as mean fold change ± standard error. Samples were run in duplicate.

Assessment of Gene Expression

Expression of DCN, MMP-1, collagen 1 alpha 1 (COL1A1) and TGF-β1 genes were quantified using reverse transcription quantitative PCR (RT-qPCR). Biopsies of tissue-engineered constructs were collected on day 17 and stored at -80ºC until total RNA was extracted from tissue samples, as previously described [32]. Tissue samples were snap-frozen in liquid nitrogen and then homogenized at 1800rpm for 2min (Mikro-Dismembrator S, B. Braun Biotech Inc., United States). The resulting powder was dissolved in TRIzol reagent (Thermo Fisher Scientific, United States) and stored at -80ºC until further use. Total RNA was then extracted using an RNeasy Mini Kit (Qiagen, Canada), according to the manufacturer's protocol. Total RNA concentration and quality (260nm/280nm ratio) was quantified using a NanoDrop

1000 spectrophotometer (Thermo Fisher Scientific, United States). 0.5µg total RNA extract was reverse-transcribed to single-stranded cDNA using a High Capacity cDNA Reverse Transcription Kit (Thermo Fisher Scientific, United States), according to the manufacturer's protocol. cDNA was diluted 1:10 in RNase/DNase-free H_2O (Hyclone, United States) and qPCR was performed with RT^2 SYBR Green/ROX Master Mix (Qiagen, Canada), according to manufacturer's protocol, using gene-specific forward and reverse primers (Eurofins MWG Operon LLC, United States) **(Table 2.3)**. Relative gene expression was calculated through a comparative C_T methodology, using glyceraldehyde 3-phosphate dehydrogenase (GAPDH) as a reference gene and normalizing data to the HTS Fb experimental group. Values were reported as mean fold change ± standard error.

Statistical Analysis

All statistical analysis was performed using STATA 12 (Stata Corporation, United States). Repeated measures ANOVA with Holm-Bonferroni post-hoc analysis was used to assess significance between experimental groups, with $p<0.05$ considered to be significant.

Results

CGAG Matrix Pore Structure

3D acellular matrices for tissue culture were successfully created from CGAG slurries using the freeze-cast, lyophilization method. Matrix cross-sections were examined using SEM after DHT crosslinking treatment and showed a heterogeneous, highly-porous structure through the entire depth of the scaffold **(Figure 2.3)**. The average pore size was determined to be 58.3µm ± 15.1µm.

Cell Viability after Ad5-DCN or Ad5-GFP Transduction

HTS Fb were plated in 2D, transduced with viral supernatant for 18 hours, and assayed at 24, 48, or 72 hours after viral exposure using a MTT assay in order to determine whether viral transduction with either Ad5-DCN or Ad5-GFP influences cell viability. No significant differences in cell viability were found at 24, 48, or 72 hours after viral exposure **(Figure 2.4)**.

Contraction in the *in vitro* Tissue-engineered Skin Model after Viral Transduction

Differences in contraction of the *in vitro* tissue-engineered skin model as a result of fibroblast viral transduction was assessed using digital photography on culture day 7, 10, 14 and 17. Contraction was measured by determining the percent change in the cell-populated-region of matrices from the original area, which was considered to be the inner area of the stainless-steel tissue culture rings ($3.976cm^2$). Contraction began on culture day 5 after the stainless-steel tissue culture rings were removed from the experimental set-up, with significant differences in contraction between experimental groups noted from culture day 10 onward **(Figure 2.5)**. On day 17, HTS Fb+Ad5-DCN constructs showed reduced contraction as compared to the HTS Fb ($p<0.05$). Contraction in the HTS Fb+Ad5-DCN constructs appears to reach a plateau from day 14 onward.

Soluble and Matrix-bound DCN Protein Levels

Medium on culture day 17 was harvested and analyzed using ELISA in order to measure the relative amount of soluble DCN protein expressed by cells cultured in the *in vitro* tissue-engineered skin model **(Figure 2.6)**. HTS Fb+Ad5-DCN exhibited an approximately 27-fold increase in expressed DCN protein, as compared to all other experimental groups ($p<0.0001$

each). Although the NS Fb group had elevated DCN protein levels as compared to the HTS Fb group (1.22-fold) the difference was not significant.

Histological sections of the *in vitro* tissue-engineered skin constructs were also stained via immunofluorescence to assess matrix-bound DCN levels **(Figure 2.7)**. HTS Fb+Ad5-DCN constructs had increased levels of matrix-bound DCN as compared to the HTS Fb+Ad5-GFP and HTS Fb groups ($p<0.0001$ each) **(Figure 2.8)**. The NS Fb group also showed an elevation in matrix-bound DCN compared to the HTS Fb+Ad5-GFP and HTS Fb groups ($p<0.01$ and $p<0.05$, respectively). The HTS Fb+Ad5-DCN group also had matrix-bound DCN levels that were higher than that of the NS Fb group ($p<0.05$).

Collagen Orientation and Packing Density in the *in vitro* Tissue-engineered Skin Model

Histological sections were stained with picrosirius red and viewed using circularly-polarized light. Type I collagen fibers can be clearly seen in these micrographs, with fibers located in the remodeled areas of the scaffold appearing as mostly yellow or orange in color and fibers of the scaffold appearing as deep red in color **(Figure 2.9)**. Moreover, the remodeled areas of the matrix also contain thin green fibers which neighbor the type I collagen fibers and are lower in illumination intensity, indicating the presence of type III collagen.

Polarized microscopy images were subsequently analyzed via a fast Fourier transformation in order to determine collagen orientation and packing density. COI in the HTS Fb+Ad5-DCN group was reduced as compared to HTS Fb and HTS Fb+Ad5-GFP ($p<0.05$ and $p<0.01$, respectively), indicating a more randomly-oriented collagen organization that is typically associated with normal skin **(Figure 2.10a)**. The NS Fb experimental group had a similar COI to HTS Fb+Ad5-DCN, which was reduced as compared to the HTS Fb and HTS Fb+Ad5-GFP

groups ($p<0.01$ and $p< 0.001$, respectively). Moreover, the CBPI in the HTS Fb+Ad5-DCN group was increased as compared to the HTS Fb and HTS Fb+Ad5-GFP groups ($p<0.05$ each) **(Figure 2.10b)**. This represents an increase in distance between collagen bundles and, therefore, a reduction in collagen packing density. The NS Fb experimental group had a similar CBPI to HTS Fb+Ad5-DCN, which was increased as compared to the HTS Fb and HTS Fb+Ad5-GFP groups ($p<0.01$ and $p< 0.001$, respectively).

Collagen Production by Fibroblasts

The amount of collagen produced by fibroblasts was determined by quantifying the relative amount of 4-hydroxyproline present in the culture medium on day 17 using LC/MS. HTS Fb+Ad5-DCN exhibited lower collagen levels in the medium than untreated HTS Fb ($p<0.05$) **(Figure 2.11)**. HTS Fb+Ad5-DCN collagen levels were also lower than those in the NS Fb experimental group ($p<0.01$). No differences in 4-hydroxyproline levels were found between HTS Fb and NS Fb experimental groups. HTS Fb+Ad5-GFP exhibited lower collagen production than untreated HTS Fb, though the difference was not found to be statistically significant. Additionally, HTS Fb+Ad5-GFP had reduced total collagen levels as compared to the NS Fb group ($p<0.05$).

Relative Gene Expression

Relative mRNA expression of DCN, MMP-1, COL1A1, and TGF-β1 was evaluated for each experimental group in order to assess the impact of Ad5-DCN transduction on genes which are commonly modulated during fibrosis. Gene expression was evaluated using a comparative C_T methodology, using GAPDH as a housekeeping gene and normalizing expression data to the HTS Fb group. The HTS Fb+Ad5-DCN group had a roughly 19-fold increase in DCN mRNA as

compared to each of the other experimental groups ($p<0.01$ each) **(Figure 2.12a)**. No significant difference was found between other experimental groups, with respect to DCN mRNA expression. MMP-1 mRNA levels were found to be 5-fold higher in the HTS Fb+Ad5-DCN group as compared to HTS Fb ($p<0.05$), with similar increases found when compared to the HTS Fb+Ad5-GFP and NS Fb groups ($p<0.01$ and $p<0.05$, respectively) **(Figure 2.12b)**. COL1A1 mRNA levels were reduced in the HTS Fb+Ad5-DCN constructs, as compared to HTS Fb+Ad5-GFP and NS Fb ($p<0.05$ each) **(Figure 2.12c)**. It should be noted that the HTS Fb+Ad5-DCN reduction in COL1A1 mRNA as compared to HTS Fb approached significance ($p<0.06$). No significant differences in TGF-β1 mRNA expression were found between experimental groups **(Figure 2.12d)**.

Discussion

Despite advances in therapies, HTS after burn injury continues to present a major clinical problem for physicians. The development of HTS involves the modulation of many cytokines and growth factors involved in wound healing, with TGF-β1 continuing to stand out as a central factor involved in the pathogenesis of this fibroproliferative disorder. Unfortunately, antibody neutralization of TGF-β1 activity does not fully reverse fibrosis, indicating a need for therapeutics that can antagonize TGF-β1 while simultaneously improving the ECM morphology of fibrotic lesions [33]. As such, novel gene therapies involving the delivery of DCN have shown promise in preventing TGF-β1-mediated fibrosis, due to its crucial involvement in collagen fibrillogenesis as well as its ability to bind to and sequester TGF-β1 in the ECM. Adenoviral vectors have been particularly effective as a vehicle for these therapies, due to their transient nature, their ease for generating high-titer stocks, and their ability to transduce dividing and quiescent cells [34]. Therefore, this study explored the impact of adenoviral-DCN therapy on the

matrix remodeling behavior of HTS Fb in an *in vitro* tissue-engineered skin model in order to evaluate its potential as a therapeutic for HTS.

After confirming that Ad5-DCN and Ad5-GFP does not impact HTS Fb viability post-transduction, transduced cells were seeded onto CGAG scaffolds in order to create organotypic skin models. CGAG matrices were the scaffold of choice for this study, due to their prior successes as an *in vitro* model for investigating dermal fibrosis [27, 35]. Additionally, these scaffolds have been used successfully in the clinic, both as a wound dressing and as a scaffold for creating tissue-engineered split-thickness skin grafts [36, 37]. SEM analysis of the CGAG scaffolds used in this study had an average pore diameter of 58.3μm ± 15.1μm, which falls well within the 20-120μm pore size range that is considered to be optimal for creating tissue-engineered skin [38]. Evaluation of the pore structure with the naked eye indicates a heterogeneous distribution (coefficient of variation = 0.259) of pore structures with slight alignment in areas of the scaffold cross-section. This is in disagreement with the findings of O'Brien, et al., who indicated that a 0.9ºC/min freezing rate during the construction of CGAG scaffolds results in a larger, more uniform pore size (coefficient of variation = 0.128) [39]. These discrepancies could be the result of the different methodologies used for freezing the CGAG scaffolds as well as the different concentrations of collagen and chondroitin-6-sulfate in the CGAG slurry. That being said, the pore size and structure of the scaffolds used in this study is in agreement with CGAG scaffolds used previously by our group for creating 3D *in vitro* skin models [40].

Fibroblasts growing in 3D collagen matrices have been found to have different mechanics when compared to those grown in 2D plastic dishes. This is because fibroblasts grown in 3D matrices can penetrate into the structure, become entangled with the matrix fibers, and remodel

the fibers in order to achieve tensional homeostasis – the restoration of a preferred mechanical microenvironment [41]. As a result, measuring the contraction of fibroblast-populated collagen lattices has been widely used to assess the impact of therapeutics on the mechanical behavior of fibroblasts [42-44]. In this study, we found that organotypic skin models created using Ad5-DCN-treated HTS Fb had reduced contraction on day 17 onward as compared to those constructed with untreated HTS Fb, indicating that Ad5-DCN gene therapy had reduced the contractile phenotype of HTS Fb. Interestingly, the Ad5-DCN-treated group had the greatest level of contraction on days 7 and 10 of culture, and then plateaued in contraction between days 14 and 17 of culture. This suggests that Ad5-DCN therapy may, in part, exert its effect via faster attainment of tensional homeostasis in the collagen-based matrix. This idea is further supported by the fact that matrices in the other experimental groups still appear to be contracting on day 17.

In order to confirm that these contraction effects during culture were the result of DCN upregulation, DCN protein levels on day 17 were measured for each experimental group. There was an almost 27-fold increase in DCN protein expressed in the medium of the Ad5-DCN-treated experimental group on day 17 as compared to the untreated HTS Fb group. DCN elevation in the HTS Fb+Ad5-DCN group also exhibited a similar increase as compared to the NS Fb control group. This protein expression behavior is particularly notable when considering that the prior adenoviral-DCN study by Kwan, et al. required a MOI of 500 to raise the DCN expression of deep dermal fibroblasts to that of superficial fibroblasts, while this study only used a MOI of 25 [25]. This inconsistency can be explained by the different cell types used in each experiment, as HTS Fb have been found to have higher expression of α_v integrins when compared to NS Fb, a cell-surface protein which is heavily involved in the cellular uptake of adenoviral vectors [45, 46].

Although elevated DCN levels in the medium indicate the proper functioning of the Ad5-DCN vector, evidence suggests that soluble DCN is ineffective at suppressing the fibrotic effects of TGF-β1 [21]. Rather, collagen-bound DCN sequesters TGF-β1 in the matrix and prevents it ability to activate fibrotic behavior. Therefore, DCN protein levels in the collagen matrix were evaluated using immunofluorescent staining, where it was found to be present in elevated levels in the Ad5-DCN-treated and NS Fb experimental groups as compared to the Ad5-GFP and HTS Fb groups. Though the Ad5-DCN-treated group was the experimental group with the highest amount of matrix-bound DCN, the elevation was not as extreme as that found in the medium via ELISA. This suggests that the CGAG matrix may have reached a saturation point with respect to DCN content in the Ad5-DCN group, with the remaining DCN being expressed into the medium. This may also explain why the DCN levels measured in the medium of the NS Fb group were not significantly higher than that of the HTS Fb or the Ad5-GFP experimental groups, as the CGAG matrix had not yet reached its saturation point with DCN.

RT-qPCR data showed a 19-fold increase in DCN mRNA present in the tissue of the Ad5-DCN-treated group, as compared to the HTS Fb group. Likewise, there was a 13-fold increase DCN mRNA in the Ad5-DCN group as compared to the NS Fb group. Moreover, there was no significant difference between the HTS Fb and NS Fb groups in terms of mRNA expression. This suggests that the elevated matrix levels of DCN seen in the Ad5-DCN and NS Fb groups are probably the result of different two mechanisms. While the DCN increase in the Ad5-DCN-transduced group can be ascribed to the transcription and translation of the transduced adenoviral genome, the matrix-bound DCN increase in the NS Fb group is most likely the result of post-translational modulation. Prior studies by our group on miRNA-181b inhibition of DCN mRNA translation in HTS Fb supports this notion [47].

Junqueira, et al. first discovered in 1979 that picrosirius red staining is a specific histological stain for collagen when used in conjunction with polarized light, due the enhanced birefringence displayed by Sirius-Red-bound collagen fibers [48]. This staining methodology becomes increasingly useful when combined with circularly-polarized light, resulting in a more accurate assessment of collagen content as compared to Masson's trichrome [49]. Moreover, picrosirius red staining can be used to differentiate between collagen types I and III histologically, due to variations in the color of collagen birefringence [50].

Interestingly, type I and type III collagens were both found in the fibroblast-populated regions of the CGAG matrix in all experimental groups. Evaluation with the naked eye appears to show an enhancement in type III collagen production in the NS Fb, due to the increased presence of thin green fibers found in these histological sections. Although HTS tissue has been shown to contain higher amounts of type III collagen, this behavior can also be an indication of immature collagen expression. During the early phases of normal wound healing, type III collagen is elevated and helps to regulate the collagen fibrillogenesis process by influencing the fibril diameter of type I collagen [51]. Notably, fetal ECM – which is characterized by a scarless wound healing phenotype – is rich with type III collagen, making up 30-60% of the total collagen content of fetal tissue [51]. Therefore, the type III collagen seen in the NS Fb experimental group histological sections are most likely the result of an enhanced capacity for collagen turnover and remodeling.

Remarkably, Ad5-DCN-treated HTS Fb showed a suppressed expression of 4-hydroxyproline in the medium as compared to the HTS Fb experimental group when measured via LC/MS. One may initially conclude that this decrease is partially due to the adenoviral vector treatment, rather than DCN gene delivery, since the Ad5-GFP-treated group also displayed a

non-significant reduction in total collagen protein expression. However, RT-qPCR data for the gene expression of COL1A1 suggests that this reduction in collagen is due to an effect on pro-alpha I chain synthesis by the Ad5-DCN treatment. This is supported by literature showing that recombinant decorin therapy suppresses type I procollagen expression, but not type III procollagen [22]. Gene expression of COL1A1 was not affected by the Ad5-GFP experimental group. Notably, both RT-qPCR and 4-hydroxyproline data indicate no apparent difference in collagen gene and protein expression between the NS Fb and HTS Fb groups. This is in agreement with prior literature indicating little to no change in the collagen content of HTS on the basis of dry weight compared to normal dermis [52].

Due to DCN's role in properly orienting collagen during fibrillogenesis, collagen organization was also assessed in order to determine the therapeutic impact of saturated DCN levels on matrix remodeling. Recently, there has been a trend towards quantitatively evaluating collagen orientation using Fourier analysis of eosin-stained histological sections in order to better understand differences between the normal and pathological ECM conditions [31, 53, 54]. Because of the enhanced specificity for collagen identification when used in conjunction with polarized light, this study used picrosirius red staining combined with fast Fourier transform digital analysis in order to assess collagen orientation and collagen packing density. Collagen was found to be more randomly-oriented in the in the Ad5-DCN group, at a level that was similar to that of the NS Fb experimental group. Moreover, the increased CBPI in the Ad5-DCN and NS Fb groups indicate a reduced packing density of collagen as compared to the Ad5-GFP and HTS Fb groups. Therefore, Ad5-DCN treatment exhibited a therapeutic effect on the matrix remodeling behavior of HTS Fb, resulting in a more normal-skin-like matrix morphology. MMP-1 suppression, either through decreased mRNA levels or TGF-β1-stimulated expression of

TIMP-1, is thought to play a significant role in mediating the abnormal collagen orientation found in HTS lesions [51]. This cell protease cleaves type I collagen into ¾ and ¼ length pieces, which can then be further digested by other metalloproteinases. Notably, MMP-1 mRNA was elevated in HTS Fb after treatment with Ad5-DCN, suggesting a mechanism for the above improvements to matrix remodeling.

Taken together, the above data indirectly suggests an inhibition of TGF-β1-mediated fibrosis in HTS Fb as a result of Ad5-DCN treatment. As such, mRNA expression for TGF-β1 was measured in order to evaluate a possible mechanism by which Ad5-DCN gene therapy suppresses TGF-β1 activity. Though a reduction in TGF-β1 mRNA was anticipated in the Ad5-DCN group, no differences were found between the Ad5-DCN and HTS Fb experimental groups. Therefore, it appears that the Ad5-DCN gene therapy does not impact the inherent nature of HTS Fb to produce TGF-β1, which is in disagreement with other DCN gene therapies used for dermal scar therapy [22, 23]. However, TGF-β1 mRNA levels may not fully reflect the protein activity of TGF-β1, given that TGF-β1 is secreted in a latent form from the cell and is extracellularly processed into its activated state [55]. Therefore, this Ad5-DCN gene therapy may exert its therapeutic effects through the elevation of matrix protein levels of DCN, which could allow for the enhanced sequestration in the ECM of active TGF-β1.

Tables

Table 2.1. Patient information for site-matched normal skin/hypertrophic scar fibroblasts and normal keratinocytes. TBSA = total body surface area burned.

Patient Number	Gender	Age	Cells Used	TBSA
1	Female	27	Matched Fibroblasts	25%
2	Female	23	Matched Fibroblasts	12%
3	Female	50	Normal Keratinocytes	0% (Abdominoplasty Tissue)
4	Male	40	Matched Fibroblasts	0% (Trauma-related Scar)
5	Male	22	Matched Fibroblasts	15%

Table 2.2. Freeze dryer system temperature during lyophilization of CGAG matrices.

Step	Initial Temp. (°C)	Final Temp. (°C)	Ramp Speed (°C/min)	Hold Time (hr)
1	-40	-40	-	-
2	-40	-30	0.2	5
3	-30	-20	0.2	4
4	-20	-4	0.2	4
5	-4	20	0.2	Indefinite

Table 2.3. Primers used for quantitative polymerase chain reaction.

Gene of Interest	Forward Primer	Reverse Primer
GAPDH	5’-ACCCCTTCATTGACCTCAAC-3’	5’-GAGATGATGACCCTTTTGGC-3’
DCN	5’-AGAAGTTCCTGATGACCGCGACTT-3’	5’-TGTTGTCCAAGTGAAGCTCCCTCA-3’
MMP-1	5’-ACACATCTGACCTACAGGATTGA-3’	5’-GTCTGACATTACTCCAGAGTTGG-3’
COL1A1	5’-AAGAGGAAGGCCAAGTCGAG-3’	5’-CACACGTCTCGGTCATGGTA-3’
TGF-β1	5’-ACCCACAACGAAATCTATGAC-3’	5’-GCTCCACTTTTAACTTGAGCC-3’

Figures

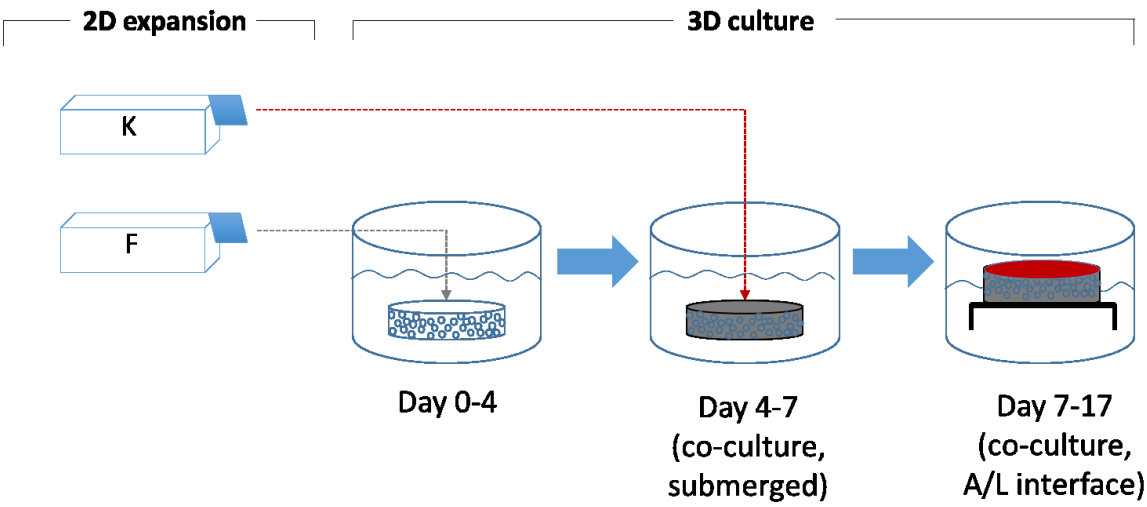

Figure 2.1. Summary of the cell culture procedure using for creating an in vitro tissue-engineered skin model. Virus-treated HTS Fb were transduced 18 hours prior to seeding on CGAG scaffolds, during the 2D expansion phase of cell culture, at a MOI of 25.

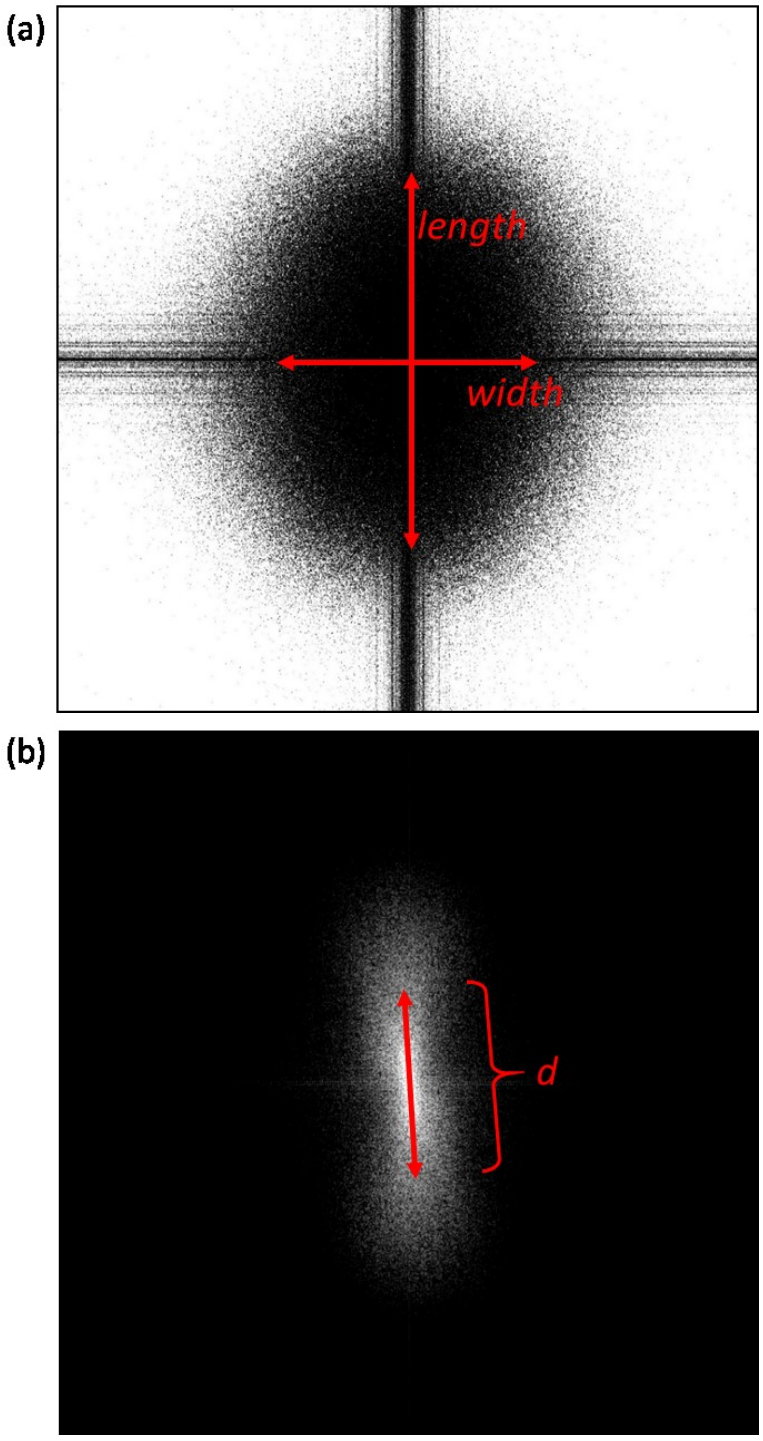

Figure 2.2. Analysis using the Fourier power plot. (a) Zeroth order maximum of the Fourier power plot showing length and width used in the calculation of the collagen orientation index. (b) First order maximum of the Fourier power plot showing the distance, d, between centers of gravity used in the calculation of the collagen bundle packing index.

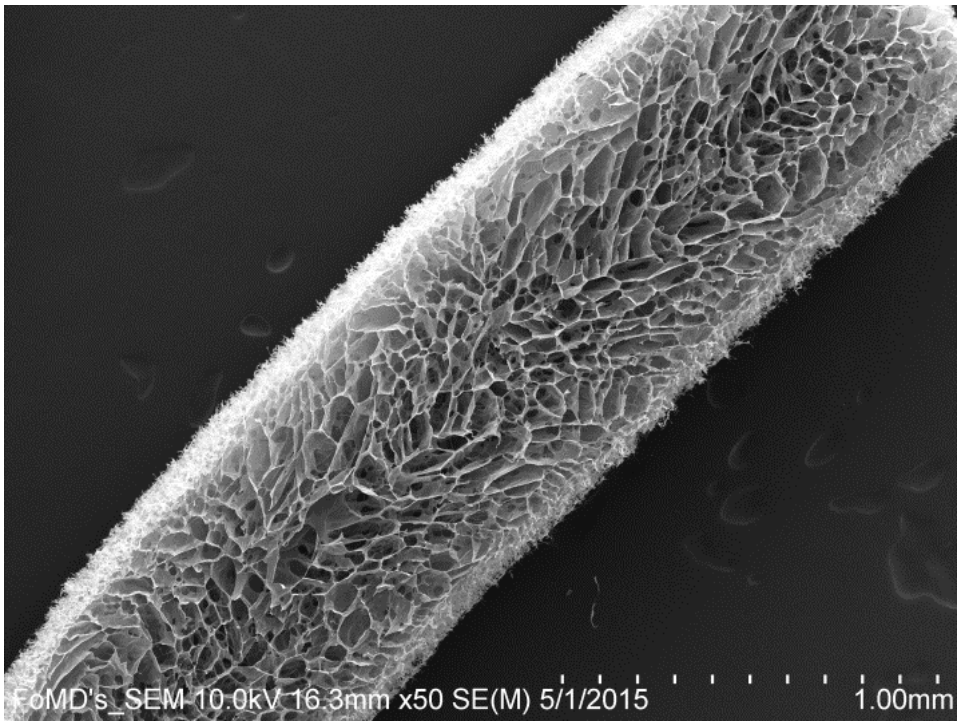

Figure 2.3. Scanning electron micrograph depicting the cross-section of a dehydrothermally-crosslinked CGAG scaffold at 50x magnification. Accelerating voltage was 10.0kV and working distance was 16.3mm. Scale bar = 1.00mm.

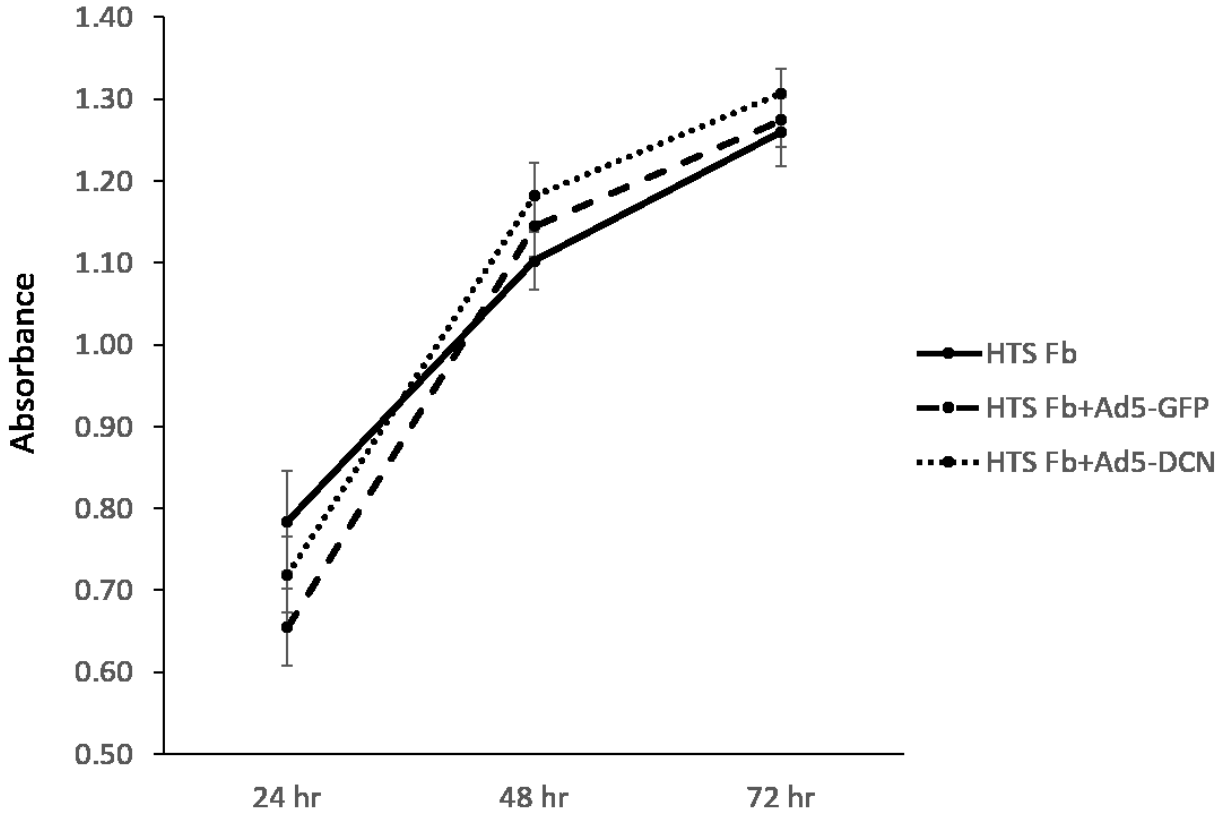

Figure 2.4. Cell viability of HTS Fb that were cultured for 24, 48, or 72 hours after exposure to either Ad5-DCN, Ad5-GFP, or no viral treatment. Absorbance at 650nm was subtracted from absorbance at 540nm in order to correct for optical imperfections in 96-well plates. Data is reported as mean corrected absorbance ± standard error.

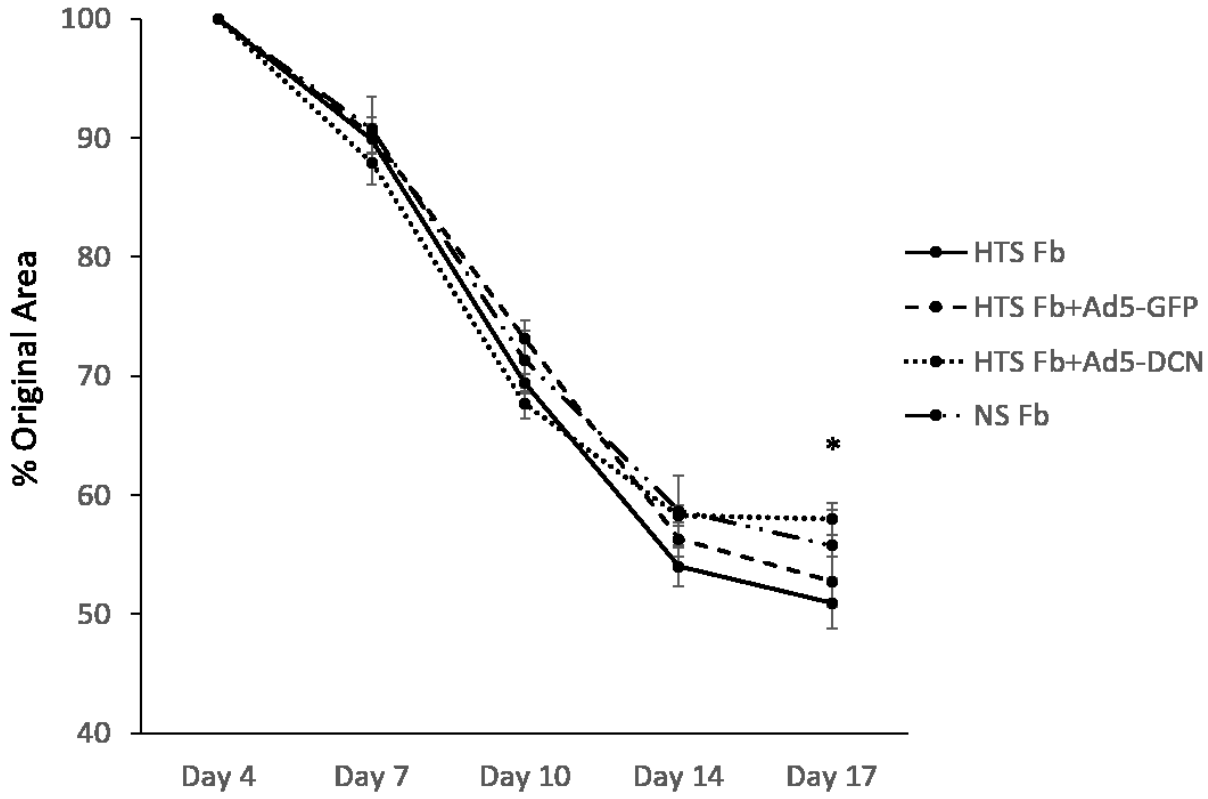

Figure 2.5. Contraction of in vitro tissue-engineered skin constructs over the course of 17 days of culture. Data is reported as mean percent original area on culture days 7, 10, 14 and 17 ± standard error. The value reported on culture day 4 represents 100% of the original area. *: $p<0.05$, HTS Fb+Ad5-DCN vs HTS Fb.

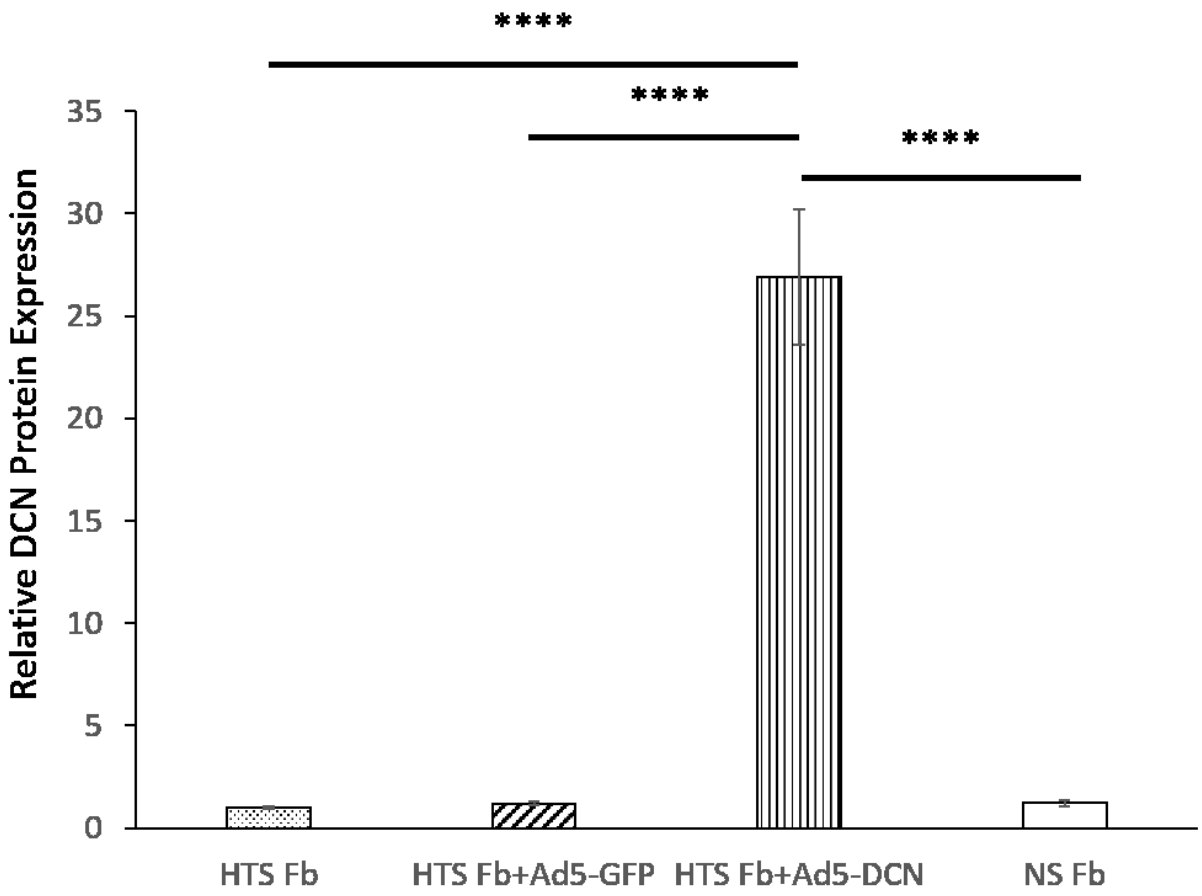

Figure 2.6. DCN protein in the culture medium on day 17 of cell culture was determined for each experimental group using ELISA. DCN levels were standardized using the total protein content of the medium. Data is normalized to the HTS Fb experimental group and reported as mean fold change ± standard error. ****: $p<0.0001$.

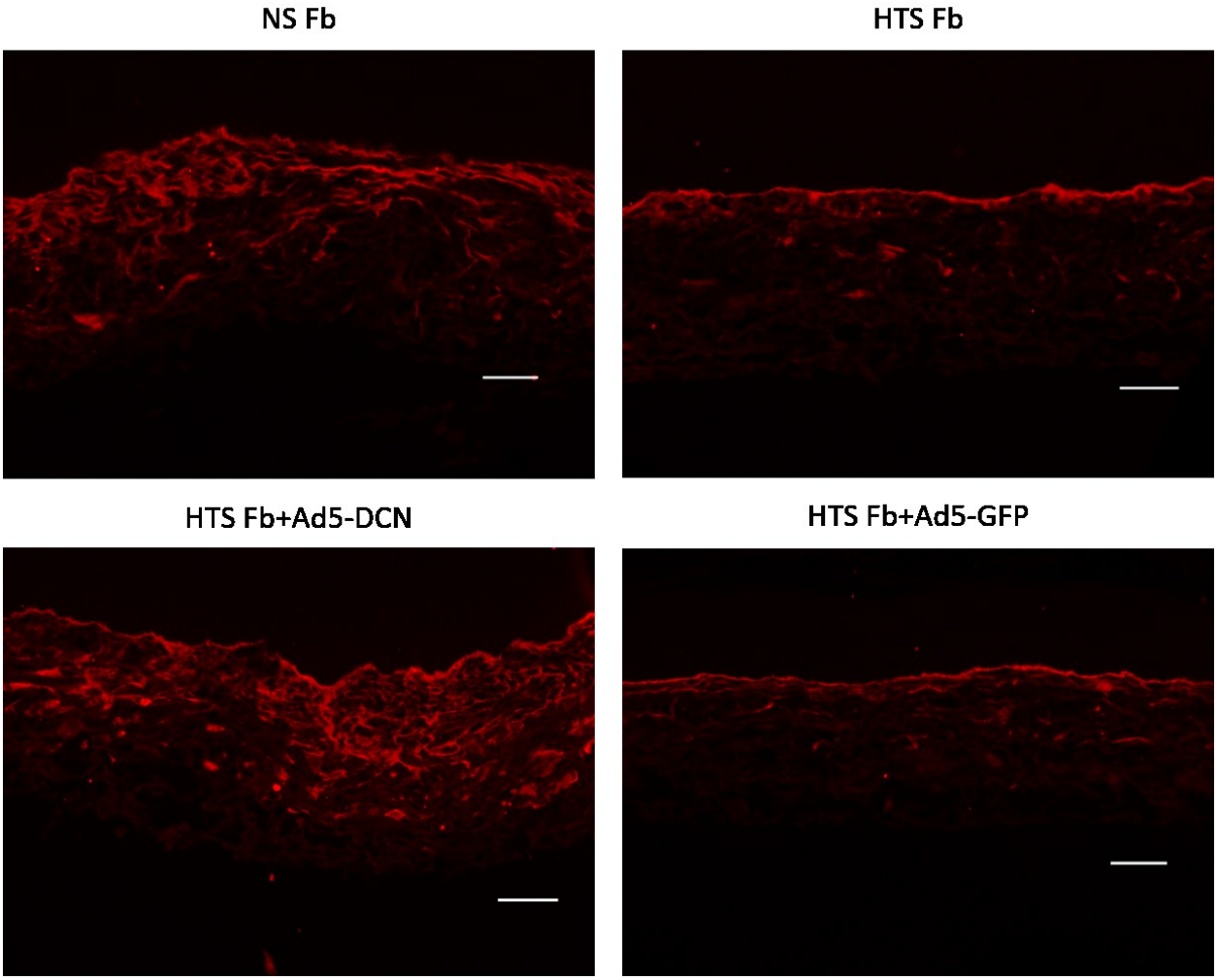

Figure 2.7. Paraffin sections of experimental tissue-engineered skin constructs stained via immunofluorescence for DCN, using a polyclonal goat anti-human DCN antibody and a Texas Red-conjugated secondary antibody (red fluorescence). Images were taken at 20x magnification. Scale bar = 50μm.

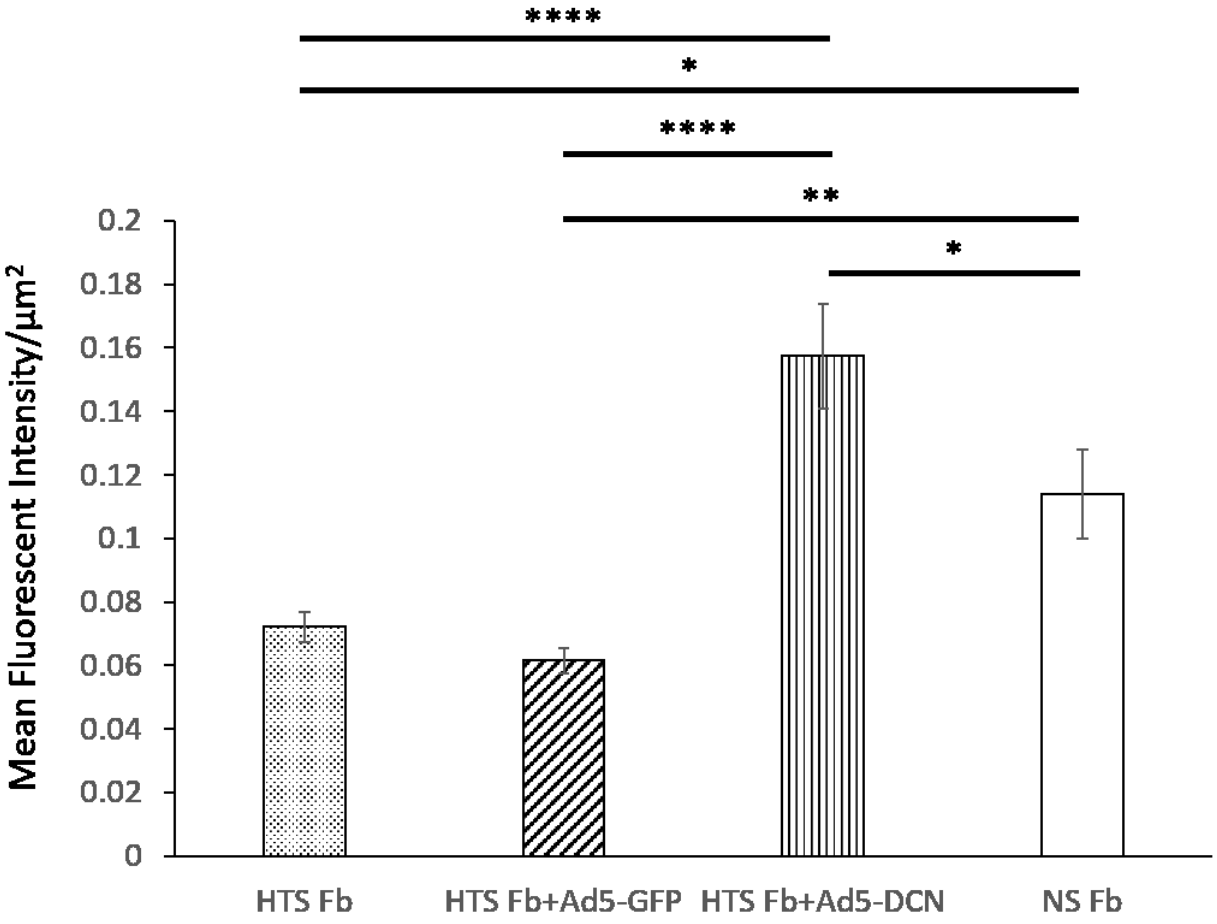

Figure 2.8. Fluorescent intensity was measured for each DCN-stained histological section using Nikon NIS-Elements BR software in order to evaluate matrix-bound DCN levels. Data is reported as mean fluorescent intensity/μm^2 ± standard error. *: $p<0.05$; **: $p<0.01$; ****: $p<0.0001$.

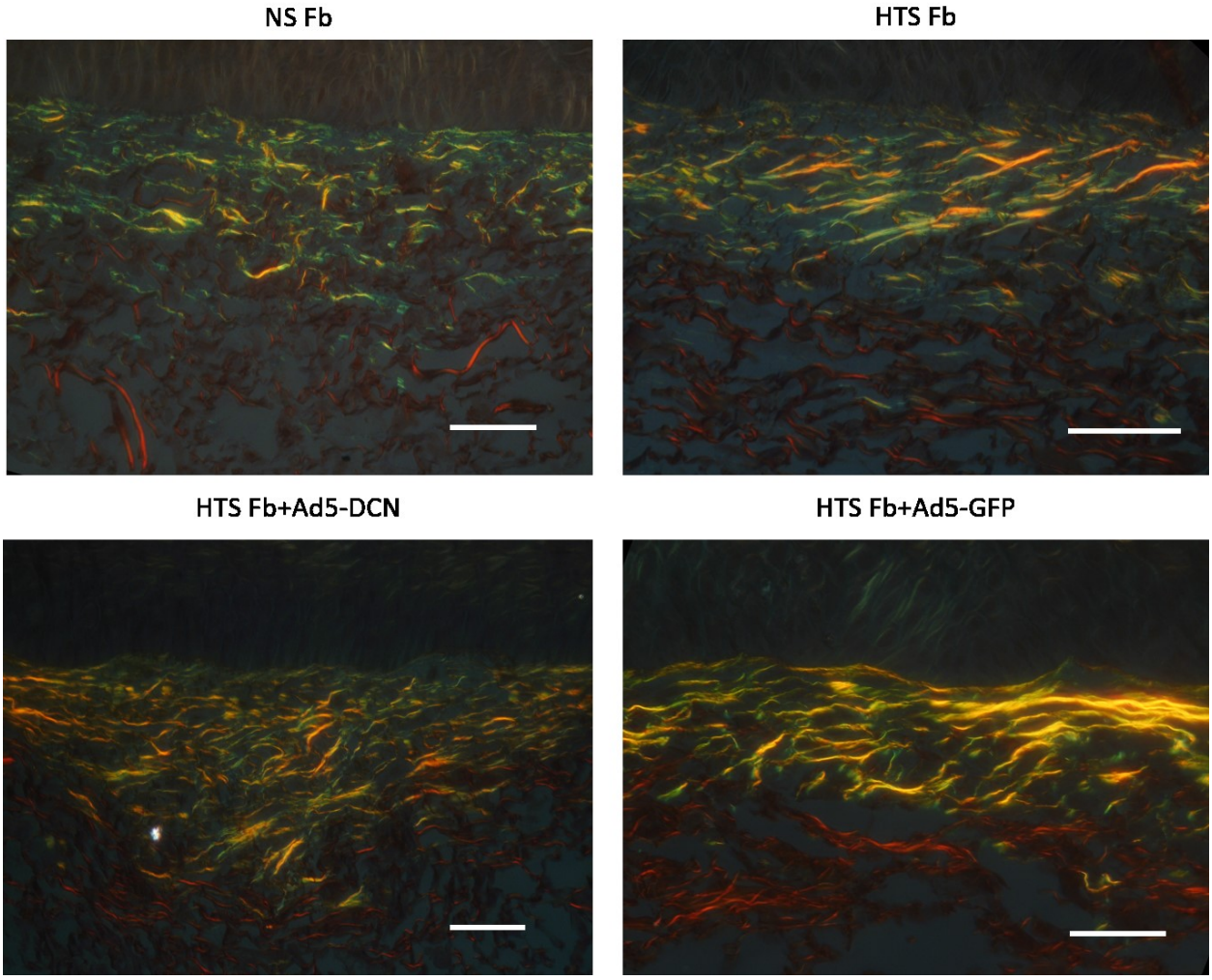

Figure 2.9. Paraffin sections of experimental tissue-engineered skin constructs stained with picrosirius red and viewed under circularly-polarized light. Type I collagen appears as bright yellow, orange, or red fibers, while type III collagen appears as thin green fibers that are lower in illumination intensity. Images were taken at 40x magnification. Scale bar = 50μm.

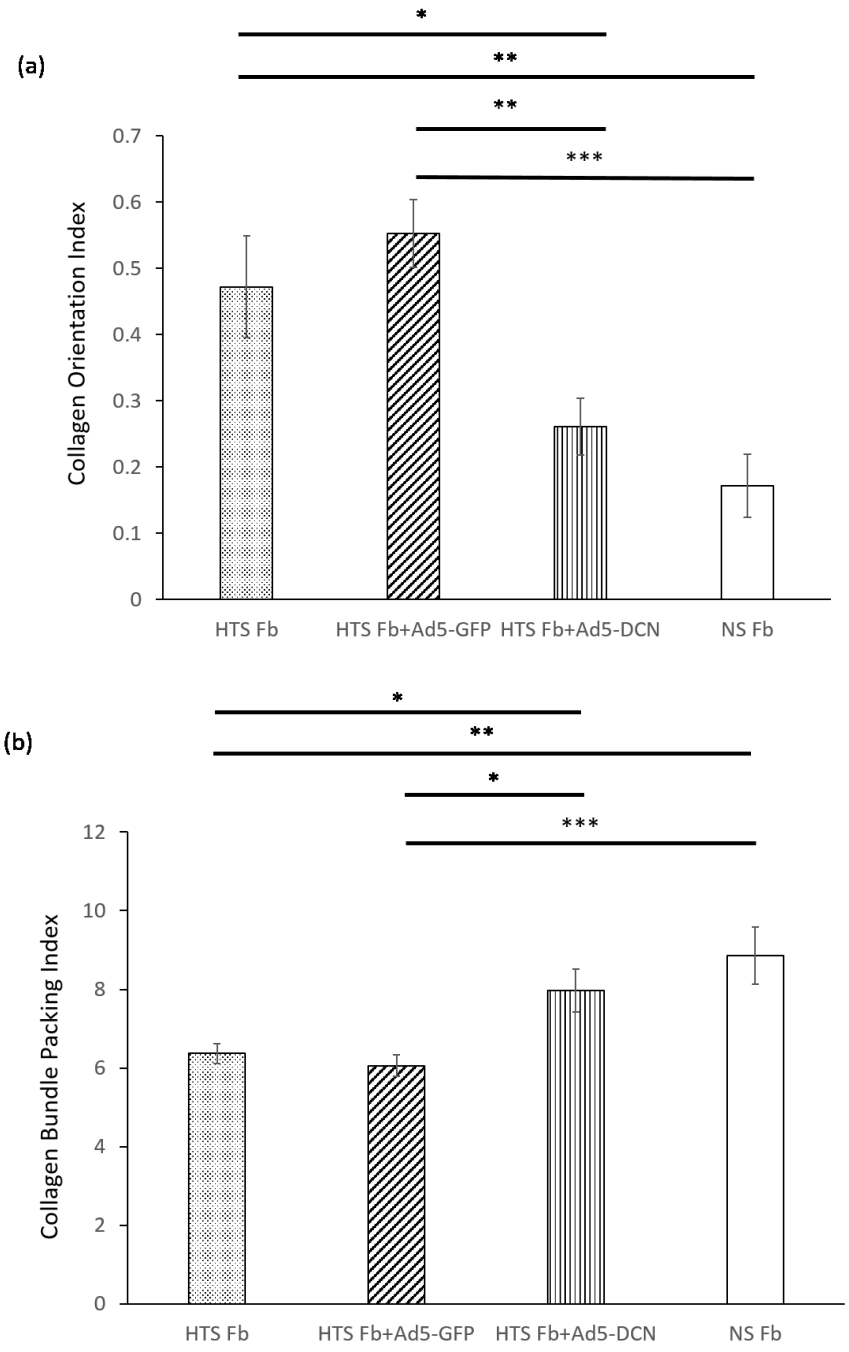

Figure 2.10. Assessment of collagen orientation and bundle packing. (a) COI was calculated in order to quantitatively assess collagen organization in the picrosirius-red-stained histological sections. Values are reported as mean COI ± standard error. (b) CBPI was calculated so as to evaluate collagen packing density in the picrosirius-red-stained histological sections. Values are reported as mean CBPI ± standard error. *: $p<0.05$; **: $p<0.01$; ***: $p<0.001$.

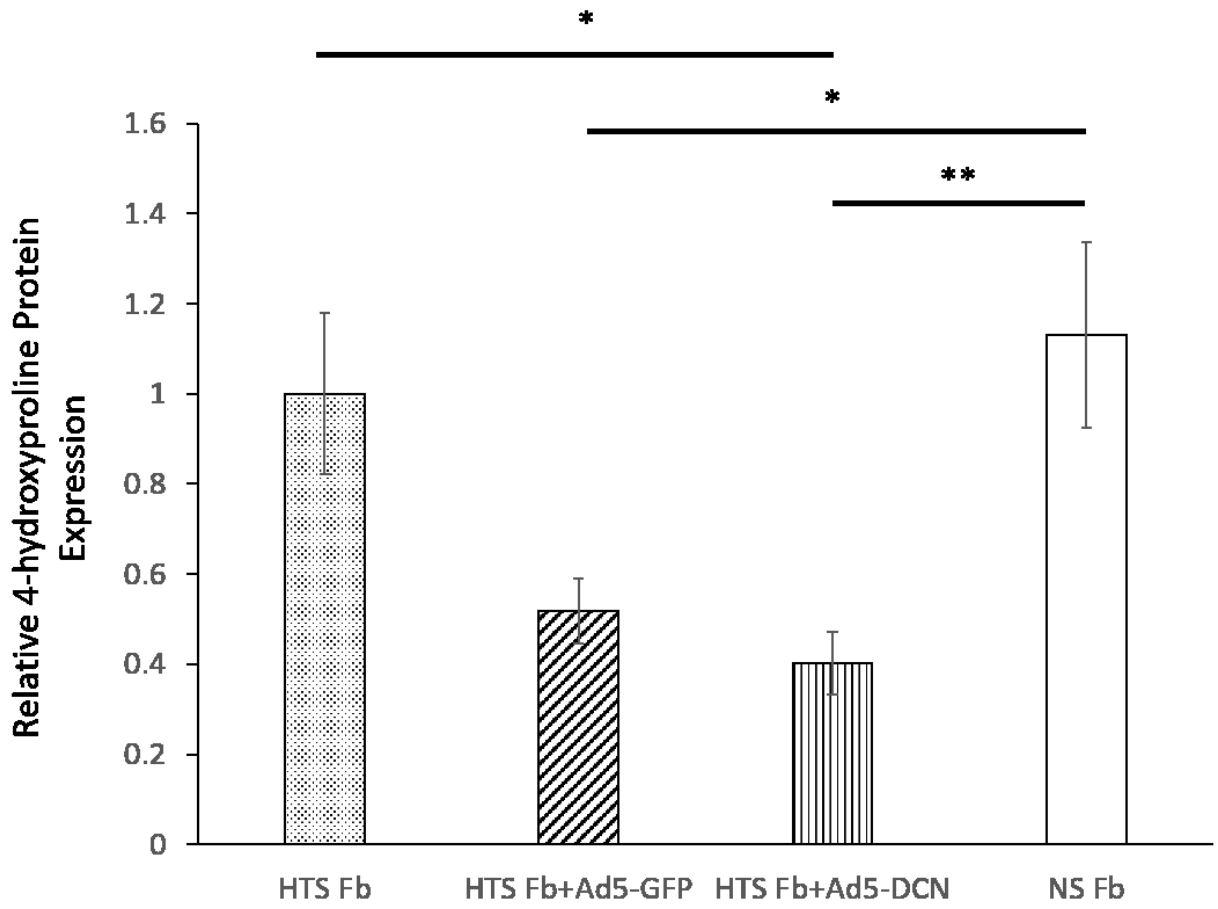

Figure 2.11. Collagen production by fibroblasts in each experimental group was measured via LC/MS using the culture medium collected on day 17. 4-hydroxyproline levels were standardized using the total protein content of the medium. Data is normalized to the HTS Fb experimental group and reported as mean fold change ± standard error. *: $p<0.05$, **: $p<0.01$.

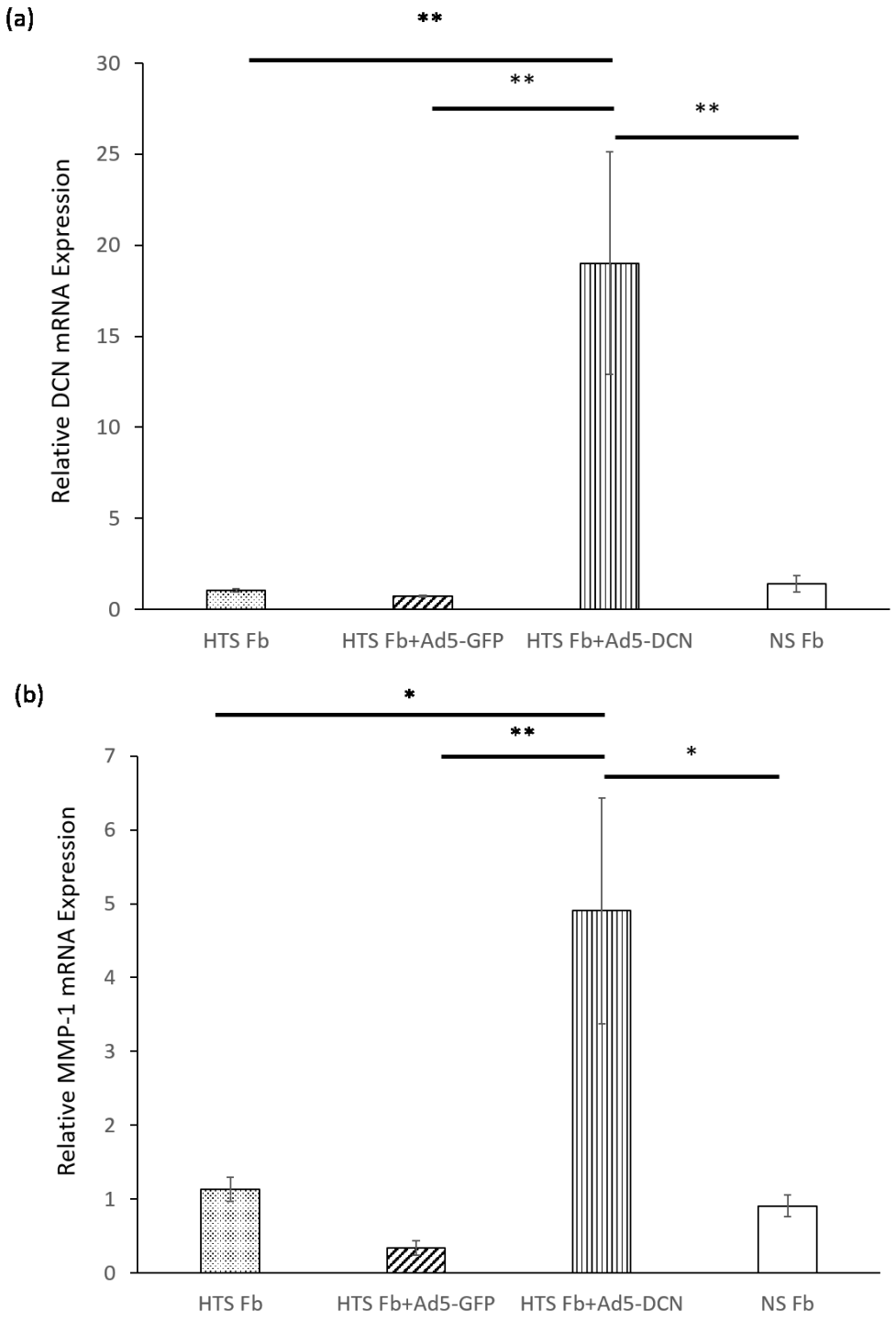
(a)
**
**
**
Relative DCN mRNA Expression
30
25
20
15
10
5
0
HTS Fb
HTS Fb+Ad5-GFP
HTS Fb+Ad5-DCN
NS Fb
(b)
*
**
*
Relative MMP-1 mRNA Expression
7
6
5
4
3
2
1
0
HTS Fb
HTS Fb+Ad5-GFP
HTS Fb+Ad5-DCN
NS Fb

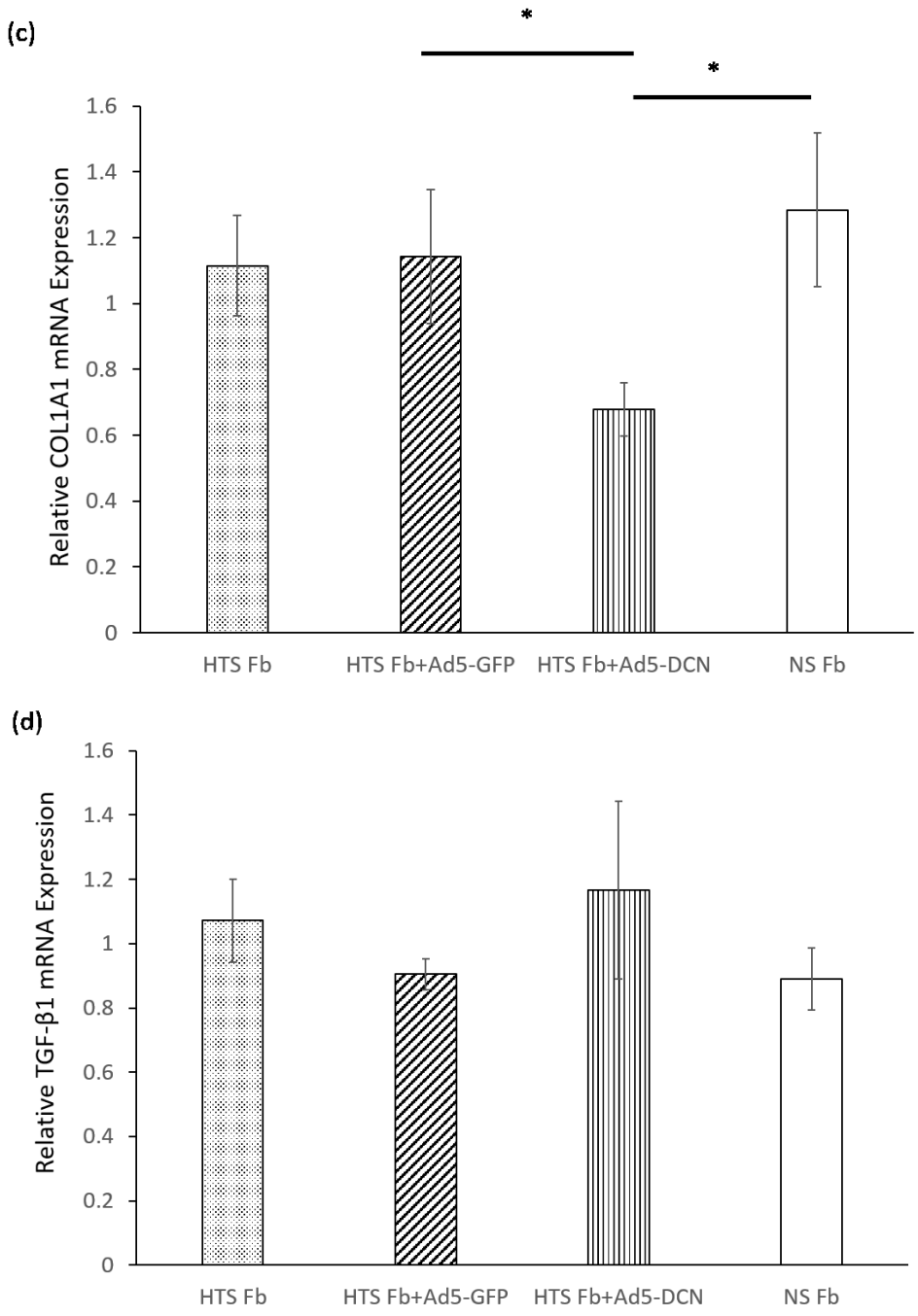

Figure 2.12. Total mRNA was extracted from *in vitro* tissue-engineered skin constructs and gene expression was quantified by RT-qPCR for relative (a) DCN mRNA, (b) MMP-1 mRNA, (c) COL1A1 mRNA, and (d) TGF-β1 mRNA levels. mRNA levels were standardized using GAPDH. Data is normalized to the HTS Fb experimental group and reported as mean fold change ± standard error. *: $p<0.05$; **: $p<0.01$.

References

1. Gangemi, E.N., Gregori, D., Berchialla, P., Zingarelli, E., Cairo, M., Bollero, D., Ganem, J., Capocelli, R., Cuccuru, F., Cassano, P., Risso, D., and Stella, M., *Epidemiology and risk factors for pathologic scarring after burn wounds.* Archives of Facial Plastic Surgery, 2008. **10**(2): p. 93-102.
2. Lawrence, J.W., Mason, S.T., Schomer, K., and Klein, M.B., *Epidemiology and impact of scarring after burn injury: a systematic review of the literature.* Journal of Burn Care & Research, 2012. **33**(1): p. 136-46.
3. Bock, O., Schmid-Ott, G., Malewski, P., and Mrowietz, U., *Quality of life of patients with keloid and hypertrophic scarring.* Archives for Dermatological Research. Archiv für Dermatologische Forschung, 2006. **297**(10): p. 433-8.
4. Penn, J.W., Grobbelaar, A.O., and Rolfe, K.J., *The role of the TGF-beta family in wound healing, burns and scarring: a review.* International Journal of Burns and Trauma, 2012. **2**(1): p. 18-28.
5. Kwan, P., Hori, K., Ding, J., and Tredget, E.E., *Scar and contracture: biological principles.* Hand Clinics, 2009. **25**(4): p. 511-28.
6. Friedman, D.W., Boyd, C.D., Mackenzie, J.W., Norton, P., Olson, R.M., and Deak, S.B., *Regulation of collagen gene expression in keloids and hypertrophic scars.* Journal of Surgical Research, 1993. **55**(2): p. 214-22.
7. Edwards, D.R., Murphy, G., Reynolds, J.J., Whitham, S.E., Docherty, A.J., Angel, P., and Heath, J.K., *Transforming growth factor beta modulates the expression of collagenase and metalloproteinase inhibitor.* EMBO Journal, 1987. **6**(7): p. 1899-904.

8. Linares, H.A., Kischer, C.W., Dobrkovsky, M., and Larson, D.L., *The histiotypic organization of the hypertrophic scar in humans.* Journal of Investigative Dermatology, 1972. **59**(4): p. 323-31.

9. Kozma, E.M., Olczyk, K., Glowacki, A., and Bobinski, R., *An accumulation of proteoglycans in scarred fascia.* Molecular and Cellular Biochemistry, 2000. **203**(1-2): p. 103-12.

10. Scott, P.G., Dodd, C.M., Tredget, E.E., Ghahary, A., and Rahemtulla, F., *Chemical characterization and quantification of proteoglycans in human post-burn hypertrophic and mature scars.* Clinical Science (London, England: 1979), 1996. **90**(5): p. 417-25.

11. Kischer, C.W., *Collagen and dermal patterns in the hypertrophic scar.* The Anatomical Record, 1974. **179**(1): p. 137-45.

12. Moulin, V., Larochelle, S., Langlois, C., Thibault, I., Lopez-Valle, C.A., and Roy, M., *Normal skin wound and hypertrophic scar myofibroblasts have differential responses to apoptotic inductors.* Journal of Cellular Physiology, 2004. **198**(3): p. 350-8.

13. Ignotz, R.A. and Massague, J., *Transforming growth factor-beta stimulates the expression of fibronectin and collagen and their incorporation into the extracellular matrix.* Journal of Biological Chemistry, 1986. **261**(9): p. 4337-45.

14. Danielson, K.G., Baribault, H., Holmes, D.F., Graham, H., Kadler, K.E., and Iozzo, R.V., *Targeted disruption of decorin leads to abnormal collagen fibril morphology and skin fragility.* Journal of Cell Biology, 1997. **136**(3): p. 729-43.

15. Schonherr, E., Broszat, M., Brandan, E., Bruckner, P., and Kresse, H., *Decorin core protein fragment Leu155-Val260 interacts with TGF-beta but does not compete for*

decorin binding to type I collagen. Archives of Biochemistry and Biophysics, 1998. **355**(2): p. 241-8.

16. Vial, C., Gutierrez, J., Santander, C., Cabrera, D., and Brandan, E., *Decorin interacts with connective tissue growth factor (CTGF)/CCN2 by LRR12 inhibiting its biological activity.* Journal of Biological Chemistry, 2011. **286**(27): p. 24242-52.
17. Kolb, M., Margetts, P.J., Galt, T., Sime, P.J., Xing, Z., Schmidt, M., and Gauldie, J., *Transient transgene expression of decorin in the lung reduces the fibrotic response to bleomycin.* American Journal of Respiratory and Critical Care Medicine, 2001. **163**(3 Pt 1): p. 770-7.
18. Baghy, K., Iozzo, R.V., and Kovalszky, I., *Decorin-TGFbeta axis in hepatic fibrosis and cirrhosis.* Journal of Histochemistry and Cytochemistry, 2012. **60**(4): p. 262-8.
19. Zhang, Z., Wu, F., Zheng, F., and Li, H., *Adenovirus-mediated decorin gene transfection has therapeutic effects in a streptozocin-induced diabetic rat model.* Nephron Experimental Nephrology, 2010. **116**(1): p. e11-21.
20. Li, L., Okada, H., Takemura, G., Kosai, K., Kanamori, H., Esaki, M., Takahashi, T., Goto, K., Tsujimoto, A., Maruyama, R., Kawamura, I., Kawaguchi, T., Takeyama, T., Fujiwara, T., Fujiwara, H., and Minatoguchi, S., *Postinfarction gene therapy with adenoviral vector expressing decorin mitigates cardiac remodeling and dysfunction.* American Journal of Physiology: Heart and Circulatory Physiology, 2009. **297**(4): p. H1504-13.
21. Markmann, A., Hausser, H., Schonherr, E., and Kresse, H., *Influence of decorin expression on transforming growth factor-beta-mediated collagen gel retraction and biglycan induction.* Matrix Biology, 2000. **19**(7): p. 631-6.

22. Zhang, Z., Li, X.J., Liu, Y., Zhang, X., Li, Y.Y., and Xu, W.S., *Recombinant human decorin inhibits cell proliferation and downregulates TGF-beta1 production in hypertrophic scar fibroblasts.* Burns, 2007. **33**(5): p. 634-41.

23. Lee, W.J., Ahn, H.M., Roh, H., Na, Y., Choi, I.K., Lee, J.H., Kim, Y.O., Lew, D.H., and Yun, C.O., *Decorin-expressing adenovirus decreases collagen synthesis and upregulates MMP expression in keloid fibroblasts and keloid spheroids.* Experimental Dermatology, 2015. **24**(8): p. 591-7.

24. Wang, J., Dodd, C., Shankowsky, H.A., Scott, P.G., Tredget, E.E., and Wound Healing Research, G., *Deep dermal fibroblasts contribute to hypertrophic scarring.* Laboratory Investigation, 2008. **88**(12): p. 1278-90.

25. Kwan, P., Ding, J., and Tredget, E.E., *Decorin gene therapy alters deep dermal fibroblast behavior to mimic that of superficial dermal fibroblasts in remodeling collagen scaffold used for cultured skin substitutes.* Tissue Engineering. Part A, 2016 (submitted).

26. Varkey, M., Ding, J., and Tredget, E.E., *Superficial dermal fibroblasts enhance basement membrane and epidermal barrier formation in tissue-engineered skin: implications for treatment of skin basement membrane disorders.* Tissue Engineering. Part A, 2014. **20**(3-4): p. 540-52.

27. Varkey, M., Ding, J., and Tredget, E.E., *Fibrotic remodeling of tissue-engineered skin with deep dermal fibroblasts is reduced by keratinocytes.* Tissue Engineering. Part A, 2014. **20**(3-4): p. 716-27.

28. Varkey, M., Ding, J., Tredget, E.E., and Wound Healing Research, G., *The effect of keratinocytes on the biomechanical characteristics and pore microstructure of tissue engineered skin using deep dermal fibroblasts.* Biomaterials, 2014. **35**(36): p. 9591-8.

29. Wang, J., Hori, K., Ding, J., Huang, Y., Kwan, P., Ladak, A., and Tredget, E.E., *Toll-like receptors expressed by dermal fibroblasts contribute to hypertrophic scarring.* Journal of Cellular Physiology, 2011. **226**(5): p. 1265-73.

30. Hitt, M.M., Ng, P., and Graham, F.L., *Construction and propagation of human adenovirus vectors*, in *Cell Biology*, J.E. Celis, Editor. 2006, Elsevier. p. 435-43.

31. van Zuijlen, P.P., Ruurda, J.J., van Veen, H.A., van Marle, J., van Trier, A.J., Groenevelt, F., Kreis, R.W., and Middelkoop, E., *Collagen morphology in human skin and scar tissue: no adaptations in response to mechanical loading at joints.* Burns, 2003. **29**(5): p. 423-31.

32. Zhu, Z., Ding, J., Ma, Z., Iwashina, T., and Tredget, E.E., *Systemic depletion of macrophages in the subacute phase of wound healing reduces hypertrophic scar formation.* Wound Repair and Regeneration, 2016.

33. Shah, M., Foreman, D.M., and Ferguson, M.W., *Neutralisation of TGF-beta 1 and TGF-beta 2 or exogenous addition of TGF-beta 3 to cutaneous rat wounds reduces scarring.* Journal of Cell Science, 1995. **108 (Pt 3)**(Pt 3): p. 985-1002.

34. McConnell, M.J. and Imperiale, M.J., *Biology of adenovirus and its use as a vector for gene therapy.* Human Gene Therapy, 2004. **15**(11): p. 1022-33.

35. Supp, D.M., Hahn, J.M., Glaser, K., McFarland, K.L., and Boyce, S.T., *Deep and superficial keloid fibroblasts contribute differentially to tissue phenotype in a novel in vivo model of keloid scar.* Plastic and Reconstructive Surgery, 2012. **129**(6): p. 1259-71.

36. Boyce, S.T., Kagan, R.J., Greenhalgh, D.G., Warner, P., Yakuboff, K.P., Palmieri, T., and Warden, G.D., *Cultured skin substitutes reduce requirements for harvesting of skin*

autograft for closure of excised, full-thickness burns. Journal of Trauma, 2006. **60**(4): p. 821-9.

37. Moiemen, N.S., Vlachou, E., Staiano, J.J., Thawy, Y., and Frame, J.D., *Reconstructive surgery with Integra dermal regeneration template: histologic study, clinical evaluation, and current practice.* Plastic and Reconstructive Surgery, 2006. **117**(7 Suppl): p. 160s-74s.

38. Yannas, I.V., Lee, E., Orgill, D.P., Skrabut, E.M., and Murphy, G.F., *Synthesis and characterization of a model extracellular matrix that induces partial regeneration of adult mammalian skin.* Proceedings of the National Academy of Sciences of the United States of America, 1989. **86**(3): p. 933-7.

39. O'Brien, F.J., Harley, B.A., Yannas, I.V., and Gibson, L., *Influence of freezing rate on pore structure in freeze-dried collagen-GAG scaffolds.* Biomaterials, 2004. **25**(6): p. 1077-86.

40. Varkey, M., Ding, J., and Tredget, E.E., *Differential collagen-glycosaminoglycan matrix remodeling by superficial and deep dermal fibroblasts: potential therapeutic targets for hypertrophic scar.* Biomaterials, 2011. **32**(30): p. 7581-91.

41. Rhee, S. and Grinnell, F., *Fibroblast mechanics in 3D collagen matrices.* Advanced Drug Delivery Reviews, 2007. **59**(13): p. 1299-305.

42. Zhang, Z., Garron, T.M., Li, X.J., Liu, Y., Zhang, X., Li, Y.Y., and Xu, W.S., *Recombinant human decorin inhibits TGF-beta1-induced contraction of collagen lattice by hypertrophic scar fibroblasts.* Burns, 2009. **35**(4): p. 527-37.

43. Huanglee, L.L.H., Wu, J.H., and Nimni, M.E., *Effects of hyaluronan on collagen fibrillar matrix contraction by fibroblasts.* Journal of Biomedical Materials Research, 1994. **28**(1): p. 123-32.

44. Kopp, J., Preis, E., Said, H., Hafemann, B., Wickert, L., Gressner, A.M., Pallua, N., and Dooley, S., *Abrogation of transforming growth factor-beta signaling by SMAD7 inhibits collagen gel contraction of human dermal fibroblasts.* Journal of Biological Chemistry, 2005. **280**(22): p. 21570-6.

45. Hu, X., Li, N., Tao, K., Fang, X., Liu, J., Wang, Y., Wang, H., Shi, J., Wang, Y., Ji, P., Cai, W., Bai, X., Zhu, X., Han, J., and Hu, D., *Effects of integrin alphanubeta3 on differentiation and collagen synthesis induced by connective tissue growth factor in human hypertrophic scar fibroblasts.* International Journal of Molecular Medicine, 2014. **34**(5): p. 1323-34.

46. Kremer, E.J. and Nemerow, G.R., *Adenovirus tales: from the cell surface to the nuclear pore complex.* PLoS Pathogens, 2015. **11**(6): p. e1004821.

47. Kwan, P., Ding, J., and Tredget, E.E., *MicroRNA 181b regulates decorin production by dermal fibroblasts and may be a potential therapy for hypertrophic scar.* PloS One, 2015. **10**(4): p. e0123054.

48. Junqueira, L.C., Bignolas, G., and Brentani, R.R., *Picrosirius staining plus polarization microscopy, a specific method for collagen detection in tissue sections.* Histochemical Journal, 1979. **11**(4): p. 447-55.

49. Whittaker, P., Kloner, R.A., Boughner, D.R., and Pickering, J.G., *Quantitative assessment of myocardial collagen with picrosirius red staining and circularly polarized light.* Basic Research in Cardiology, 1994. **89**(5): p. 397-410.

50. Junqueira, L.C., Cossermelli, W., and Brentani, R., *Differential staining of collagens type I, II and III by Sirius Red and polarization microscopy.* Archivum Histologicum Japonicum. Nippon Soshikigaku Kiroku, 1978. **41**(3): p. 267-74.

51. Xue, M. and Jackson, C.J., *Extracellular matrix reorganization during wound healing and its impact on abnormal scarring.* Advances in Wound Care, 2015. **4**(3): p. 119-36.

52. Shetlar, M.R., Dobrkovsky, M., Linares, H., Villarante, R., Shetlar, C.L., and Larson, D.L., *The hypertrophic scar. Glycoprotein and collagen components of burn scars.* Proceedings of the Society for Experimental Biology and Medicine, 1971. **138**(1): p. 298-300.

53. Verhaegen, P.D., van Zuijlen, P.P., Pennings, N.M., van Marle, J., Niessen, F.B., van der Horst, C.M., and Middelkoop, E., *Differences in collagen architecture between keloid, hypertrophic scar, normotrophic scar, and normal skin: An objective histopathological analysis.* Wound Repair and Regeneration, 2009. **17**(5): p. 649-56.

54. de Vries, H.J., Enomoto, D.N., van Marle, J., van Zuijlen, P.P., Mekkes, J.R., and Bos, J.D., *Dermal organization in scleroderma: the fast Fourier transform and the laser scatter method objectify fibrosis in nonlesional as well as lesional skin.* Laboratory Investigation, 2000. **80**(8): p. 1281-9.

55. Shi, M., Zhu, J., Wang, R., Chen, X., Mi, L., Walz, T., and Springer, T.A., *Latent TGF-beta structure and activation.* Nature, 2011. **474**(7351): p. 343-9.

Chapter 3 : Conclusions and Future Directions

To conclude, treating HTS Fb using Ad5-DCN gene therapy results in a reduction of TGF-β1-mediated fibrotic effects. Ad5-DCN therapy was found to reduce collagen matrix contraction after 17 days of culture and also accelerated the achievement of tensional homeostasis in 3D culture. Moreover, the extracellular matrix environment of 3D scaffolds was significantly improved after treatment with Ad5-DCN for 17 days, as determined via an assessment of collagen fiber orientation and collagen bundle packing density. MMP-1, which was found to have elevated gene expression after Ad5-DCN treatment, is most likely the key agent responsible for these enhancements in matrix remodeling. Ad5-DCN therapy also resulted in the downregulation of collagen synthesis. Because TGF-β1 gene expression was not modified in treated fibroblasts, it is believed that Ad5-DCN exerts its therapeutic effect by saturating the extracellular matrix with DCN, thus allowing for efficient sequestration of TGF-β1 away from its cell-surface receptors.

The findings from this study, in combination with those of Kwan, et al., suggest that this viral vector has the potential to improve wound healing, particularly HTS after burn injury [1]. In order to further test this hypothesis, studies involving an animal model would need to be carried out. Our lab has established an *in vivo* HTS model by grafting split-thickness human skin on to the back of an athymic nude mice, an *in vivo* model which may be suitable for initially exploring Ad5-DCN gene therapy [2]. The aforementioned xenografting procedure results in the development of a scar lesion – characterized by redness, contracture, and a disorganized extracellular matrix environment – which becomes elevated over the course of 4 weeks before beginning to remodel into a mature scar, similar to HTS in humans [2]. This model has been

recently used with success to study the effects of a CXCR4 inhibitor, as well as systemic macrophage depletion, on the development of HTS [3, 4]. Systemic delivery of Ad5-DCN after xenografting human skin onto nude mice may improve the characteristics of the resulting scar lesion and lead to a new therapeutic for HTS.

One additional advantage to this *in vivo* model is the presence of an intact innate immune system. Recent studies have indicated that DCN is an endogenous ligand for TLRs [5]. Notably, DCN has been shown to bind to TLR-2 and TLR-4 on macrophages, triggering the production of proinflammatory cytokines like TNF-α and IL-12 [5]. Considering the extreme elevation in soluble DCN produced by Ad5-DCN gene therapy in this study, the hypertrophic-scar-like nude mouse model would be useful for evaluating the proinflammatory effect of this gene therapy *in vivo*.

Moreover, due to the E3-deletion prevalent in most adenovirus-based vectors (including the viral vector used in this study), systemically-delivered adenoviral gene therapies are susceptible to attack by the adaptive immune system [6]. Therefore, the therapeutic efficacy of this vector would need to be evaluated prior to use in humans through the use of an immune-competent animal model. Because the deleted E3 region was not used for transgene insertion in the development of the Ad5-DCN vector, this issue might be solved by adding the E3 region back into the genome of this vector. However, this may result in cytotoxicity if E1 recombination occurs during viral propagation, as this would generate replication-competent adenoviruses. The issue of adaptive immune system stimulation might also be solved by using a next generation viral vector that does not contain any viral components or by delivering recombinant DCN using gold nanoparticles [6, 7].

Alternatively, Ad5-DCN gene therapy may be more effective as a therapeutic for HTS when used in combination with a tissue-engineered skin graft. In the Ad5-DCN study by Kwan, et al., it was found that the presence of the adenoviral backbone was negligible after three weeks of culture in 3D, though the elevation in DCN mRNA was persistent [1]. Therefore, tissue-engineered skin grafts created using Ad5-DCN-transduced fibroblasts may serve as a novel medical device which can deliver DCN directly to the site of burn injury. Hypothetically, this would result in the faster resolution of TGF-β1-mediated fibrotic effects in the wound microenvironment, potentially leading to a reduction in scarring. Moreover, this medical device may find value as a way of reducing the contraction and wound-margin scarring typically seen after autograft or tissue-engineered skin graft therapy [8, 9].

References

1. Kwan, P., Ding, J., and Tredget, E.E., *Decorin gene therapy alters deep dermal fibroblast behavior to mimic that of superficial dermal fibroblasts in remodeling collagen scaffold used for cultured skin substitutes.* Tissue Engineering. Part A, 2016 (submitted).
2. Wang, J., Ding, J., Jiao, H., Honardoust, D., Momtazi, M., Shankowsky, H.A., and Tredget, E.E., *Human hypertrophic scar-like nude mouse model: characterization of the molecular and cellular biology of the scar process.* Wound Repair and Regeneration, 2011. **19**(2): p. 274-85.
3. Zhu, Z., Ding, J., Ma, Z., Iwashina, T., and Tredget, E.E., *Systemic depletion of macrophages in the subacute phase of wound healing reduces hypertrophic scar formation.* Wound Repair and Regeneration, 2016.
4. Ding, J., Ma, Z., Liu, H., Kwan, P., Iwashina, T., Shankowsky, H.A., Wong, D., and Tredget, E.E., *The therapeutic potential of a C-X-C chemokine receptor type 4 (CXCR-4) antagonist on hypertrophic scarring in vivo.* Wound Repair and Regeneration, 2014. **22**(5): p. 622-30.
5. Frey, H., Schroeder, N., Manon-Jensen, T., Iozzo, R.V., and Schaefer, L., *Biological interplay between proteoglycans and their innate immune receptors in inflammation.* FEBS Journal, 2013. **280**(10): p. 2165-79.
6. McConnell, M.J. and Imperiale, M.J., *Biology of adenovirus and its use as a vector for gene therapy.* Human Gene Therapy, 2004. **15**(11): p. 1022-33.
7. Chaudhary, K., Moore, H., Tandon, A., Gupta, S., Khanna, R., and Mohan, R.R., *Nanotechnology and adeno-associated virus-based decorin gene therapy ameliorates*

peritoneal fibrosis. American Journal of Physiology: Renal Physiology, 2014. **307**(7): p. F777-82.

8. Harrison, C.A., Gossiel, F., Layton, C.M., Bullock, A.J., Johnson, T., Blumsohn, A., and MacNeil, S., *Use of an in vitro model of tissue-engineered skin to investigate the mechanism of skin graft contraction.* Tissue Engineering, 2006. **12**(11): p. 3119-33.
9. Boyce, S.T., Kagan, R.J., Greenhalgh, D.G., Warner, P., Yakuboff, K.P., Palmieri, T., and Warden, G.D., *Cultured skin substitutes reduce requirements for harvesting of skin autograft for closure of excised, full-thickness burns.* Journal of Trauma, 2006. **60**(4): p. 821-9.

Bibliography

Alberts, B., Bray, D., Lewis, J., Raff, M., Roberts, K., and Watson, J.D., *Molecular biology of the cell*. Vol. 1st. 1983, New York, NY: Garland Publishing, Inc.

Amadeu, T.P., Braune, A.S., Porto, L.C., Desmouliere, A., and Costa, A.M.A., *Fibrillin-1 and elastin are differentially expressed in hypertrophic scars and keloids.* Wound Repair and Regeneration, 2004. **12**(2): p. 169-74.

Anderson, R.R., Donelan, M.B., Hivnor, C., Greeson, E., Ross, E.V., Shumaker, P.R., Uebelhoer, N.S., and Waibel, J.S., *Laser treatment of traumatic scars with an emphasis on ablative fractional laser resurfacing: consensus report.* JAMA Dermatology, 2014. **150**(2): p. 187-93.

Armour, A., Scott, P.G., and Tredget, E.E., *Cellular and molecular pathology of HTS: basis for treatment.* Wound Repair and Regeneration, 2007. **15 Suppl 1**: p. S6-17.

Arnberg, N., *Adenovirus receptors: implications for targeting of viral vectors.* Trends in Pharmacological Sciences, 2012. **33**(8): p. 442-8.

Atiyeh, B.S., Hayek, S.N., and Gunn, S.W., *New technologies for burn wound closure and healing - Review of the literature.* Burns, 2005. **31**(8): p. 944-56.

Baghy, K., Iozzo, R.V., and Kovalszky, I., *Decorin-TGFbeta axis in hepatic fibrosis and cirrhosis.* Journal of Histochemistry and Cytochemistry, 2012. **60**(4): p. 262-8.

Bellemare, J., Roberge, C.J., Bergeron, D., Lopez-Valle, C.A., Roy, M., and Moulin, V.J., *Epidermis promotes dermal fibrosis: role in the pathogenesis of hypertrophic scars.* The Journal of Pathology, 2005. **206**(1): p. 1-8.

Blackstone, B.N., Drexler, J.W., and Powell, H.M., *Tunable engineered skin mechanics via coaxial electrospun fiber core diameter.* Tissue Engineering. Part A, 2014. **20**(19-20): p. 2746-55.

Bock, O., Schmid-Ott, G., Malewski, P., and Mrowietz, U., *Quality of life of patients with keloid and hypertrophic scarring.* Archives for Dermatological Research. Archiv für Dermatologische Forschung, 2006. **297**(10): p. 433-8.

Bombaro, K.M., Engrav, L.H., Carrougher, G.J., Wiechman, S.A., Faucher, L., Costa, B.A., Heimbach, D.M., Rivara, F.P., and Honari, S., *What is the prevalence of hypertrophic scarring following burns?* Burns, 2003. **29**(4): p. 299-302.

Boyce, S.T. *Tissue engineering*. in *American Burn Association*. 2007. San Diego, CA.

Boyce, S.T., Kagan, R.J., Greenhalgh, D.G., Warner, P., Yakuboff, K.P., Palmieri, T., and Warden, G.D., *Cultured skin substitutes reduce requirements for harvesting of skin autograft for closure of excised, full-thickness burns.* Journal of Trauma, 2006. **60**(4): p. 821-9.

Breitkreutz, D., Mirancea, N., and Nischt, R., *Basement membranes in skin: unique matrix structures with diverse functions?* Histochemistry and Cell Biology, 2009. **132**(1): p. 1-10.

Brodsky, S., Chen, J., Lee, A., Akassoglou, K., Norman, J., and Goligorsky, M.S., *Plasmin-dependent and -independent effects of plasminogen activators and inhibitor-1 on ex vivo angiogenesis.* American Journal of Physiology: Heart and Circulatory Physiology, 2001. **281**(4): p. 1784-92.

Brych, S.B., Engrav, L.H., Rivara, F.P., Ptacek, J.T., Lezotte, D.C., Esselman, P.C., Kowalske, K.J., and Gibran, N.S., *Time off work and return to work rates after burns: systematic*

review of the literature and a large two-center series. The Journal of Burn Care & Rehabilitation, 2001. **22**(6): p. 401-05.

Bucala, R., Spiegel, L.A., Chesney, J., Hogan, M., and Cerami, A., *Circulating fibrocytes define a new leukocyte subpopulation that mediates tissue repair.* Molecular Medicine, 1994. **1**(1): p. 71-81.

Catalano, E., Cochis, A., Varoni, E., Rimondini, L., and Azzimonti, B., *Tissue-engineered skin substitutes: an overview.* Journal of Artificial Organs, 2013. **16**(4): p. 397-403.

Chamberlain, L.J. and Yannas, I.V., *Preparation of collagen-glycosaminoglycan copolymers for tissue regeneration.* Methods in Molecular Medicine, 1999. **18**: p. 3-17.

Chaudhary, K., Moore, H., Tandon, A., Gupta, S., Khanna, R., and Mohan, R.R., *Nanotechnology and adeno-associated virus-based decorin gene therapy ameliorates peritoneal fibrosis.* American Journal of Physiology: Renal Physiology, 2014. **307**(7): p. F777-82.

Choi, I.K., Lee, Y.S., Yoo, J.Y., Yoon, A.R., Kim, H., Kim, D.S., Seidler, D.G., Kim, J.H., and Yun, C.O., *Effect of decorin on overcoming the extracellular matrix barrier for oncolytic virotherapy.* Gene Therapy, 2010. **17**(2): p. 190-201.

Choi, J.E., Oh, G.N., Kim, J.Y., Seo, S.H., Ahn, H.H., and Kye, Y.C., *Ablative fractional laser treatment for hypertrophic scars: comparison between Er:YAG and CO2 fractional lasers.* Journal of Dermatological Treatment, 2014. **25**(4): p. 299-303.

Clark, R.A.F. and Singer, A.J., *Wound repair: basic biology to tissue engineering*, in *Principles of tissue engineering*, R.P. Lanza, R. Langer, and J. Vacanti, Editors. 2000, Academic Press: San Diego, CA. p. 857-78.

Connolly, K.L., Chaffins, M., and Ozog, D., *Vascular patterns in mature hypertrophic burn scars treated with fractional CO2 laser.* Lasers in Surgery and Medicine, 2014. **46**(8): p. 597-600.

Danielson, K.G., Baribault, H., Holmes, D.F., Graham, H., Kadler, K.E., and Iozzo, R.V., *Targeted disruption of decorin leads to abnormal collagen fibril morphology and skin fragility.* Journal of Cell Biology, 1997. **136**(3): p. 729-43.

de Vries, H.J., Enomoto, D.N., van Marle, J., van Zuijlen, P.P., Mekkes, J.R., and Bos, J.D., *Dermal organization in scleroderma: the fast Fourier transform and the laser scatter method objectify fibrosis in nonlesional as well as lesional skin.* Laboratory Investigation, 2000. **80**(8): p. 1281-9.

Deitch, E.A., Wheelahan, T.M., Rose, M.P., Clothier, J., and Cotter, J., *Hypertrophic burn scars: analysis of variables.* The Journal of Trauma, 1983. **23**(10): p. 895-98.

Ding, J., Hori, K., Zhang, R., Marcoux, Y., Honardoust, D., Shankowsky, H.A., and Tredget, E.E., *Stromal cell-derived factor 1 (SDF-1) and its receptor CXCR4 in the formation of postburn hypertrophic scar (HTS).* Wound Repair and Regeneration, 2011. **19**(5): p. 568-78.

Ding, J., Ma, Z., Liu, H., Kwan, P., Iwashina, T., Shankowsky, H.A., Wong, D., and Tredget, E.E., *The therapeutic potential of a C-X-C chemokine receptor type 4 (CXCR-4) antagonist on hypertrophic scarring in vivo.* Wound Repair and Regeneration, 2014. **22**(5): p. 622-30.

Dunkin, C.S.J., Pleat, J.M., Gillespie, P.H., Tyler, M.P.H., Roberts, A.H.N., and McGrouther, D.A., *Scarring occurs at a critical depth of skin injury: Precise measurement in a*

graduated dermal scratch in human volunteers. Plastic and Reconstructive Surgery, 2007. **119**(6): p. 1722-32.

Eckhart, L., Lippens, S., Tschachler, E., and Declercq, W., *Cell death by cornification.* Biochimica et Biophysica Acta, 2013. **1833**(12): p. 3471-80.

Edelstein, M. *Vectors used in gene therapy clinical trials*. Gene Therapy Clinical Trials Worldwide 2016 [cited 2016 May]; Available from: http://www.wiley.com//legacy/wileychi/genmed/clinical/.

Edwards, D.R., Murphy, G., Reynolds, J.J., Whitham, S.E., Docherty, A.J., Angel, P., and Heath, J.K., *Transforming growth factor beta modulates the expression of collagenase and metalloproteinase inhibitor.* EMBO Journal, 1987. **6**(7): p. 1899-904.

Ehrlich, H.P., Desmouliere, A., Diegelmann, R.F., Cohen, I.K., Compton, C.C., Garner, W.L., Kapanci, Y., and Gabbiani, G., *Morphological and immunochemical differences between keloid and hypertrophic scar.* American Journal of Pathology, 1994. **145**(1): p. 105-13.

Engrav, L.H., Covey, M.H., Dutcher, K.D., Heimbach, D.M., Walkinshaw, M.D., and Marvin, J.A., *Impairment, time out of school, and time off from work after burns.* Plastic and Reconstructive Surgery, 1987. **79**(6): p. 927-34.

Fang, T., Lineaweaver, W.C., Sailes, F.C., Kisner, C., and Zhang, F., *Clinical application of cultured epithelial autografts on acellular dermal matrices in the treatment of extended burn injuries.* Annals of Plastic Surgery, 2014. **73**(5): p. 509-15.

Fenner, J. and Clark, R.A.F., *Anatomy, physiology, histology, and immunohistochemistry of human skin*, in *Skin Tissue Engineering and Regenerative Medicine*, M.Z. Albanna and J.H. Holmes, Editors. 2016, Elsevier. p. 1-17.

Flaten, G.E., Palac, Z., Engesland, A., Filipovic-Grcic, J., Vanic, Z., and Skalko-Basnet, N., *In vitro skin models as a tool in optimization of drug formulation.* European Journal of Pharmaceutical Sciences, 2015. **75**: p. 10-24.

Foley, T.T. and Ehrlich, H.P., *Through gap junction communications, co-cultured mast cells and fibroblasts generate fibroblast activities allied with hypertrophic scarring.* Plastic and Reconstructive Surgery, 2013. **131**(5): p. 1036-44.

Frey, H., Schroeder, N., Manon-Jensen, T., Iozzo, R.V., and Schaefer, L., *Biological interplay between proteoglycans and their innate immune receptors in inflammation.* FEBS Journal, 2013. **280**(10): p. 2165-79.

Friedman, D.W., Boyd, C.D., Mackenzie, J.W., Norton, P., Olson, R.M., and Deak, S.B., *Regulation of collagen gene expression in keloids and hypertrophic scars.* Journal of Surgical Research, 1993. **55**(2): p. 214-22.

Gangemi, E.N., Gregori, D., Berchialla, P., Zingarelli, E., Cairo, M., Bollero, D., Ganem, J., Capocelli, R., Cuccuru, F., Cassano, P., Risso, D., and Stella, M., *Epidemiology and risk factors for pathologic scarring after burn wounds.* Archives of Facial Plastic Surgery, 2008. **10**(2): p. 93-102.

Gauglitz, G.G., Korting, H.C., Pavicic, T., Ruzicka, T., and Jeschke, M.G., *Hypertrophic scarring and keloids: pathomechanisms and current and emerging treatment strategies.* Molecular Medicine, 2011. **17**(1-2): p. 113-25.

Ghahary, A., Shen, Y.J., Nedelec, B., Scott, P.G., and Tredget, E.E., *Interferons gamma and alpha-2b differentially regulate the expression of collagenase and tissue inhibitor of metalloproteinase-1 messenger RNA in human hypertrophic and normal dermal fibroblasts.* Wound Repair and Regeneration, 1995. **3**(2): p. 176-84.

Ghahary, A., Shen, Y.J., Nedelec, B., Wang, R., Scott, P.G., and Tredget, E.E., *Collagenase production is lower in post-burn hypertrophic scar fibroblasts than in normal fibroblasts and is reduced by insulin-like growth factor-1.* Journal of Investigative Dermatology, 1996. **106**(3): p. 476-81.

Goldoni, S., Humphries, A., Nystrom, A., Sattar, S., Owens, R.T., McQuillan, D.J., Ireton, K., and Iozzo, R.V., *Decorin is a novel antagonistic ligand of the Met receptor.* Journal of Cell Biology, 2009. **185**(4): p. 743-54.

Gomez, C., Galan, J.M., Torrero, V., Ferreiro, I., Perez, D., Palao, R., Martinez, E., Llames, S., Meana, A., and Holguin, P., *Use of an autologous bioengineered composite skin in extensive burns: Clinical and functional outcomes. A multicentric study.* Burns, 2011. **37**(4): p. 580-89.

Harrison, C.A., Gossiel, F., Layton, C.M., Bullock, A.J., Johnson, T., Blumsohn, A., and MacNeil, S., *Use of an in vitro model of tissue-engineered skin to investigate the mechanism of skin graft contraction.* Tissue Engineering, 2006. **12**(11): p. 3119-33.

Haugh, M.G., Jaasma, M.J., and O'Brien, F.J., *The effect of dehydrothermal treatment on the mechanical and structural properties of collagen-GAG scaffolds.* Journal of Biomedical Materials Research, Part A, 2009. **89**(2): p. 363-69.

Haugh, M.G., Murphy, C.M., and O'Brien, F.J., *Novel freeze-drying methods to produce a range of collagen-glycosaminoglycan scaffolds with tailored mean pore sizes.* Tissue Engineering. Part C, Methods, 2010. **16**(5): p. 887-94.

Hildebrand, A., Romaris, M., Rasmussen, L.M., Heinegard, D., Twardzik, D.R., Border, W.A., and Ruoslahti, E., *Interaction of the small interstitial proteoglycans biglycan, decorin*

and fibromodulin with transforming growth factor beta. Biochemical Journal, 1994. **302 (Pt 2)**(Pt 2): p. 527-34.

Hitt, M.M., Ng, P., and Graham, F.L., *Construction and propagation of human adenovirus vectors*, in *Cell Biology*, J.E. Celis, Editor. 2006, Elsevier. p. 435-43.

Honardoust, D., Varkey, M., Hori, K., Ding, J., Shankowsky, H.A., and Tredget, E.E., *Small leucine-rich proteoglycans, decorin and fibromodulin, are reduced in postburn hypertrophic scar.* Wound Repair and Regeneration, 2011. **19**(3): p. 368-78.

Honardoust, D., Varkey, M., Marcoux, Y., Shankowsky, H.A., and Tredget, E.E., *Reduced decorin, fibromodulin, and transforming growth factor-beta3 in deep dermis leads to hypertrophic scarring.* Journal of Burn Care & Research, 2012. **33**(2): p. 218-27.

Hu, X., Li, N., Tao, K., Fang, X., Liu, J., Wang, Y., Wang, H., Shi, J., Wang, Y., Ji, P., Cai, W., Bai, X., Zhu, X., Han, J., and Hu, D., *Effects of integrin alphanubeta3 on differentiation and collagen synthesis induced by connective tissue growth factor in human hypertrophic scar fibroblasts.* International Journal of Molecular Medicine, 2014. **34**(5): p. 1323-34.

Huanglee, L.L.H., Wu, J.H., and Nimni, M.E., *Effects of hyaluronan on collagen fibrillar matrix contraction by fibroblasts.* Journal of Biomedical Materials Research, 1994. **28**(1): p. 123-32.

Ignotz, R.A. and Massague, J., *Transforming growth factor-beta stimulates the expression of fibronectin and collagen and their incorporation into the extracellular matrix.* Journal of Biological Chemistry, 1986. **261**(9): p. 4337-45.

Iozzo, R.V., Buraschi, S., Genua, M., Xu, S.Q., Solomides, C.C., Peiper, S.C., Gomella, L.G., Owens, R.C., and Morrione, A., *Decorin antagonizes IGF receptor I (IGF-IR) function*

by interfering with IGF-IR activity and attenuating downstream signaling. Journal of Biological Chemistry, 2011. **286**(40): p. 34712-21.

Iozzo, R.V., Moscatello, D.K., McQuillan, D.J., and Eichstetter, I., *Decorin is a biological ligand for the epidermal growth factor receptor.* Journal of Biological Chemistry, 1999. **274**(8): p. 4489-92.

Iozzo, R.V. and Schaefer, L., *Proteoglycans in health and disease: novel regulatory signaling mechanisms evoked by the small leucine-rich proteoglycans.* FEBS Journal, 2010. **277**(19): p. 3864-75.

Ito, M., Liu, Y., Yang, Z., Nguyen, J., Liang, F., Morris, R.J., and Cotsarelis, G., *Stem cells in the hair follicle bulge contribute to wound repair but not to homeostasis of the epidermis.* Nature Medicine, 2005. **11**(12): p. 1351-54.

Jean, J., Lapointe, M., Soucy, J., and Pouliot, R., *Development of an in vitro psoriatic skin model by tissue engineering.* Journal of Dermatological Science, 2009. **53**(1): p. 19-25.

Junqueira, L.C., Bignolas, G., and Brentani, R.R., *Picrosirius staining plus polarization microscopy, a specific method for collagen detection in tissue sections.* Histochemical Journal, 1979. **11**(4): p. 447-55.

Junqueira, L.C., Cossermelli, W., and Brentani, R., *Differential staining of collagens type I, II and III by Sirius Red and polarization microscopy.* Archivum Histologicum Japonicum. Nippon Soshikigaku Kiroku, 1978. **41**(3): p. 267-74.

Kamel, R.A., Ong, J.F., Eriksson, E., Junker, J.P., and Caterson, E.J., *Tissue engineering of skin.* Journal of the American College of Surgeons, 2013. **217**(3): p. 533-55.

Kischer, C.W., *Collagen and dermal patterns in the hypertrophic scar.* The Anatomical Record, 1974. **179**(1): p. 137-45.

Koide, M., Osaki, K., Konishi, J., Oyamada, K., Katakura, T., Takahashi, A., and Yoshizato, K., *A new type of biomaterial for artificial skin: dehydrothermally cross-linked composites of fibrillar and denatured collagens.* Journal of Biomedical Materials Research, 1993. **27**(1): p. 79-87.

Kolb, M., Margetts, P.J., Galt, T., Sime, P.J., Xing, Z., Schmidt, M., and Gauldie, J., *Transient transgene expression of decorin in the lung reduces the fibrotic response to bleomycin.* American Journal of Respiratory and Critical Care Medicine, 2001. **163**(3 Pt 1): p. 770-7.

Kolb, M., Margetts, P.J., Sime, P.J., and Gauldie, J., *Proteoglycans decorin and biglycan differentially modulate TGF-beta-mediated fibrotic responses in the lung.* American Journal of Physiology: Lung Cellular and Molecular Physiology, 2001. **280**(6): p. L1327-34.

Kopp, J., Preis, E., Said, H., Hafemann, B., Wickert, L., Gressner, A.M., Pallua, N., and Dooley, S., *Abrogation of transforming growth factor-beta signaling by SMAD7 inhibits collagen gel contraction of human dermal fibroblasts.* Journal of Biological Chemistry, 2005. **280**(22): p. 21570-76.

Kozma, E.M., Olczyk, K., Glowacki, A., and Bobinski, R., *An accumulation of proteoglycans in scarred fascia.* Molecular and Cellular Biochemistry, 2000. **203**(1-2): p. 103-12.

Kremer, E.J. and Nemerow, G.R., *Adenovirus tales: from the cell surface to the nuclear pore complex.* PLoS Pathogens, 2015. **11**(6): p. e1004821.

Kresse, H. and Schonherr, E., *Proteoglycans of the extracellular matrix and growth control.* Journal of Cellular Physiology, 2001. **189**(3): p. 266-74.

Kwan, P., Ding, J., and Tredget, E.E., *Decorin gene therapy alters deep dermal fibroblast behavior to mimic that of superficial dermal fibroblasts in remodeling collagen scaffold used for cultured skin substitutes.* Tissue Engineering. Part A, 2016 (submitted).

Kwan, P., Ding, J., and Tredget, E.E., *MicroRNA 181b regulates decorin production by dermal fibroblasts and may be a potential therapy for hypertrophic scar.* PloS One, 2015. **10**(4): p. e0123054.

Kwan, P., Hori, K., Ding, J., and Tredget, E.E., *Scar and contracture: biological principles.* Hand Clinics, 2009. **25**(4): p. 511-28.

Kwan, P.O., Ding, J., and Tredget, E.E., *Serum decorin, IL-1beta, and TGF-beta predict hypertrophic scarring postburn.* Journal of Burn Care & Research, 2015.

Lai, H.J., Kuan, C.H., Wu, H.C., Tsai, J.C., Chen, T.M., Hsieh, D.J., and Wang, T.W., *Tailored design of electrospun composite nanofibers with staged release of multiple angiogenic growth factors for chronic wound healing.* Acta Biomaterialia, 2014. **10**(10): p. 4156-66.

Lamy, J., Yassine, A.H., Gourari, A., Forme, N., and Zakine, G., *The role of skin substitutes in the surgical treatment of extensive burns covering more than 60 % of total body surface area. A review of patients over a 10-year period at the Tours University Hospital.* Annales de Chirurgie Plastique et Esthétique, 2013.

Lawrence, J.W., Mason, S.T., Schomer, K., and Klein, M.B., *Epidemiology and impact of scarring after burn injury: a systematic review of the literature.* Journal of Burn Care & Research, 2012. **33**(1): p. 136-46.

Lee, J.Y.Y., Yang, C.C., Chao, S.C., and Wong, T.W., *Histopathological differential diagnosis of keloid and hypertrophic scar.* American Journal of Dermatopathology, 2004. **26**(5): p. 379-84.

Lee, W.J., Ahn, H.M., Roh, H., Na, Y., Choi, I.K., Lee, J.H., Kim, Y.O., Lew, D.H., and Yun, C.O., *Decorin-expressing adenovirus decreases collagen synthesis and upregulates MMP expression in keloid fibroblasts and keloid spheroids.* Experimental Dermatology, 2015. **24**(8): p. 591-7.

Leeson, C.R. and Leeson, T.S., *Histology*. Vol. 3rd. 1976, Philadelphia, PA: W.B. Saunders Company.

Levy, V., Lindon, C., Zheng, Y., Harfe, B.D., and Morgan, B.A., *Epidermal stem cells arise from the hair follicle after wounding.* FASEB Journal, 2007. **21**(7): p. 1358-66.

Lewis, W.H.P. and Sun, K.K.Y., *Hypertrophic scar: a genetic hypothesis.* Burns, 1990. **16**(3): p. 176-78.

Li-Tsang, C.W.P., Lau, J.C.M., and Chan, C.C.H., *Prevalence of hypertrophic scar formation and its characteristics among the Chinese population.* Burns, 2005. **31**(5): p. 610-16.

Li, L., Fukunaga-Kalabis, M., and Herlyn, M., *The three-dimensional human skin reconstruct model: a tool to study normal skin and melanoma progression.* Journal of Visualized Experiments, 2011(54).

Li, L., Okada, H., Takemura, G., Kosai, K., Kanamori, H., Esaki, M., Takahashi, T., Goto, K., Tsujimoto, A., Maruyama, R., Kawamura, I., Kawaguchi, T., Takeyama, T., Fujiwara, T., Fujiwara, H., and Minatoguchi, S., *Postinfarction gene therapy with adenoviral vector expressing decorin mitigates cardiac remodeling and dysfunction.* American Journal of Physiology: Heart and Circulatory Physiology, 2009. **297**(4): p. H1504-13.

Linares, H.A., Kischer, C.W., Dobrkovsky, M., and Larson, D.L., *The histiotypic organization of the hypertrophic scar in humans.* Journal of Investigative Dermatology, 1972. **59**(4): p. 323-31.

Lloyd, C., Besse, J., and Boyce, S., *Controlled-rate freezing to regulate the structure of collagen-glycosaminoglycan scaffolds in engineered skin substitutes.* Journal of Biomedical Materials Research, Part B: Applied Biomaterials, 2014.

Maas-Szabowski, N., Shimotoyodome, A., and Fusenig, N.E., *Keratinocyte growth regulation in fibroblast cocultures via a double paracrine mechanism.* Journal of Cell Science, 1999. **112 (Pt 12)**: p. 1843-53.

Mackenzie, I.C. and Hill, M.W., *Connective tissue influences on patterns of epithelial architecture and keratinization in skin and oral mucosa of the adult mouse.* Cell and Tissue Research, 1984. **235**(3): p. 551-9.

Makboul, M., Makboul, R., Abdelhafez, A.H., Hassan, S.S., and Youssif, S.M., *Evaluation of the effect of fractional CO2 laser on histopathological picture and TGF-beta1 expression in hypertrophic scar.* Journal of Cosmetic Dermatology, 2014. **13**(3): p. 169-79.

Markmann, A., Hausser, H., Schonherr, E., and Kresse, H., *Influence of decorin expression on transforming growth factor-beta-mediated collagen gel retraction and biglycan induction.* Matrix Biology, 2000. **19**(7): p. 631-6.

McConnell, M.J. and Imperiale, M.J., *Biology of adenovirus and its use as a vector for gene therapy.* Human Gene Therapy, 2004. **15**(11): p. 1022-33.

Meaume, S., Le Pillouer-Prost, A., Richert, B., Roseeuw, D., and Vadoud, J., *Management of scars: updated practical guidelines and use of silicones.* European Journal of Dermatology, 2014. **24**(4): p. 435-43.

Moiemen, N.S., Vlachou, E., Staiano, J.J., Thawy, Y., and Frame, J.D., *Reconstructive surgery with Integra dermal regeneration template: histologic study, clinical evaluation, and current practice.* Plastic and Reconstructive Surgery, 2006. **117**(7 Suppl): p. 160s-74s.

Mosmann, T.R. and Coffman, R.L., *TH1 and TH2 cells: different patterns of lymphokine secretion lead to different functional properties.* Annual Review of Immunology, 1989. **7**: p. 145-73.

Moulin, V., Larochelle, S., Langlois, C., Thibault, I., Lopez-Valle, C.A., and Roy, M., *Normal skin wound and hypertrophic scar myofibroblasts have differential responses to apoptotic inductors.* Journal of Cellular Physiology, 2004. **198**(3): p. 350-58.

Musgrave, M.A., Umraw, N., Fish, J.S., Gomez, M., and Cartotto, R.C., *The effect of silicone gel sheets on perfusion of hypertrophic burn scars.* The Journal of Burn Care & Rehabilitation, 2002. **23**(3): p. 208-14.

Nanchahal, J., Dover, R., and Otto, W.R., *Allogeneic skin substitutes applied to burns patients.* Burns, 2002. **28**(3): p. 254-57.

Nedelec, B., Shankowsky, H., Scott, P.G., Ghahary, A., and Tredget, E.E., *Myofibroblasts and apoptosis in human hypertrophic scars: The effect of interferon-α2b.* Surgery, 2001. **130**(5): p. 798-808.

Niessen, F.B., Andriessen, M.P., Schalkwijk, J., Visser, L., and Timens, W., *Keratinocyte-derived growth factors play a role in the formation of hypertrophic scars.* Journal of Pathology, 2001. **194**(2): p. 207-16.

Niessen, F.B., Spauwen, P.H., Schalkwijk, J., and Kon, M., *On the nature of hypertrophic scars and keloids: a review.* Plastic and Reconstructive Surgery, 1999. **104**(5): p. 1435-58.

O'Brien, F.J., Harley, B.A., Waller, M.A., Yannas, I.V., Gibson, L.J., and Prendergast, P.J., *The effect of pore size on permeability and cell attachment in collagen scaffolds for tissue engineering.* Technology and Health Care, 2007. **15**(1): p. 3-17.

O'Brien, F.J., Harley, B.A., Yannas, I.V., and Gibson, L., *Influence of freezing rate on pore structure in freeze-dried collagen-GAG scaffolds.* Biomaterials, 2004. **25**(6): p. 1077-86.

O'Connor, N.E., Mulliken, J.B., Banks-Schlegel, S., Kehinde, O., and Green, H., *Grafting of burns with cultured epithelium prepared from autologous epidermal cells.* Lancet, 1981. **1**(8211): p. 75-78.

Okazaki, M., Yoshimura, K., Suzuki, Y., and Harii, K., *Effects of subepithelial fibroblasts on epithelial differentiation in human skin and oral mucosa: heterotypically recombined organotypic culture model.* Plastic and Reconstructive Surgery, 2003. **112**(3): p. 784-92.

Orgel, J.P., Eid, A., Antipova, O., Bella, J., and Scott, J.E., *Decorin core protein (decoron) shape complements collagen fibril surface structure and mediates its binding.* PloS One, 2009. **4**(9): p. e7028.

Penn, J.W., Grobbelaar, A.O., and Rolfe, K.J., *The role of the TGF-beta family in wound healing, burns and scarring: a review.* International Journal of Burns and Trauma, 2012. **2**(1): p. 18-28.

Reijnders, C.M., van Lier, A., Roffel, S., Kramer, D., Scheper, R.J., and Gibbs, S., *Development of a full-thickness human skin equivalent In vitro model derived from TERT-immortalized keratinocytes and fibroblasts.* Tissue Engineering. Part A, 2015. **21**(17-18): p. 2448-59.

Reinke, J.M. and Sorg, H., *Wound repair and regeneration.* European Surgical Research, 2012. **49**(1): p. 35-43.

Rhee, S. and Grinnell, F., *Fibroblast mechanics in 3D collagen matrices.* Advanced Drug Delivery Reviews, 2007. **59**(13): p. 1299-305.

Rheinwald, J.G. and Green, H., *Serial cultivation of strains of human epidermal keratinocytes: the formation of keratinizing colonies from single cells.* Cell, 1975. **6**(3): p. 331-43.

Rnjak-Kovacina, J., Wise, S.G., Li, Z., Maitz, P.K., Young, C.J., Wang, Y., and Weiss, A.S., *Electrospun synthetic human elastin:collagen composite scaffolds for dermal tissue engineering.* Acta Biomaterialia, 2012. **8**(10): p. 3714-22.

Salem, A.K., Stevens, R., Pearson, R.G., Davies, M.C., Tendler, S.J., Roberts, C.J., Williams, P.M., and Shakesheff, K.M., *Interactions of 3T3 fibroblasts and endothelial cells with defined pore features.* Journal of Biomedical Materials Research, 2002. **61**(2): p. 212-17.

Sayani, K., Dodd, C.M., Nedelec, B., Shen, Y.J., Ghahary, A., Tredget, E.E., and Scott, P.G., *Delayed appearance of decorin in healing burn scars.* Histopathology, 2000. **36**(3): p. 262-72.

Schmid, P., Itin, P., Cherry, G., Bi, C., and Cox, D.A., *Enhanced expression of transforming growth factor-beta type I and type II receptors in wound granulation tissue and hypertrophic scar.* American Journal of Pathology, 1998. **152**(2): p. 485-93.

Schonherr, E., Broszat, M., Brandan, E., Bruckner, P., and Kresse, H., *Decorin core protein fragment Leu155-Val260 interacts with TGF-beta but does not compete for decorin binding to type I collagen.* Archives of Biochemistry and Biophysics, 1998. **355**(2): p. 241-8.

Scott, P.G., Dodd, C.M., Tredget, E.E., Ghahary, A., and Rahemtulla, F., *Chemical characterization and quantification of proteoglycans in human post-burn hypertrophic and mature scars.* Clinical Science (London, England: 1979), 1996. **90**(5): p. 417-25.

Scott, P.G., Dodd, C.M., Tredget, E.E., Ghahary, A., and Rahemtulla, F., *Immunohistochemical localization of the proteoglycans decorin, biglycan and versican and transforming growth factor-beta in human post-burn hypertrophic and mature scars.* Histopathology, 1995. **26**(5): p. 423-31.

Seo, D.K., Kym, D., and Hur, J., *Management of neck contractures by single-stage dermal substitutes and skin grafting in extensive burn patients.* Annals of Surgical Treatment and Research, 2014. **87**(5): p. 253-59.

Shah, M., Foreman, D.M., and Ferguson, M.W., *Neutralisation of TGF-beta 1 and TGF-beta 2 or exogenous addition of TGF-beta 3 to cutaneous rat wounds reduces scarring.* Journal of Cell Science, 1995. **108 (Pt 3)**(Pt 3): p. 985-1002.

Shepherd, J., Douglas, I., Rimmer, S., Swanson, L., and MacNeil, S., *Development of three-dimensional tissue-engineered models of bacterial infected human skin wounds.* Tissue Engineering. Part C, Methods, 2009. **15**(3): p. 475-84.

Shetlar, M.R., Dobrkovsky, M., Linares, H., Villarante, R., Shetlar, C.L., and Larson, D.L., *The hypertrophic scar. Glycoprotein and collagen components of burn scars.* Proceedings of the Society for Experimental Biology and Medicine, 1971. **138**(1): p. 298-300.

Shi, M., Zhu, J., Wang, R., Chen, X., Mi, L., Walz, T., and Springer, T.A., *Latent TGF-beta structure and activation.* Nature, 2011. **474**(7351): p. 343-9.

Simon, F., Bergeron, D., Larochelle, S., Lopez-Valle, C.A., Genest, H., Armour, A., and Moulin, V.J., *Enhanced secretion of TIMP-1 by human hypertrophic scar keratinocytes could contribute to fibrosis.* Burns, 2012. **38**(3): p. 421-27.

Smith, M.M. and Melrose, J., *Proteoglycans in normal and healing skin.* Advances in Wound Care, 2015. **4**(3): p. 152-73.

Smola, H., Thiekotter, G., and Fusenig, N.E., *Mutual induction of growth factor gene expression by epidermal-dermal cell interaction.* Journal of Cell Biology, 1993. **122**(2): p. 417-29.

Sorrell, J.M. and Caplan, A.I., *Fibroblast heterogeneity: more than skin deep.* Journal of Cell Science, 2004. **117**(5): p. 667-75.

Supp, D.M., Hahn, J.M., Glaser, K., McFarland, K.L., and Boyce, S.T., *Deep and superficial keloid fibroblasts contribute differentially to tissue phenotype in a novel in vivo model of keloid scar.* Plastic and Reconstructive Surgery, 2012. **129**(6): p. 1259-71.

Tredget, E.E., *Pathophysiology and treatment of fibroproliferative disorders following thermal injury.* Annals of the New York Academy of Sciences, 1999. **888**: p. 165-82.

Tredget, E.E., Levi, B., and Donelan, M.B., *Biology and principles of scar management and burn reconstruction.* Surgical Clinics of North America, 2014. **94**(4): p. 793-815.

Tredget, E.E., Shankowsky, H.A., Pannu, R., Nedelec, B., Iwashina, T., Ghahary, A., Taerum, T.V., and Scott, P.G., *Transforming growth factor-beta in thermally injured patients with hypertrophic scars: effects of interferon alpha-2b.* Plastic and Reconstructive Surgery, 1998. **102**(5): p. 1317-28; discussion 29-30.

Tredget, E.E., Wang, R., Shen, Q., Scott, P.G., and Ghahary, A., *Transforming growth factor-beta mRNA and protein in hypertrophic scar tissues and fibroblasts: antagonism by IFN-alpha and IFN-gamma in vitro and in vivo.* Journal of Interferon & Cytokine Research, 2000. **20**(2): p. 143-51.

Tredget, E.E., Yang, L., Delehanty, M., Shankowsky, H., and Scott, P.G., *Polarized Th2 cytokine production in patients with hypertrophic scar following thermal injury.* Journal of Interferon & Cytokine Research, 2006. **26**(3): p. 179-89.

van Zuijlen, P.P., Ruurda, J.J., van Veen, H.A., van Marle, J., van Trier, A.J., Groenevelt, F., Kreis, R.W., and Middelkoop, E., *Collagen morphology in human skin and scar tissue: no adaptations in response to mechanical loading at joints.* Burns, 2003. **29**(5): p. 423-31.

Varkey, M., Ding, J., and Tredget, E.E., *Differential collagen-glycosaminoglycan matrix remodeling by superficial and deep dermal fibroblasts: potential therapeutic targets for hypertrophic scar.* Biomaterials, 2011. **32**(30): p. 7581-91.

Varkey, M., Ding, J., and Tredget, E.E., *Fibrotic remodeling of tissue-engineered skin with deep dermal fibroblasts is reduced by keratinocytes.* Tissue Engineering. Part A, 2014. **20**(3-4): p. 716-27.

Varkey, M., Ding, J., and Tredget, E.E., *Superficial dermal fibroblasts enhance basement membrane and epidermal barrier formation in tissue-engineered skin: implications for treatment of skin basement membrane disorders.* Tissue Engineering. Part A, 2014. **20**(3-4): p. 540-52.

Varkey, M., Ding, J., Tredget, E.E., and Wound Healing Research, G., *The effect of keratinocytes on the biomechanical characteristics and pore microstructure of tissue engineered skin using deep dermal fibroblasts.* Biomaterials, 2014. **35**(36): p. 9591-98.

Verhaegen, P.D., van Zuijlen, P.P., Pennings, N.M., van Marle, J., Niessen, F.B., van der Horst, C.M., and Middelkoop, E., *Differences in collagen architecture between keloid, hypertrophic scar, normotrophic scar, and normal skin: An objective histopathological analysis.* Wound Repair and Regeneration, 2009. **17**(5): p. 649-56.

Vial, C., Gutierrez, J., Santander, C., Cabrera, D., and Brandan, E., *Decorin interacts with connective tissue growth factor (CTGF)/CCN2 by LRR12 inhibiting its biological activity.* Journal of Biological Chemistry, 2011. **286**(27): p. 24242-52.

Wang, J., Ding, J., Jiao, H., Honardoust, D., Momtazi, M., Shankowsky, H.A., and Tredget, E.E., *Human hypertrophic scar-like nude mouse model: characterization of the molecular and*

cellular biology of the scar process. Wound Repair and Regeneration, 2011. **19**(2): p. 274-85.

Wang, J., Dodd, C., Shankowsky, H.A., Scott, P.G., Tredget, E.E., and Wound Healing Research, G., *Deep dermal fibroblasts contribute to hypertrophic scarring.* Laboratory Investigation, 2008. **88**(12): p. 1278-90.

Wang, J., Hori, K., Ding, J., Huang, Y., Kwan, P., Ladak, A., and Tredget, E.E., *Toll-like receptors expressed by dermal fibroblasts contribute to hypertrophic scarring.* Journal of Cellular Physiology, 2011. **226**(5): p. 1265-73.

Wang, J., Jiao, H., Stewart, T.L., Shankowsky, H.A., Scott, P.G., and Tredget, E.E., *Increased TGF-beta-producing CD4+ T lymphocytes in postburn patients and their potential interaction with dermal fibroblasts in hypertrophic scarring.* Wound Repair and Regeneration, 2007. **15**(4): p. 530-39.

Wang, J.F., Jiao, H., Stewart, T.L., Shankowsky, H.A., Scott, P.G., and Tredget, E.E., *Fibrocytes from burn patients regulate the activities of fibroblasts.* Wound Repair and Regeneration, 2007. **15**(1): p. 113-21.

Wang, Y.W., Liou, N.H., Cherng, J.H., Chang, S.J., Ma, K.H., Fu, E., Liu, J.C., and Dai, N.T., *siRNA-targeting transforming growth factor-beta type I receptor reduces wound scarring and extracellular matrix deposition of scar tissue.* Journal of Investigative Dermatology, 2014. **134**(7): p. 2016-25.

Weadock, K.S., Miller, E.J., Keuffel, E.L., and Dunn, M.G., *Effect of physical crosslinking methods on collagen-fiber durability in proteolytic solutions.* Journal of Biomedical Materials Research, 1996. **32**(2): p. 221-26.

Whittaker, P., Kloner, R.A., Boughner, D.R., and Pickering, J.G., *Quantitative assessment of myocardial collagen with picrosirius red staining and circularly polarized light.* Basic Research in Cardiology, 1994. **89**(5): p. 397-410.

Wilgus, T.A. and Wulff, B.C., *The importance of mast cells in dermal scarring.* Advances in Wound Care, 2014. **3**(4): p. 356-65.

Wu, Y. and Tredget, E.E., *Pathology of tissue regeneration repair: skin regeneration*, in *Pathobiology of human disease*, L.M. McManus and R.N. Mitchell, Editors. 2014, Elsevier: San Diego, CA. p. 558-66.

Wynn, T.A., *Fibrotic disease and the T(H)1/T(H)2 paradigm.* Nature Reviews: Immunology, 2004. **4**(8): p. 583-94.

Xue, M. and Jackson, C.J., *Extracellular matrix reorganization during wound healing and its impact on abnormal scarring.* Advances in Wound Care, 2015. **4**(3): p. 119-36.

Yamaguchi, Y., Itami, S., Tarutani, M., Hosokawa, K., Miura, H., and Yoshikawa, K., *Regulation of keratin 9 in nonpalmoplantar keratinocytes by palmoplantar fibroblasts through epithelial-mesenchymal interactions.* Journal of Investigative Dermatology, 1999. **112**(4): p. 483-8.

Yamaguchi, Y., Mann, D.M., and Ruoslahti, E., *Negative regulation of transforming growth factor-beta by the proteoglycan decorin.* Nature, 1990. **346**(6281): p. 281-4.

Yang, H., Tan, Q., and Zhao, H., *Progress in various crosslinking modification for acellular matrix.* Chinese Medical Journal, 2014. **127**(17): p. 3156-64.

Yang, L., Scott, P.G., Dodd, C., Medina, A., Jiao, H., Shankowsky, H.A., Ghahary, A., and Tredget, E.E., *Identification of fibrocytes in postburn hypertrophic scar.* Wound Repair and Regeneration, 2005. **13**(4): p. 398-404.

Yannas, I.V. and Burke, J.F., *Design of an artificial skin. I. Basic design principles.* Journal of Biomedical Materials Research, 1980. **14**(1): p. 65-81.

Yannas, I.V., Lee, E., Orgill, D.P., Skrabut, E.M., and Murphy, G.F., *Synthesis and characterization of a model extracellular matrix that induces partial regeneration of adult mammalian skin.* Proceedings of the National Academy of Sciences of the United States of America, 1989. **86**(3): p. 933-7.

Yuan, Z., Zhao, J., Chen, Y., Yang, Z., Cui, W., and Zheng, Q., *Regulating inflammation using acid-responsive electrospun fibrous scaffolds for skin scarless healing.* Mediators of Inflammation, 2014. **2014**: p. 858045.

Zeltinger, J., Sherwood, J.K., Graham, D.A., Mueller, R., and Griffith, L.G., *Effect of pore size and void fraction on cellular adhesion, proliferation, and matrix deposition.* Tissue Engineering, 2001. **7**(5): p. 557-72.

Zhang, Z., Garron, T.M., Li, X.J., Liu, Y., Zhang, X., Li, Y.Y., and Xu, W.S., *Recombinant human decorin inhibits TGF-beta1-induced contraction of collagen lattice by hypertrophic scar fibroblasts.* Burns, 2009. **35**(4): p. 527-37.

Zhang, Z., Li, X.J., Liu, Y., Zhang, X., Li, Y.Y., and Xu, W.S., *Recombinant human decorin inhibits cell proliferation and downregulates TGF-beta1 production in hypertrophic scar fibroblasts.* Burns, 2007. **33**(5): p. 634-41.

Zhang, Z., Wu, F., Zheng, F., and Li, H., *Adenovirus-mediated decorin gene transfection has therapeutic effects in a streptozocin-induced diabetic rat model.* Nephron Experimental Nephrology, 2010. **116**(1): p. e11-21.

Zhu, Z., Ding, J., Ma, Z., Iwashina, T., and Tredget, E.E., *Systemic depletion of macrophages in the subacute phase of wound healing reduces hypertrophic scar formation.* Wound Repair and Regeneration, 2016.